



MEDICAL UNIVERSITY OF GDAŃSK

EUROPEAN JOURNAL OF TRANSLATIONAL AND CLINICAL MEDICINE





EUROPEAN JOURNAL OF TRANSLATIONAL AND CLINICAL MEDICINE

Editor-in-Chief

Dariusz Kozłowski

Vice-Editor-in-Chief

Tomasz Szmuda

Secretary

Justyna Fercho

Advisory Board

John J. Bissler

*University of Tennessee,
Health Science Center (TN, USA)*

Jean-Luc Cracowski

Grenoble Alpes University (France)

Lawrence W. Dobrucki

University of Illinois at Urbana-Champaign (IL, USA)

Anna Dominiczak

University of Glasgow (GB)

Zbigniew Gaciong

Medical University of Warsaw (Poland)

Jerzy B. Gajewski

Dalhousie University (Canada)

Paul Grundeman

University Medical Center Utrecht (Netherlands)

Jacek Jassem

Medical University of Gdańsk (Poland)

Lukasz Konopka

*Institute for Personal Development, Spectrum
Center for Integrative Neuroscience (USA)*

Paweł M. Kozłowski

University of Louisville (KY, USA)

Bengt Lindholm

Karolinska Institutet (Sweden)

Jan-Eric Litton

Karolinska Institutet (Sweden)

Eva M. Martinez-Caceres

*Universitat Autònoma
de Barcelona Medical School (Spain)*

Olle Melander

Lund University Diabetes Centre (Sweden)

Krzysztof Narkiewicz

Medical University of Gdańsk (Poland)

Waldemar Priebe

University of Texas (TX, USA)

Thomas Ritter

National University of Ireland (Ireland)

Paweł Tacik

*University of Bonn Medical Center
(Germany)*

Anna Tomaszuk-Kazberuk

Medical University of Białystok (Poland)

Piotr Witkowski

University of Chicago (IL, USA)

Finance Administrator

Beata Dudzik-Richter

Managing Editor

Małgorzata Omilian-Mucharska

Technical Editors

Małgorzata Omilian-Mucharska
Małgorzata Gusman
Maksymilian Wroniszewski

DTP Editor

Małgorzata Gusman
Janusz Tarasiewicz

Language Editor

Janusz Springer

Web Developer

Piotr Samplawski

Statistical Consultant

Paweł Zagożdżon

Photo on the cover of the issue
by Maciej Broda et al.
(page 80)

Editorial Office

Medical University of Gdańsk
European Journal
of Translational Medicine
Dębinki 7 Street, Building 1
80-211 Gdańsk, Poland

Phone: +48 58 349 15 37

E-mail: ejtcm@gumed.edu.pl
www.ejtcm.gumed.edu.pl

Publisher

Medical University of Gdańsk
M. Skłodowskiej-Curie 3 A
80-210 Gdańsk, Poland
© Copyright by Medical
University of Gdańsk

Gdańsk 2023
e-ISSN 2657-3156

Online edition is the
original version of the journal.

INVITED EDITORIAL

- Emergency Medicine: a specialty that deserves "re-branding", because it enables large financial savings! (This may seem counter-intuitive, but it's true)** **5**
Gary Michael Gaddis

RESEARCH ARTICLE

- Optimisation of osteosynthesis positioning in mandibular body fracture management using finite element analysis** **10**
Omid Daqiq, Charlotte Christina Roossien, Friederik Wilhelm Wubs, Rudolf Robert Maria Bos, Baucke van Minnen
- An echocardiographic tool for the interatrial conduction disorders – old dog, new tricks?** **26**
Jacek Marcin Zawadzki, Jacek Jerzy Gajek, Agnieszka Sławuta, Dariusz Kozłowski, Gabriel Zaborniak, Bartosz Kudliński
- Prevalence of tuberculosis and drug-resistant tuberculosis in tertiary care rural hospital in Gujarat, India: a retrospective study** **36**
Reena Ughreja, Vaibhav Bhatt, Sunny Shah, Devang Boxa
- His bundle pacing in patients with permanent atrial fibrillation and heart failure with non-reduced ejection fraction – retrospective study** **45**
Bartosz Skonieczny, Agnieszka Sławuta, Jadwiga Radziejewska, Dariusz Jagielski, Jacek Gajek, Dariusz Kozłowski
- The impact of ginger and curcumin on diabetic nephropathy induced by streptozotocin in rats** **51**
Alaa Taha, Hanaa Ashour, Manar Reffat, Omali Yousef Elkhawaga
- ST segment depression in atrioventricular reentrant tachycardia** **66**
Jakub Szymon Mercik, Marcin Kuniewicz, Jadwiga Radziejewska, Katarzyna Pach, Dorota Zyśko, Jacek Gajek
- Internet searching may predict novel symptoms, but not new outbreaks. A long-term evaluation of infoveillance in COVID-19** **71**
Jakub Aleksander Radziwon, Maciej Lubiejewski, Przemysław Waszak, Zbigniew Heleniak, Maria Alicja Dębska-Ślizień

TECHNICAL REPORT

- Interdisciplinary interventional and physiotherapy management of facet joint syndrome** **78**
Maciej Broda, Julia Miler, Konrad Jankowski, Bartosz Rogowski, Mateusz Krakowiak, Paweł Sokal

REVIEW ARTICLE

- Histopathological characteristics of myocarditis following COVID-19 vaccination: a scoping review** **85**
Datis Kalali, Doxakis Anastakis
- Usage of pregabalin in the treatment of pain associated with chronic pancreatitis – a clinically oriented narrative review** **91**
Jakub Krzysztof Gałązka, Barbara Skrzydło-Radomańska, Beata Kasztelan-Szczerbińska, Halina Cichoż-Lach
- Remember by heart – the importance of post-mortem cardiac implantable electronic device analysis** **95**
Szymon Rzepczyk, Marcin Migiel, Bartosz Bijata, Paweł Świdorski

Emergency Medicine: a specialty that deserves “re-branding”, because it enables large financial savings! (This may seem counter-intuitive, but it’s true)

Gary Michael Gaddis 

Department of Biomedical and Health Informatics, University of Missouri-Kansas City School of Medicine, Kansas City, MO, USA

Abstract

Emergency departments are costly to maintain. They remain open every hour of the year to provide care for those who need it, when they need it. Therefore, emergency departments are a crucial resource for any modern society, and no sensible person would want to close them, despite their cost. However, the view held by many, that the care provided in an emergency department is excessively costly, is just plain wrong. When our doctors’ and our specialty’s performance is viewed objectively, it becomes clear that emergency physicians have become crucial agents of cost savings. Therefore, EPs have earned the right to proudly “re-brand” themselves not as high-cost care providers, but as indispensable, money-savers in any nation’s health care enterprise. If you don’t believe that, continue reading this commentary.

Keywords: health care costs • emergency medicine • dogmas • savings

Citation

Gaddis GM. Emergency Medicine: a specialty that deserves “re-branding”, because it enables large financial savings! Eur J Transl Clin Med. 2023;6(2):5-9.

DOI: [10.31373/ejtcmm/171885](https://doi.org/10.31373/ejtcmm/171885)

Corresponding author:

Gary Michael Gaddis, Department of Biomedical and Health Informatics, University of Missouri-Kansas City School of Medicine, Kansas City, MO, USA

e-mail: garymgaddis86@gmail.com

Available online: www.ejtcmm.gumed.edu.pl

Copyright © Medical University of Gdańsk

This is Open Access article distributed under the terms of the Creative Commons Attribution-ShareAlike 4.0 International.



Roles and availability of Emergency Departments

As “background information,” those who allege that emergency care is too costly and should in most cases be provided in outpatient clinics overlook at least four critical facts:

First, much of the emergency care we provide could not be provided in an outpatient clinic or a doctor’s office. Could you imagine treating a polytrauma patient, a cerebrovascular accident (“stroke”) patient or acute S-T elevation myocardial infarction (STEMI) patient in an outpatient clinic? Of course not!

Second, most urgent and emergent medical problems don’t happen just on weekdays, while the sun is in the sky. Patients often need to be able to access medical care when doctors’ offices are closed. If an outpatient clinic remains open from 09:00 until 17:00 on weekdays, even if these clinicians in that facility are able to accommodate a few “urgent” appointment requests, they are available for only 40 hours, or 23.8%, of a 168-hour week.

Third, we have implemented research findings to safely decrease costs of care via processes which did not exist when I entered emergency medicine (EM) residency training in 1986. This implementation of research findings saves considerable sums of money.

Fourth, the public’s need for inpatient care ebbs and flows, and when a hospital is operating “above capacity,” the emergency department is typically where that care is provided. Provision of inpatient-level care in an emergency department is less expensive than would be the case if a hospital spent money to add sufficient bed capacity to enable that happy day when ED boarding of patients never had to occur.

Points number 1 and 2, and especially point 4, should all be obvious, yet are sometimes not overtly acknowledged. They will not be further discussed, except for asking you, the readers, to imagine the cost to a hospital system, if it expanded its inpatient capacity sufficiently such that ED boarding of to-be-admitted patients was rarely required!

We leverage research findings to save money

Regarding the third point, the leveraging of research findings, an important development that can easily be taken for granted, here are some illustrative examples demonstrating how EPs save health care systems money every day, when 1986 is compared to 2023:

- In 1986, all patients with acute pyelonephritis were admitted for several days of inpatient intravenous (IV) antibiotic therapy. Now, many of these patients receive one dose of an IV antibiotic, plus analgesia and an antiemetic, in the ED.

Once they demonstrate that their nausea and vomiting is controlled, most of these patients are then prescribed oral antibiotics, analgesics and antiemetics, and discharged. Acute pyelonephritis has become a disease for which emergency physicians can contribute cost savings, because less expensive outpatient management is often feasible and appropriate [1].

- In 1986, most patients with pelvic inflammatory disease (PID) were admitted for several days of IV antibiotics, under the now-disproven dogma that IV antibiotics decreased the scarring of the Fallopian tubes and enhanced the patient’s future fertility. Now, many patients with PID are treated and released after ED administration of appropriate antibiotics to eradicate possible infection by *Neisseria gonorrhea* and *Chlamydia trachomatis*, often with added treatment for anaerobic microbes, and an oral antibiotic upon home-going. Female upper genital tract disease has been transformed to another disease for which emergency physicians can contribute cost savings, because less expensive outpatient management is often feasible and appropriate [2].

- In 1986 all patients diagnosed with the venous thromboembolic (VTE) diseases of deep venous thrombosis (DVT) or acute pulmonary embolism (PE) were admitted for several days of inpatient care to enable therapy with intravenous heparin as a bridge to oral warfarin. Warfarin pills are inexpensive, but the associated care is not. Warfarin is a drug highly prone to drug-drug and drug-food interactions [3]. Further, warfarin dosing requires regular monitoring of the International Normalized Ratio (INR), both a cost and an inconvenience to patients. Fortunately, we first learned we could safely treat most patients with DVT as outpatients by prescribing direct oral anticoagulants (DOACs) such as Factor Xa Inhibitors. Subsequently, we also learned that patients with PE without hypoxia or evidence of right heart failure can safely be discharged home with DOAC prescriptions. DVT and PE have been transformed to diseases for which emergency physicians can contribute cost savings, because they usually can implement feasible and appropriate outpatient management [4].

- In 1986, chest pain patients without an S-T Elevation Acute Myocardial Infarction (STEMI), whose pain was suspected to be cardiac in nature, became inpatients for sequential monitoring of their Lactate Dehydrogenase (LDH) and Creatine Kinase (CK) isozyme profiles. This process required at least a full day and an overnight inpatient stay. Now, for selected patients, EPs can leverage low and non-rising high sensitivity troponin values and a low “HEART score” to safely implement outpatient follow-up plans, within hours, sparing an inpatient admission. Chest pain has been transformed to a chief complaint for which emergency physicians can contribute cost savings, because outpatient management can be feasible and appropriate [5].

- In 1986, a complete workup of many other diseases also required several days of inpatient care. Thanks to improved systems of care and better implementation of medical evidence, patients who used to be admitted for their multi-day “workup” can occasionally be “treated and released”. For example, a hospital at which I had worked in the past had a dedicated fast track pathway for patients diagnosed with transient ischemic attacks (TIA). Most of our patients with TIA who did not need an urgent vascular procedure to protect them against a near-term stroke were treated and released from the ED observation area within 12 hours of their arrival. This expedites hospital throughput and saves significant sums of money.
- A further benefit of all of these examples is that patients with these diseases can be returned to work much more quickly than in past years, enhancing overall workforce productivity in a nation’s economy.

Further improvements are possible

We could do even better at implementing cost savings, if only our patients would permit it. We already know how to apply validated and highly reliable clinical decision rules (CDRs) such as the Ottawa Ankle Rules, the Ottawa Knee Rules, the NEXUS and Canadian C Spine Rules, and the PECARN (for children) and Canadian Head CT (for adults) Rules [6-11]. All perform with high accuracy and validity. However, we know that patients often expect radiographs that these CDRs would establish as contraindicated.

Our collective experience is that there is a significantly long time required to explain these CDRs to patients, so it becomes more cost- and time-effective to simply obtain the non-indicated imaging. Consider this idea for the future: create educational modules that present advocacy to patients to allow doctors to implement these CDRs. This education could be efficiently accomplished if patients were enabled to view effective bedside “plug and play” teaching tools, explaining those CDRs. Such resources could dissuade patients of their false beliefs and persuade them to agree that omission of the contraindicated radiographs, tests which they believed they needed upon their ED arrival, represents appropriate care. This would both save money and shorten the patient’s ED stay. Added benefit would accrue when a pediatric patient avoids a head CT by decreasing their risk for a subsequent cancer [12].

To enable this vision and further enhance our role toward cost savings will require emergency medicine researchers to complement

validated CDRs with the creation, testing and validation of accurate and persuasive patient education tools, sufficient to dissuade most patients of their dogmatic and erroneous beliefs regarding radiographs. EPs have abolished incorrect dogmas before. For instance, consider the well-deserved death at the hands of academic EPs of the previous dogmatic belief that no abdominal pain patient can be administered an opiate until they have been examined by a surgeon [13]. Hopefully, patients’ dogmatic beliefs regarding radiographs can also become consigned to the dustbin of history.

Certain myths need to die

In re-branding ourselves, we should also work to abolish other dogmatic myths that plague us, by refuting certain misleading beliefs that cause the public to wrongly conclude that ED care is a larger source of health care expenditures than is the case.

Consider the myth of Medicaid expenditures in the United States. Medicaid, contrary to popular belief, is not health insurance. It is a government welfare program. It provides a payment mechanism for low-income individuals to obtain health care, while shielding them from the costs and charges for that care. When I ask my friends and neighbors what percentage of a state’s Medicaid budget is spent for emergency department care of persons living in poverty, most of them estimate that number to be about 50%. In truth, 52% of Medicaid spending goes for managed care organizations (MCOs) and health plans, 20% pays for fee-for-service acute care and

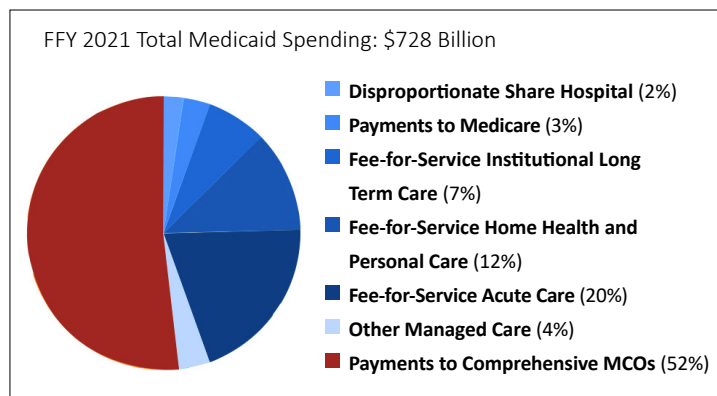


Figure Total national Medicaid spending in the United States [14]

FFY 2021 – Federal fiscal year (October 1, 2020-September 30, 2021), MCOs – managed care organizations. “Other managed care” includes prepaid health plans (PHP), primary care case management (PCCM), programs of all-inclusive care for the elderly (PACE) and premiums and coinsurance paid toward employer group insurance plans and premiums paid for other insurance or remedial care. Managed care prescription drug spending is included in “Payments to Comprehensive MCOs”. “Fee-for-Service Acute Care” includes inpatient hospital services, physician, lab and x-ray services, prescription drugs and other services. “Fee-for-Service Institutional Long-Term Care” includes spending on nursing facilities, intermediate care facilities for individuals with intellectual disabilities and mental health facilities. Data shown above exclude administrative spending, adjustments and payments to the territories. Source: The Urban Institute based on FY 2019 data from the CMS-64, prepared for the Kaiser Program on Medicaid and the Uninsured [14].

19% is spent for long term care (e.g. “nursing homes”) [14]. The Figure parses the spending by MCOs. Spending for ED care is not large enough to merit its own “share” of that “pie”! [14]. I’d bet that a similar misconception about how much of the nation’s health care budget is spent for emergency department care exists in every voivodeship in Poland!

In the United States, patients who ideally would be receiving their medical care in an inpatient department often receive much of that care in an emergency department, when surges in patient demand occur. By pitching in and providing inpatient-type care to “boarders” in the emergency department, we help the hospital system avoid the considerable expense of expanding their inpatient capacity in such a manner that the hospital’s “percent occupancy” would fall, while enabling them to better accommodate occasional surges in demand for inpatient medical care.

The “take-home message”

In summary, rather than repeatedly serving as the “whipping boy” in the “court of public opinion” for our provision of what is incorrectly perceived to be high-cost medical care, EPs should proudly call attention to the numerous ways by which EPs and EDs in which they work help save their nations and patients significant sums of money.

Hopefully, you are now convinced that as EPs, we deserve to be valued not only for being available 24 x 7 x 365, but also for the numerous cost savings that our training permits us to enable.

Brian Zink captured a wonderful initial “vision statement” for EM with the title of his book documenting the history

of our specialty, “Anyone, Anything, Anytime”. That book was first published in 2006. However, in 2023, it is time to move beyond that title. We need a new “vision statement” to “re-brand” EM in a manner that captures how EPs help not only save lives, but also save significant sums of money, 24 x 7 x 365.

I offer for consideration: “Emergency Medicine: Saving not only lives, money, by delivering life-saving, life-enhancing evidence-based medical care quickly, efficiently and effectively”.

Emergency physicians should deservedly take pride in the numerous ways that they help save their nations’ money, via application of their tools and their training, as they accurately and expeditiously work up patients and implement therapy plans that were unthinkable when I entered my emergency medicine residency in 1986. As the citizens of your nation learn of this story, perhaps a few words of their words of praise could usefully offset the “burnout” that plagues many physicians of our specialty.

Now that you know the story that justifies the claim that emergency medicine should be “re-branded” as a cost-saving specialty, it is up to all of us to adopt and spread this message.

Conflicts of interest

None.

Founding

None.

References

1. Herness J, Buttolph A, Hammer NC. Acute pyelonephritis in adults: rapid evidence review. Am Fam Physician [Internet]. 2020;102(3):173-80. Available from: <https://www.aafp.org/pubs/afp/issues/2020/0801/p173.html>
2. CDC sexually transmitted disease guidelines 2021. Pelvic Inflammatory Disease (PID) [Internet]. Centers for Disease Control and Prevention. 2021 [cited 2023 Sep 4]. Available from: <https://www.cdc.gov/std/treatment-guidelines/pid.htm>
3. Warfarin side effects: watch for interactions print [Internet]. Mayo Clinic. 2022 [cited 2023 Sep 4]. Available from: <https://www.mayoclinic.org/diseases-conditions/deep-vein-thrombosis/in-depth/warfarin-side-effects/art-20047592>
4. Stubblefield WB, Kline JA. Outpatient treatment of emergency department patients diagnosed with venous thromboembolism. Postgrad Med [Internet]. 2021 Aug 6;133(sup1):11-9. Available from: <https://www.tandfonline.com/doi/full/10.1080/00325481.2021.1916299>
5. Gulati M, Levy PD, Mukherjee D, Amsterdam E, Bhatt DL, Birtcher KK, et al. 2021 AHA/ACC/ASE/CHEST/SAEM/SCCT/SCMR Guideline for the evaluation and diagnosis of chest pain. J Am Coll Cardiol [Internet]. 2021 Nov;78(22):e187-285. Available from: <https://linkinghub.elsevier.com/retrieve/pii/S0735109721057958>
6. Shell IG. Decision rules for the use of radiography in acute ankle injuries. JAMA [Internet]. 1993 Mar 3;269(9):1127. Available from: <http://jama.jamanetwork.com/article.aspx?doi=10.1001/jama.1993.03500090063034>
7. Stiell IG. Prospective validation of a decision rule for the use of radiography in acute knee injuries. JAMA J Am Med Assoc [Internet]. 1996 Feb 28;275(8):611. Available from: <http://jama.jamanetwork.com/article.aspx?doi=10.1001/jama.1996.03530320035031>

8. Hoffman JR, Mower WR, Wolfson AB, Todd KH, Zucker MI. Validity of a set of clinical criteria to rule out injury to the cervical spine in patients with blunt trauma. *N Engl J Med* [Internet]. 2000 Jul 13;343(2):94-9. Available from: <http://www.nejm.org/doi/abs/10.1056/NEJM200007133430203>
9. Stiell IG, Clement CM, McKnight RD, Brison R, Schull MJ, Rowe BH, et al. The Canadian C-Spine Rule versus the NEXUS Low-Risk Criteria in Patients with Trauma. *N Engl J Med* [Internet]. 2003 Dec 25;349(26):2510-8. Available from: <http://www.nejm.org/doi/abs/10.1056/NEJMoa031375>
10. Schonfeld D, Bressan S, Da Dalt L, Henien MN, Winnett JA, Nigrovic LE. Pediatric Emergency Care Applied Research Network head injury clinical prediction rules are reliable in practice. *Arch Dis Child* [Internet]. 2014 May 1;99(5):427-31. Available from: <https://adc.bmj.com/lookup/doi/10.1136/archdischild-2013-305004>
11. Stiell IG. Comparison of the Canadian CT Head Rule and the New Orleans Criteria in Patients With Minor Head Injury. *JAMA* [Internet]. 2005 Sep 28;294(12):1511. Available from: <http://jama.jamanetwork.com/article.aspx?doi=10.1001/jama.294.12.1511>
12. Sheppard JP, Nguyen T, Alkhalid Y, Beckett JS, Salamon N, Yang I. Risk of brain tumor induction from pediatric head CT procedures: a systematic literature review. *Brain Tumor Res Treat* [Internet]. 2018;6(1):1. Available from: <https://btrt.org/DOIx.php?id=10.14791/btrt.2018.6.e4>
13. Brewster GS, Herbert ME, Hoffman JR. Medical myth: analgesia should not be given to patients with an acute abdomen because it obscures the diagnosis. *West J Med* [Internet]. 2000 Mar;172(3):209-10. Available from: <http://www.ncbi.nlm.nih.gov/pubmed/10734818>
14. Williams E, Rudowitz R, Burns A. Medicaid financing: the basics [Internet]. KFF. 2023. Available from: <https://www.kff.org/medicaid/issue-brief/medicaid-financing-the-basics/>

Optimisation of osteosynthesis positioning in mandibular body fracture management using finite element analysis

Omid Daqiq¹ , Charlotte Christina Roossien² , Friederik Wilhelm Wubs³ , Rudolf Robert Maria Bos¹, Baucke van Minnen¹ 

¹Department of Oral and Maxillofacial Surgery, University Medical Center Groningen, University of Groningen, The Netherlands

²Department of Rehabilitation Medicine, University Medical Center Groningen, University of Groningen, The Netherlands

³Bernoulli Institute for Mathematics, Computer Science and Artificial Intelligence, University of Groningen, The Netherlands

Abstract

Background: This proof of principle study aims to investigate the applicability of finite element analysis (FEA) in Oral and Maxillofacial (OMF) surgery, by studying the effect of mandibular body height and osteosynthesis positioning on unilateral mandibular body fractures based on Champy's technique. **Material and methods:** Mandibles made of polyurethane foam (Synbone®), with heights of 18, 14, and 10 mm were used to create a FEA model with a unilateral straight-line fracture, fixated with a standard commercially available 6-hole 2 mm titanium miniplate. Two different FEA programs were used for the comparison, namely: Solidworks and Comsol Multiphysics. The FEA outcomes were compared with a series of mechanical tests with polymeric models fixed in a customised device and loaded onto a mechanical test bench. **Results:** First, the study illustrated that the optimal plate position appeared to be the upper border. Second, lower mandibular height increases instability and requires a stronger osteosynthesis system. **Conclusions:** FEA's and polymeric model testing outcomes of unilateral non-communited fractures were highly comparable with current opinions of mandibular fracture management. The promising outcome of this study makes it worthwhile to do more extensive analysis in order to determine whether FEA alone is sufficient for optimisation of fracture management.

Keywords: mandibular body fracture · finite element analysis (FEA) · polymeric model testing · mandibular body height · miniplate positioning

Citation

Daqiq O, Roossien CC, Wubs FW, Bos RRM, van Minnen B. Optimisation of osteosynthesis positioning in mandibular body fracture management using finite element analysis. Eur J Transl Clin Med. 2023;6(2):10-25.

DOI: [10.31373/ejtcmed/163427](https://doi.org/10.31373/ejtcmed/163427)

Corresponding author:

Omid Daqiq, Department of Oral and Maxillofacial Surgery, University Medical Center Groningen, University of Groningen
e-mail: o.daqiq@umcg.nl

Available online: www.ejtcmed.gumed.edu.pl

Copyright © Medical University of Gdańsk

This is Open Access article distributed under the terms of the Creative Commons Attribution-ShareAlike 4.0 International.



Introduction

Osteosynthesis plates and screws are routinely used in oral and maxillofacial (OMF) surgery [1-5]. In OMF surgery, mandibular fracture management is based on two completely different principles: (1) the osteosynthesis plate must provide enough rigidity to avoid fragment displacement during functional movement achieved through rigid fixation by placing solid plates at the lower border (load-bearing principle), and (2) the Champy technique suggesting the use of semi-rigid fixation with miniplates in which the tensile forces are neutralized by placing the plates in the so-called ideal line of osteosynthesis, resulting in interfragmentary stability between the bone segments (load-sharing principle) [6-8].

The applied (mastication) forces on the mandible cause different tension and compression zones [9]. The mandibular body's upper border is a tension zone, whereas the lower border is a compression zone [8-9]. According to current clinical understanding and literature, a decrease in mandibular body height in an atrophic mandible results in a narrow range between the tension and compression zones [10-13]. In a severely atrophic mandible, the tension and compression zones more or less overlap each other and the load-sharing principle is not valid anymore [6-8, 14-15].

Following Champy's theory, many studies started using expensive and time-consuming cadaveric or polymeric bone models [16-19]. It could be beneficial to use three-dimensional (3D) modelling and finite element analysis (FEA) instead of model testing. FEA is a non-invasive computational method to evaluate the stress distribution and displacement within a structure on load application [20-21]. It is a reliable and accurate numerical simulation tool for studying force distribution in the OMF area [21-22]. FEA enables the studying of mandibular fracture fixation, possibly leading to solutions regarding plate positioning and predicting the consequences of mandibular height decrease [23-26]. So far, the use of FEA to address clinical issues has been limited. In OMF surgery, not every issue regarding the best possible osteosynthesis has been resolved, e.g. complex comminuted fractures or extremely atrophic mandibles [14-15]. As these cases are less common than non-complex fractures, any subsequent clinical studies are very time-consuming or impossible without the required inclusions [15, 27]. Therefore, there is a need for a validated three-dimensional (3D) computer modelling and FEA simulation method to analyse these fractures and to plan the best osteosynthesis system for each clinical

scenario, possibly by introducing new implants (e.g. degradable or patient-specific 3D printed plates) [23].

Hence, the purpose of our study was to compare mandibular model testing with FEA as a first step towards developing a validated 3D computer model for optimising mandibular fracture management. As proof of principle, we studied the effect of plate positioning and the effect of reduced mandibular body height in mandibular body fracture management based on the FEA simulations. In this initial study, the model was simplified by using mandibles with a unilateral straight-line body fracture only. Our first hypothesis was that the clinical observations of plate positioning and its effect on fracture stability, according to the load-bearing versus load-sharing principles, are reproducible in the 3D computer model. The second hypothesis was that the 3D computer model will confirm the theory that a reduction in atrophic mandible height leads to a decrease in interfragmentary stability making load-bearing fixation necessary. Finally, we hypothesized that FEA is a suitable tool to facilitate the visualisation of fixation stability which may subsequently help the surgeon in selecting an appropriate osteosynthesis system and in positioning the plate correctly.

Material and methods

Study design

We used FEA to analyse the effect of plate positioning for different mandibular body heights with a unilateral mandibular body fracture. The FEA simulations were conducted primarily in the computer simulation software Solidworks version SP5.0, 2020, 3D Modelling and Simulation, Waltham, Massachusetts, USA). The eligibility, reproducibility and accuracy of the outcomes generated in Solidworks were compared with those from a second simulation software Comsol Multiphysics (version 5.5, 3D Modelling and Simulation, Stockholm, Sweden). Further validation was done by comparing the results with a series of polymeric models fixated in a customized device on a mechanical test bench (DYNA-MESS Prüfsysteme, Stolberg, Germany). All the mandibles were fixated with the same type of osteosynthesis system (2.0 mm titanium miniplates, KLS Martin Group, Tuttlingen, Germany) and identical simulations were conducted for each study.

Assembly modelling

Synbone (Zizers, Switzerland) mandibles with body heights of 18, 14, and 10 mm (representing the slightly, moderately and severely atrophic mandibles, respectively) were used to create the 3D computer models of the mandible. Cone beam computed tomography (CBCT) (Planmeca, Promax 3D Max ProFace, Helsinki, Finland) was conducted on each Synbone mandible and digital imaging and communication in medicine (DICOM) files were generated. The CBCT scans were made at the bone setting with a voxel size of 400 μ m, tube current of 2.5 mA, and tube voltage of 120 kV. DICOM files were used for the 3D modelling of the mandibles. The 3D computer modelling dimension measurements were performed using the Mimics software (version 25.0, Materialise, Leuven, Belgium). The 3D mandible

models were then created in Solidworks after which they were geometrically simplified to eliminate mesh errors and simplify the simulation computations (Figure 1). In the study, the same type of straight-line unilateral mandibular body fracture was applied to each model. The distance between the fracture surfaces was set at 0.1 mm. The fracture type, size, and placement were identical in all the 3D models. The fracture was placed in the middle of the mandibular body, in between the first molar and second premolar. A standard commercially available 6-hole 2 mm osteosynthesis titanium miniplate (KLS Martin Group, Tuttlingen, Germany) with a length of 36.3 mm and 6 x 2 mm diameter screws with a length of 18.4 mm were modelled in Solidworks. The 6-hole miniplate was used for all the FEA computer simulation analyses (Figure 2).

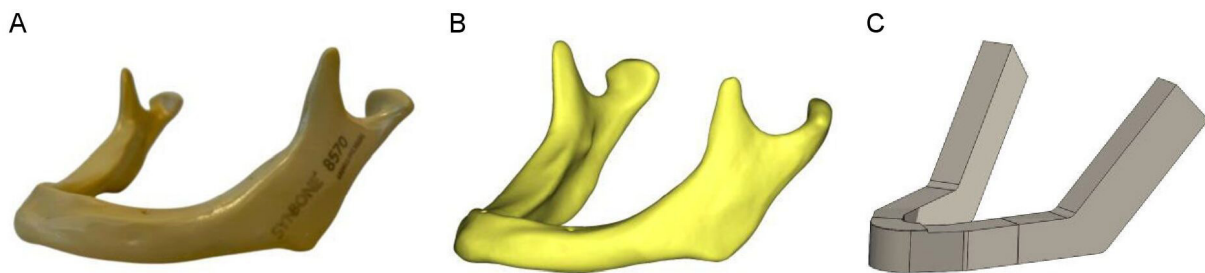


Figure 1. 3D computer modelling of the mandible: (A) Synbone® mandible, (B) DICOM file from CBCT, and (C) a simplified 3D model of a mandible

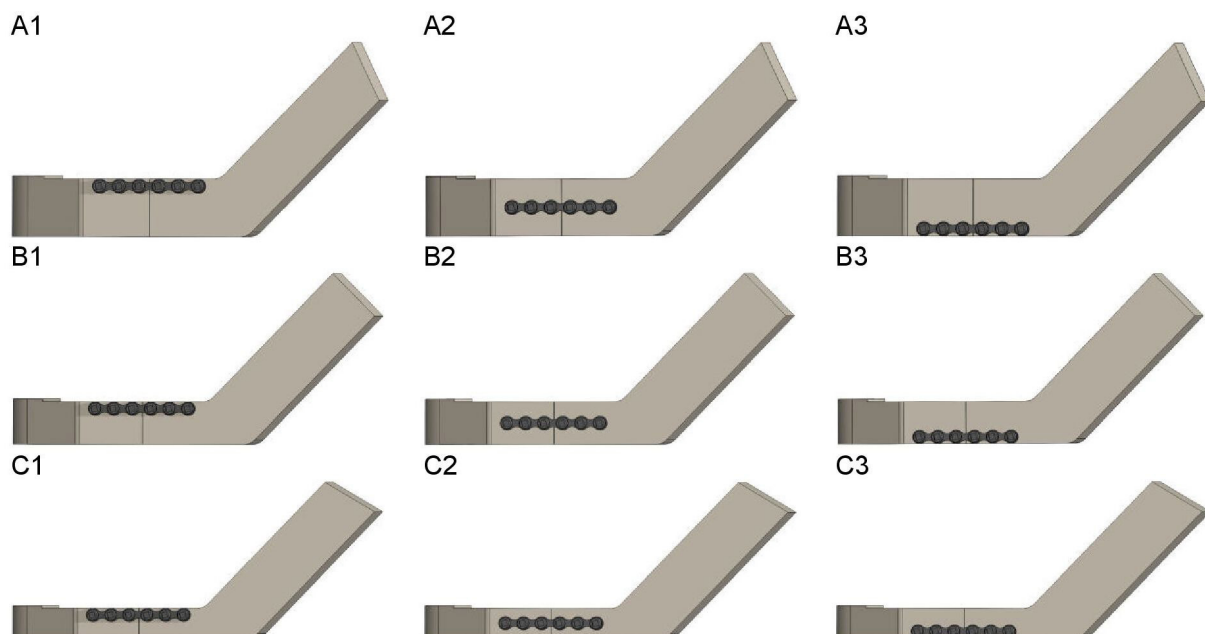


Figure 2. Plate positioning at the (A) 18 mm, (B) 14 mm, and (C) 10 mm mandibular body heights: (1) miniplate positioned at the upper border, (2) in the middle, and (3) at the lower border of the mandible

FEA Solidworks

FEA was primarily performed in the Solidworks software. The analysis started with positioning the osteosynthesis miniplate at the mandible's upper border and subsequently lowering it towards the lower border along the fracture line. This was done to determine the effect of plate positioning at different mandibular body heights (Figure 2). Plate positions 1 to 3 represent the miniplate at the upper border, in the middle, and at the lower border of the mandible, respectively.

The average mastication force (200 N) was applied downward on the symphysis of the mandible (Figure 3A) [28-29]. The mandibles were fixed at the condylar head to replicate the temporomandibular joint by applying the fixed geometry option from the Solidworks fixture property manager tab (Figure 3B). Furthermore, the effect of fixation site was evaluated by conducting a series of sensitivity tests for different fixation locations (Supplementary Figure S1).

The chosen mandible material properties were similar to those of the Synbone® polyurethane foam mandible to allow for a comparison with polymeric model

testing. The mandible material properties were set at an elastic modulus of 2410 MPa, shear modulus of 862.2 MPa, mass density of 1.26 g/cm³, tensile strength of 40 MPa, and a Poisson's ratio of 0.39 [30-32]. The properties of the titanium miniplates and screws were as follows: an elastic modulus of 104800 MPa, mass density of 4.43 g/cm³, tensile strength of 1100 MPa, yield strength of 827.4 MPa, and a Poisson's ratio of 0.31 [1]. Using the Solidworks contact-sets property manager tab we defined the boundary conditions between the mandibles, miniplates, and screws (Figure 3C). The connection between the two fracture surfaces was defined by using the contact-sets with a fixed distance of 0.1 mm between the fracture surfaces (Figure 3D), representing optimal fracture reduction. When the fracture surfaces touch, only the forces normal to the surfaces would be exchanged and there was no friction force present. The mandible screw holes and the screws were set as bounded, meaning that the screws were fixed tightly in the mandible, pressing the plate against the mandibular body. The connection between the miniplate and the screws, as well as the connection between the miniplate and the mandible, were set using the contact

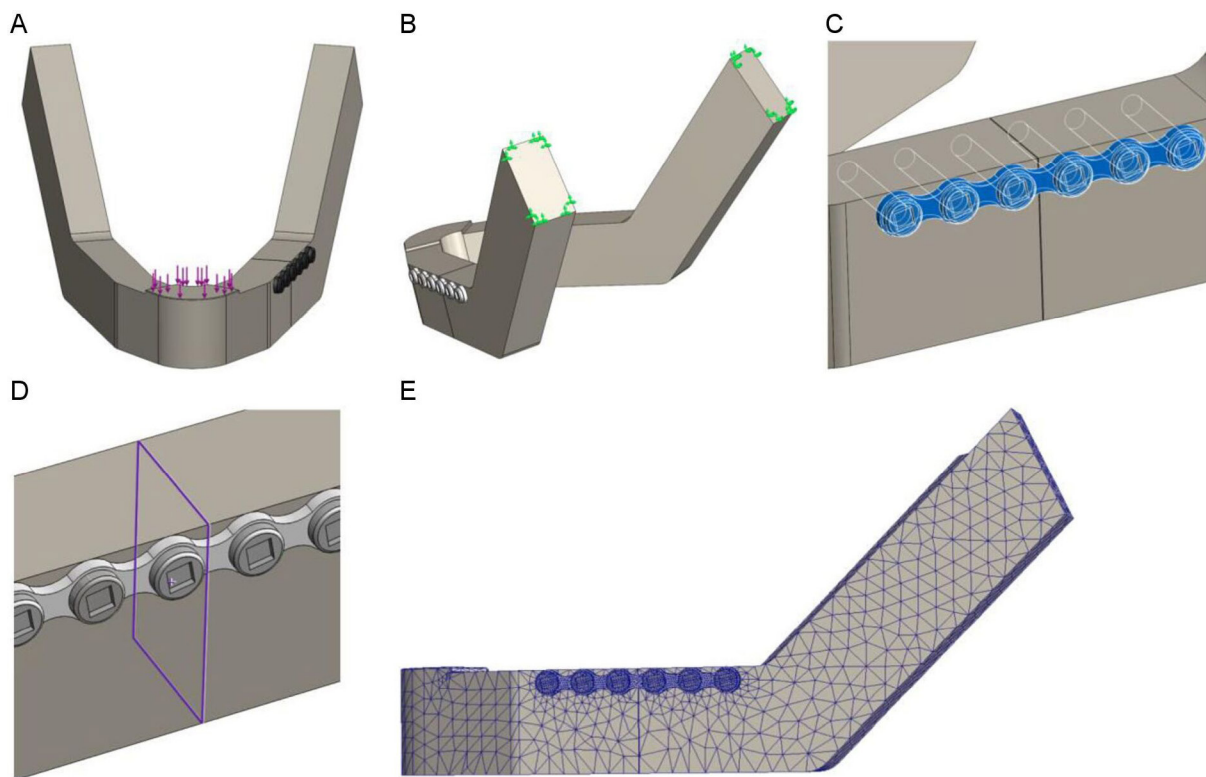
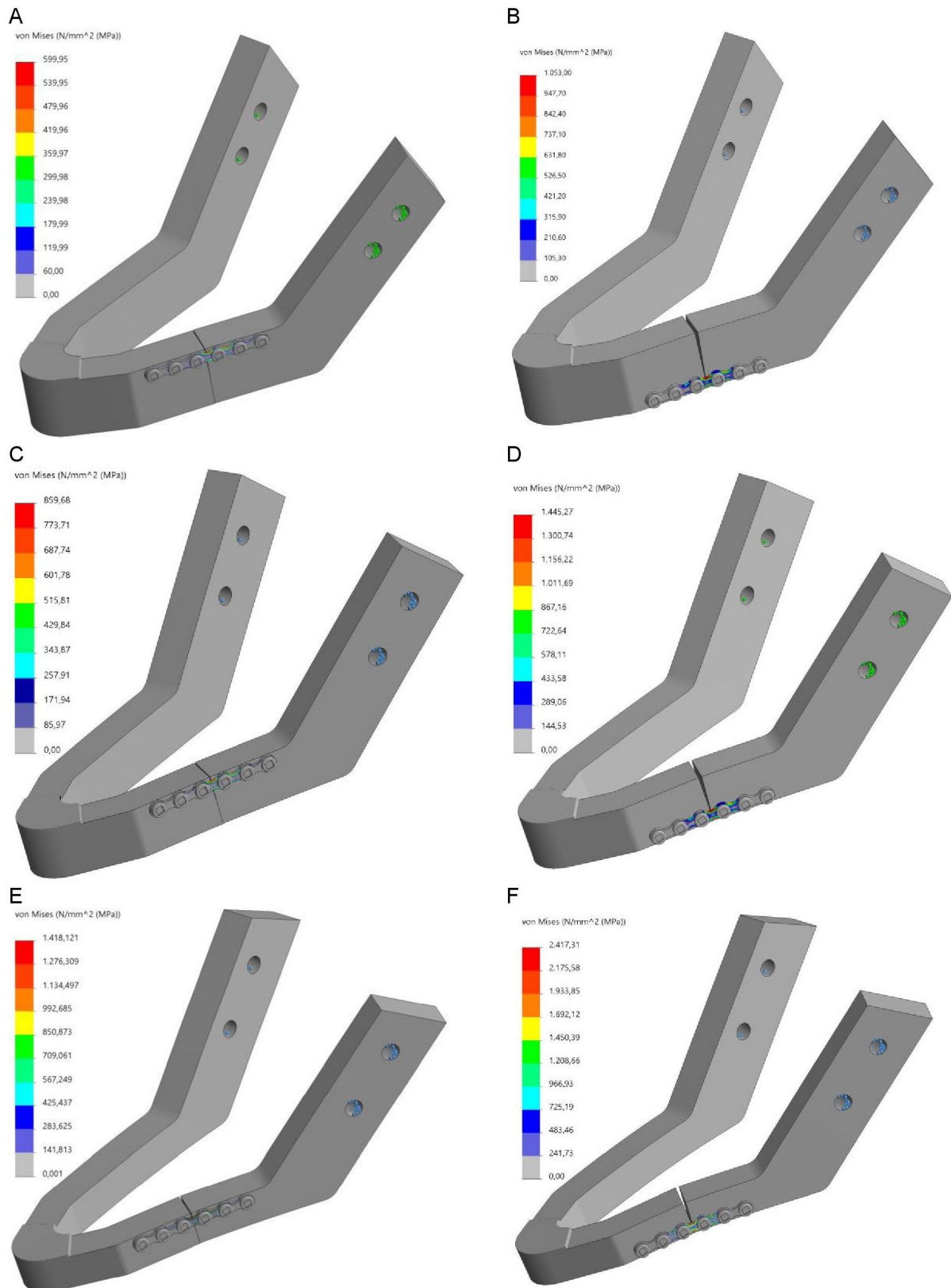
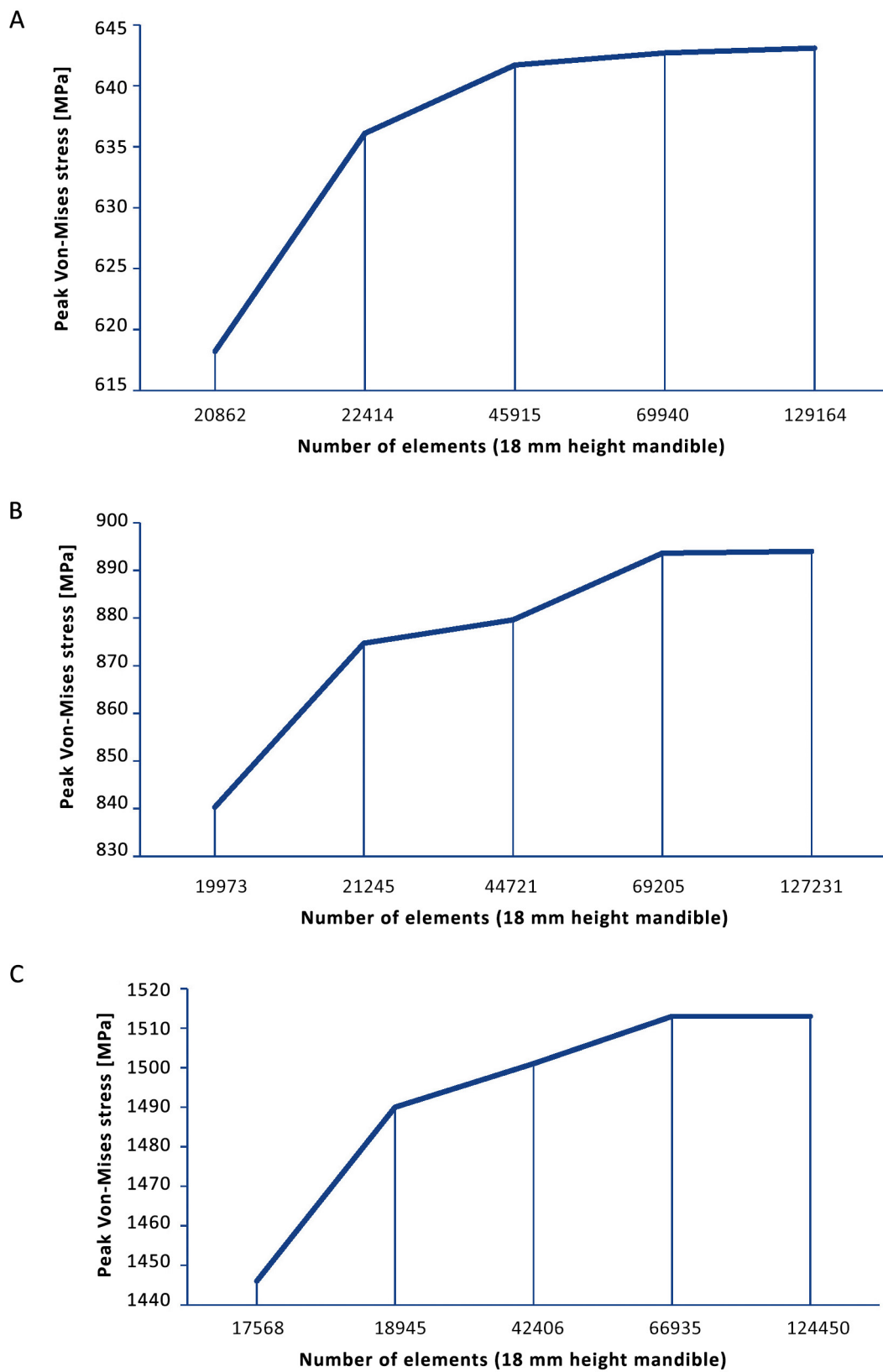


Figure 3. FEA set up in Solidworks: (A) Mastication force of 200 N is applied downward on the symphysis, (B) Fixation at the condylar head, (C) Contact boundary condition between the mandible and osteosynthesis system, (D) Contact-set boundaries between the fracture surfaces with a fracture distance of 0.1 mm and no penetration, and (E) Impression of the used mesh.



Supplementary Figure S1. FEA Von-Mises stress [MPa] for different fixation location: (A-B) 18 mm height mandible, (C-D) 14 mm height mandible, and (E-F) 10 mm height mandible; note: plate positioned at the upper border (right) and plate positioned at the lower border of the mandible (left)



Supplementary Figure S2. Mesh convergence plots: (A) 18 mm height mandible, (B) 12 mm height mandible, and (C) 10 mm height mandible

option from the contact-sets property manager. Only normal forces and no friction were present here, which is in accordance with the current opinion on stabilising mandibular fractures using non-locking plates. The boundary conditions and parameters were identical in all of the FEA studies.

FEA Comsol

Comsol was used to verify the Solidworks results and to evaluate whether the outcomes were reproducible, reliable, and accurate. The 3D computer model assemblies of each mandible and the osteosynthesis miniplate were imported from Solidworks in STEP file format. The imported assemblies were processed and saved in the Comsol 3D environment. All the FEA inputs were performed identically as in Solidworks. A force of 200 N was applied downwards on the symphysis of the mandible and fixation was set at the condylar head. The connections between the miniplate and the screws, as well as between the miniplate and the mandible, were set using the contact constraint option. The connection between the mandible and the screws was set as fixed using the continuity constraint option. The applied mesh was similar to the one in Solidworks.

FEA mesh convergence

The chosen mesh dimensions were checked in the simulation models to determine whether they were correct. The mesh size was reduced until the results were independent of the mesh size and mesh convergence was reached (Supplementary Figure S2). The converged mesh was used for the remaining FEA studies (Figure 3E). The mesh applied in Solidworks was similar to the mesh in Comsol.

Polymeric model testing

A polymeric mandible is made of polyurethane foam and is an adequate substitute for cadaveric human bone for testing purposes [30-32]. It has been shown to be a successful simulator for a similar sized and shaped human bone [30, 33-34]. Polymeric model testing was conducted on a mechanical test bench to validate the FEA. Polymeric mandible replicas with body heights of 18, 14, and 10 mm were obtained from Synbone. A straight-line unilateral fracture was applied to each mandibular body and fixated with the osteosynthesis miniplate system. Polymeric model testing of 18 and 14 mm mandibular heights entailed using a 4-hole miniplate with four screws. A 6-hole miniplate

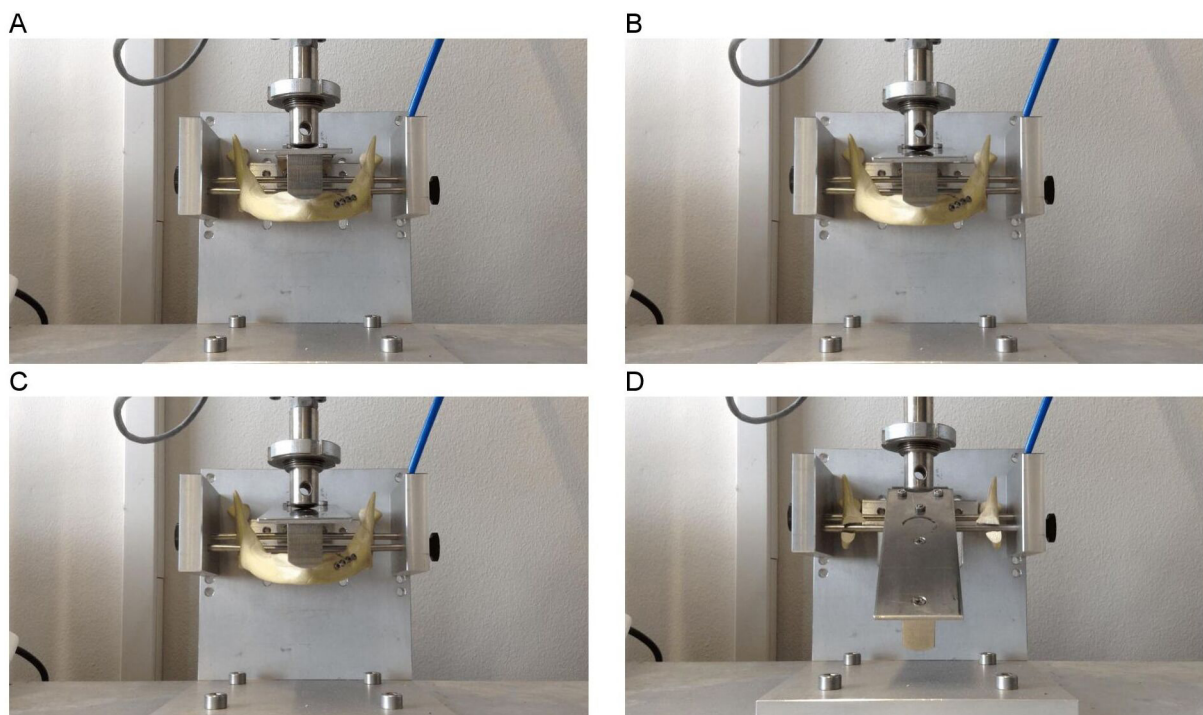


Figure 4. Mandible (with straight-line fracture and miniplate fixation) positioned on the custom-made device and loaded in a mechanical test bench; the starting point is (A) until it reaches the breaking point (D)

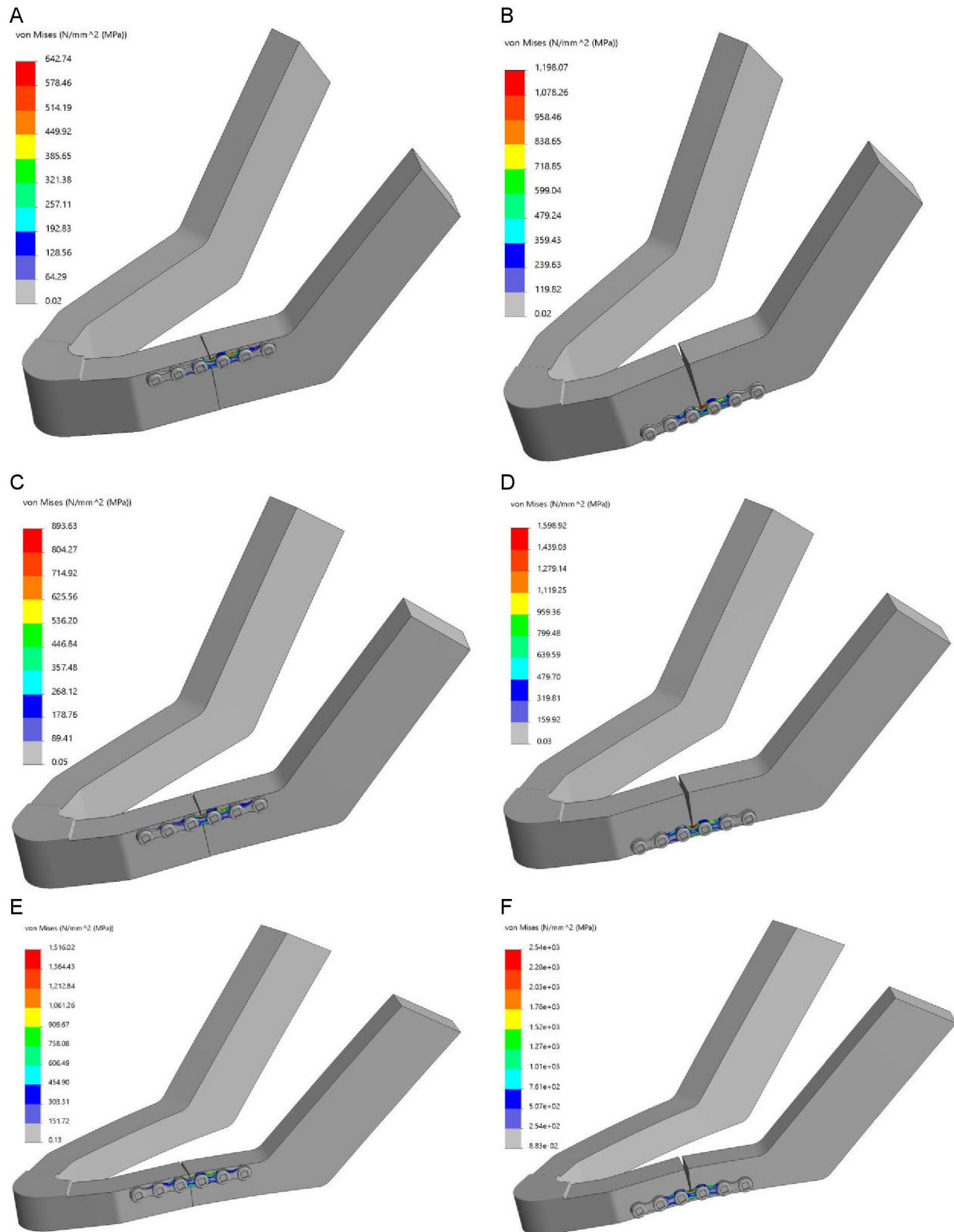


Figure 5. FEA Von-Mises stress [MPa]: (A-B) 18 mm height mandible, (C-D) 14 mm height mandible, and (E-F) 10 mm height mandible; note: plate positioned at the upper border (right) and plate positioned at the lower border of the mandible (left)

with six screws was used for the 10 mm mandibular height. Only the osteosynthesis miniplates positioned at the upper border of the mandible were

tested. Each of the three polymeric mandible replicas (the 18, 14 and 10 mm heights) was tested three times. A custom device was built to position the mandibles on

the mechanical test bench (Figure 4). A load representing the mastication force was applied to the mandible and gradually increased at a rate of 10 N/s (Figure 4A). The values were set in the computer system of the mechanical test bench. The force on the mandible was increased continuously until the failure point where the mandible breaks down was reached (Figure 4D). Computerised sensors on the mechanical test bench recorded the data. All three mandible heights were tested using the same technique.

Data analysis

The FEA Solidworks outcomes were compared with the Comsol outcomes. This was done by first meas-

uring the amount and the location of the maximum Von-Mises stress (Figure 7A-B). Then the displacement in the Z-axis was compared (Figure 7C-D). Finally, the Von-Mises stress pattern at a selected stress point was compared between the two FEA studies (Figure 6). The FEA outcomes were also compared with the polymeric model testing by observing the displacement patterns of the miniplates positioned at the upper borders of the mandibles with the different fracture heights (Figure 8). The displacement in the Z-axis of the FEA was used for the comparisons with the displacement in the polymeric model testing. Finally, data were evaluated with help of experts in statistics, however due to the small sample size statistical analysis did not make sense in this study.

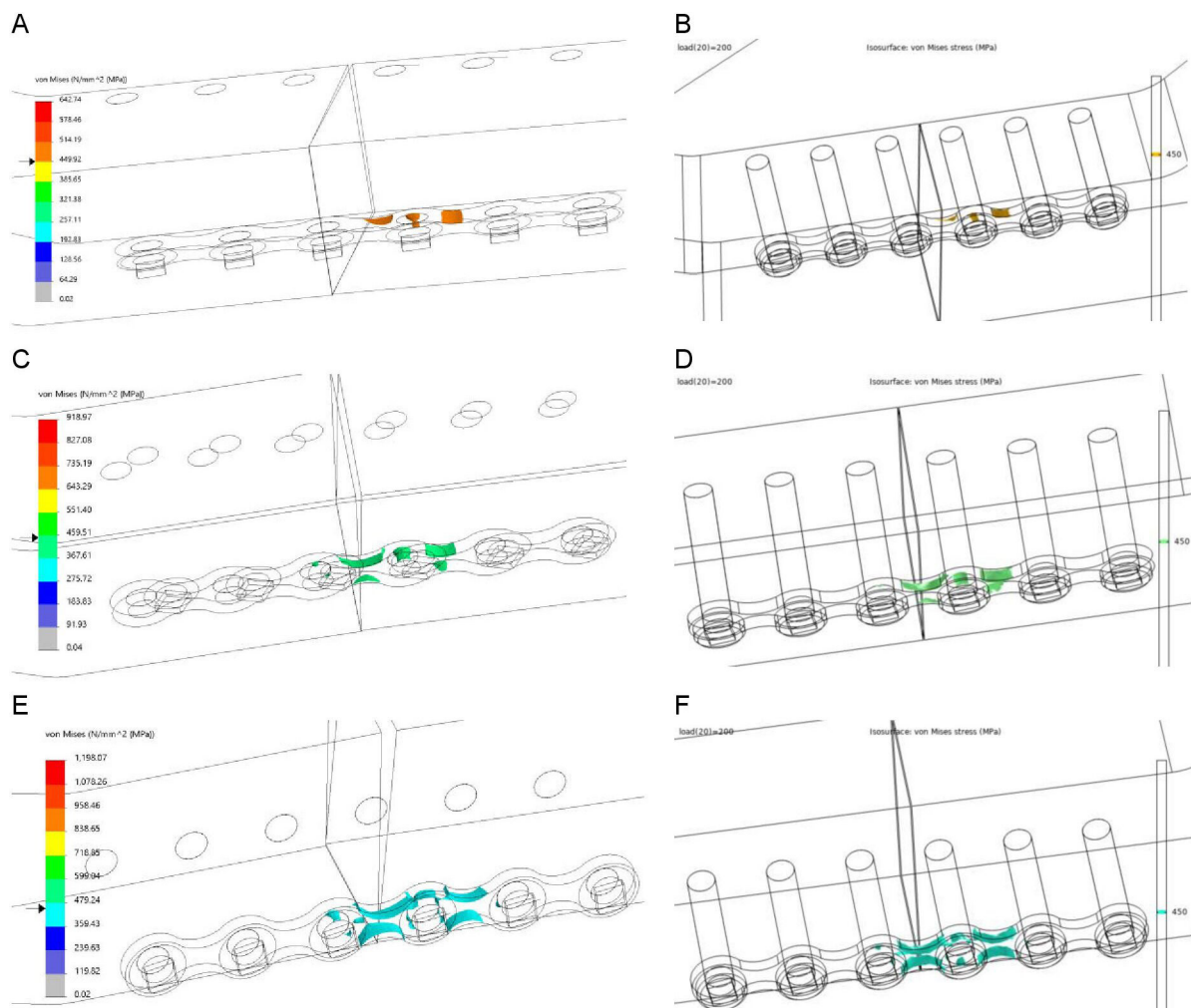


Figure 6. Comparison of Von-Mises stress between Solidworks (right) and Comsol (left) at 450 MPa for the 18 mm mandible height: (A-B) plate positioned at the upper border, (C-D) in the middle, and (E-F) at the lower border of the mandible

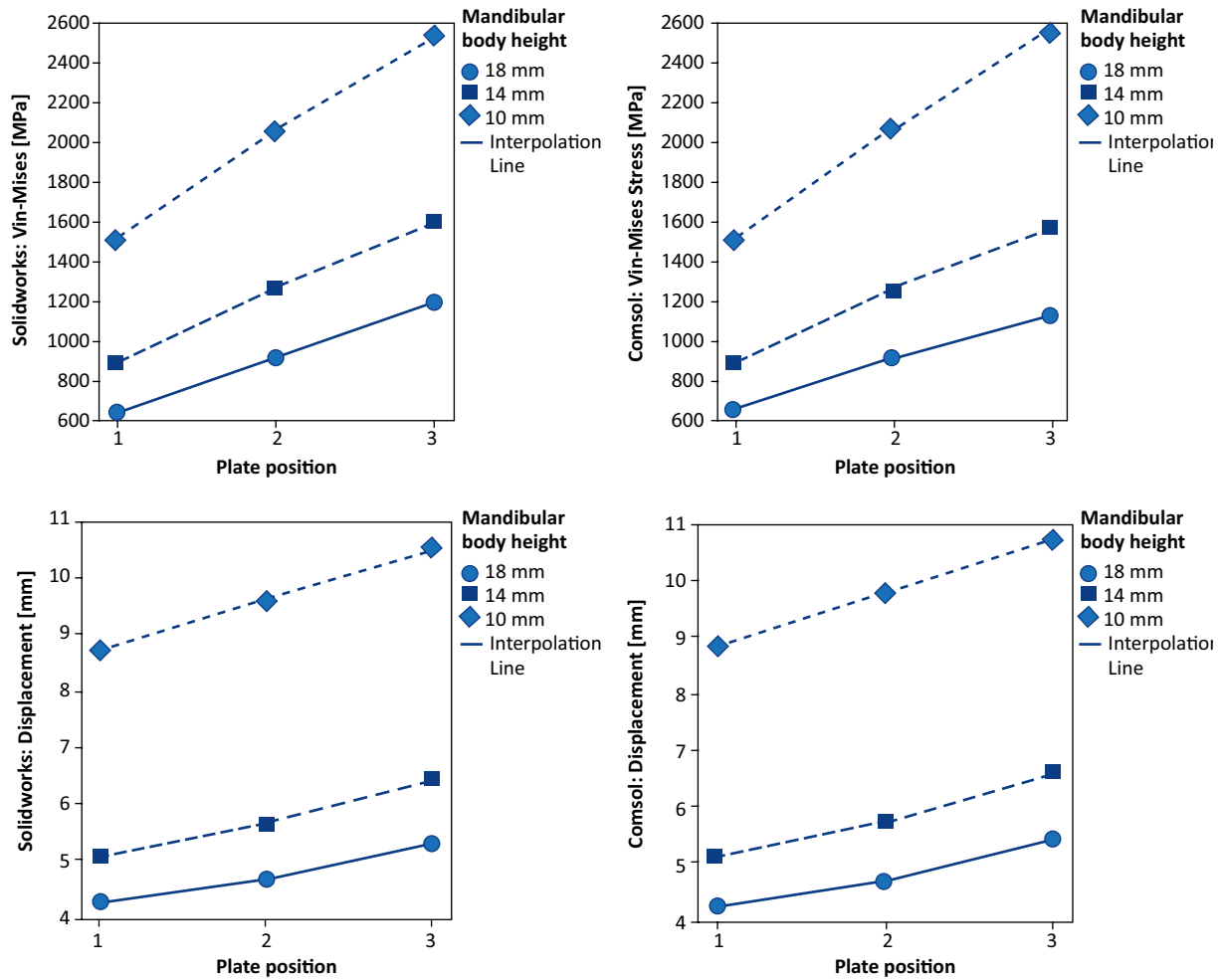


Figure 7. (A-B) FEA Von-Mises stress plots: (A) Solidworks and (B) Comsol; (C-D) FEA displacement plots: (C) Solidworks and (D) Comsol

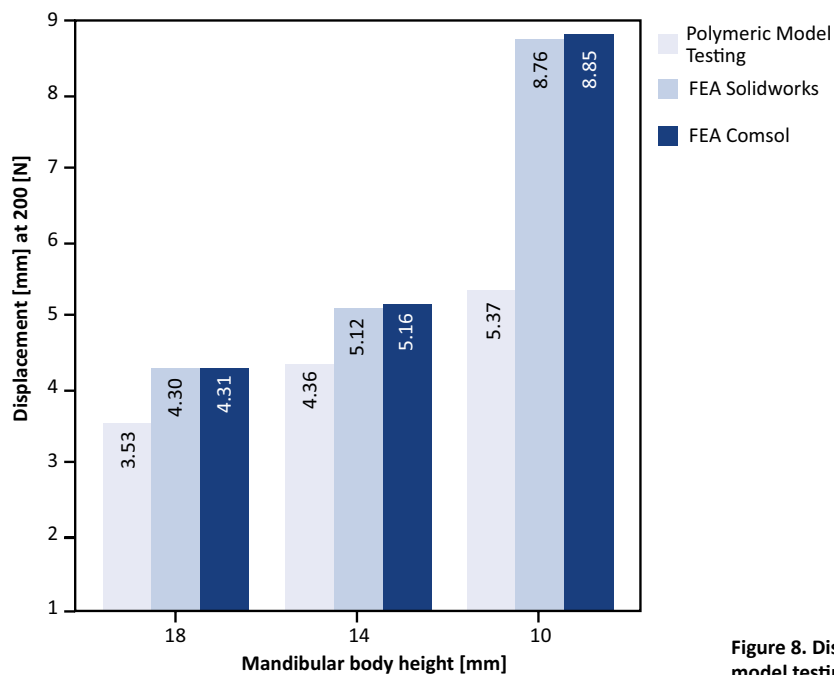


Figure 8. Displacement comparison between polymeric model testing and FEA at 200 N; the displacements are in the z-axis; the same direction as the applied mastication force.

Results

FEA Solidworks

The results of the FEA are presented in Table 1, showing the maximum Von-Mises stress [MPa] and displacement [mm] outcomes. The maximum Von-Mises stress was located at the miniplates curvature between the third and the fourth screw holes, specifically at the edge of the plate where it was touching the mandibular body at the unilateral fracture site (Figure 5A-F). The table shows that stress and displacement increased with a decrease in mandibular body height. The same applies to when the miniplate was lowered from the mandibular upper border towards the lower border along the fracture line. The ratio of the Von-Mises stress and the ratio of the displacement in relation to plate positioning (miniplate at the lower border versus the upper border) and mandibular body height (10 mm versus 18 mm)

are presented in Table 2. Observing the fracture surfaces shows that when the miniplate was positioned at the upper border, the fractures remained closed, intact, and stable. This was due to the tension zone at the upper border of the mandible and the compression zone at the lower border. However, when the miniplate was lowered, particularly when positioned at the lower border, the fracture surfaces tended to open from the upper border in a wedge-shaped form. In this situation the fixation was unstable (Figure 5).

FEA Comsol

Comsol was used to check the reproducibility and accuracy of the Solidworks simulations. The Von-Mises stress [MPa] and displacement [mm] are shown in Table 1. The maximum stress location according to Comsol was identical to all the Solidworks FEA outcomes, namely at the edge of the plate where it was touching

Table 1. FEA outcomes in Solidworks and Comsol regarding the maximum Von-Mises stress and displacement

Mandible height [mm]	Plate position	Solidworks		Comsol	
		Von-Mises stress [MPa]	Displacement z-axis [mm]	Von-Mises stress [MPa]	Displacement z-axis [mm]
18	1	643	4.30	646	4.31
	2	919	4.69	911	4.73
	3	1198	5.35	1120	5.47
14	1	894	5.12	880	5.16
	2	1273	5.69	1253	5.78
	3	1599	6.46	1560	6.64
10	1	1516	8.76	1521	8.85
	2	2065	9.65	2072	9.76
	3	2536	10.53	2560	10.70

Plate position: (1) upper border, (2) middle, and (3) lower border of the mandible. The z-axis was in the same direction as the applied 200 [N] force

Table 2. Ratio of the Von-Mises stress [MPa] and displacement [mm] (Z-axis) for plate positioning and mandibular body height

Ratio		Solidworks		Comsol	
		Von-Mises stress	Displacement	Von-Mises stress	Displacement
Plate positioning *	18	1.86	1.24	1.73	1.27
	14	1.79	1.26	1.77	1.29
	10	1.67	1.20	1.68	1.21
Mandibular body height **	1	2.36	2.04	2.35	2.05
	2	2.25	2.06	2.27	2.06
	3	2.12	1.97	2.29	1.96

* Ratio of the miniplate positioned at the lower border compared to the upper border for the 18, 14 and 10 mm mandibular body heights

** Ratio between the 10 mm versus the 18 mm mandibular body heights for the plates positioned at the upper (1), in the middle (2) and the lower borders (3)

the mandibular body at the unilateral fracture site (Figure 5). The Von-Mises stress pattern comparison illustrates that the stress pattern remained identical in both FEA simulations at any selected stress point (Figure 6). This demonstrates that the Solidworks FEA outcomes are reproducible, accurate and correct. Furthermore, the Von-Mises stress ratio and the displacement ratio for the plate positioning and mandibular body height were similar to those generated in Solidworks (Table 2).

Fixation location sensitivity test

Sensitivity test evaluations of the different fixation locations illustrated a change of less than 10% for the maximum stress and displacement values. However, no changes were observed in the stress or displacement distribution patterns, as they remained identical. Furthermore, the FEA outcomes for analysing the effect of different mandibular body heights and plate positioning remained identical with no changes observed for the different fixation locations (Supplementary Figure S2).

Polymeric model testing

The displacement outcomes of the polymeric model testing are displayed in Table 3, showing that a decrease in mandibular body height resulted in an increased displacement. This indicates that the probability of failure increases when the mandibular body height decreases. Furthermore, the polymeric testing patterns were similar to the FEA, namely: a decrease in mandibular body height increased the fixation instability leading to implant failure.

Outcomes comparison

The FEA plots show that the Von-Mises stress (Figure 7A-B) and displacement (Figure 7C-D) increased with a decrease in mandibular body height. The same applies when the miniplate was lowered from the mandibular upper border towards the lower border along the fracture line (Figure 7). The maximum Von-Mises stress location at any selected stress point was similar in both simulation software (Figure 6). Furthermore, Figure 8 shows the 200 N displacement comparisons between the FEA and polymeric model testing, where displacement increased with a decrease in mandibular body height. Both the FEA simulations and polymeric model testing illustrated a similar pattern: a decrease in height resulted in an increase in displacement (Figure 8). Finally, the FEA

outcomes were similar and highly comparable with those from the polymeric model testing.

Discussion

According to the literature, FEA has been a promising applicable tool in OMF surgery to analyse different types of fracture management and osteosynthesis implants [20-24, 35]. The outcomes of our study are consistent with some of the data that can be found in the literature. According to Tams et al. plate positioning is a crucial factor for mandibular fracture fixation stability [9]. Lowering the plate along the fracture line from the mandibular upper border toward the lower border decreases the fracture fixation stability. Therefore, locating the plate on the upper border results in better stability, even with small plates. Based on Champy et al., upper border plate placement is based on the fact that mastication creates a tensile force in the upper border and a compression force at the lower border resulting in the closure of the fracture (Figure 5) [8]. This study's FEA simulation results are similar, whereby the Von-Mises stress and displacement increase when the plate is moved along the fracture line from the upper border towards the lower border of the mandibular body (Table 1, Figure 7).

According to Ellis et al. and Gerbino et al., the mandibular body height significantly affects fracture fixation stability [36-37]. A decrease in mandibular height increases fracture fixation instability [38]. It is more difficult to achieve fixation stability with a miniplate in the atrophic mandible than in cases with a normal mandibular height. In terms of stability, it means that a miniplate that does well in slightly or moderately atrophied mandibles (18 or 14 mm height) and performs poorly in severely atrophic mandibles (10 mm) (Table 2). The literature suggests several solutions for instability in the management of mandibular fractures with decreased height: e.g. thicker plates and/or more screws at each side of the fracture [36-38].

We used the polymeric model testing method to verify the FEA simulation outcomes. They both showed that displacement increases when the mandibular body height decreases (Table 3, Figure 8). This is in line with the literature [5, 8, 37] and the current clinical observation. This suggests that both FEA studies are good models for analysing mandibular fractures. Furthermore, the polymeric model testing outcomes indicate that using a 6-hole miniplate is not sufficient for lower mandibular height fracture management. It is plausible that a 4-hole miniplate would have performed even worse in

this case. Therefore, 10 mm or lower mandibular height fracture fixation requires a stronger osteosynthesis system. In this case, the load-sharing principle is not valid and the load-bearing principle should be applied [6-7].

There are some limitations regarding the polymeric model testing. Namely, only displacement outcomes in the Z-axis (the same direction as the applied force) could be compared between the polymeric tests and the FEA studies. This is because the mechanical test bench used in this study could only calculate the displacement as the output result. Furthermore, the displacement values between the FEA studies compared to polymeric model testing were not exactly similar (Table 3) due to: (1) the shape of mandibles (the geometrical shapes of the polymeric models were similar to human mandibles, whereas the FEA mandibles were simplified models to eliminate mesh errors, (2) FEA uses numerical simulation to calculate the amount of displacement. However, on the mechanical test bench, displacement was measured based on the movement of the loading bar from the predetermined zero position to the end position where the mandible fractured or fixation failed. Nevertheless, the displacement results from the FEA studies and polymeric model testing are highly comparable (Table 3, Figure 8).

Finally, our FEA and polymeric model testing outcomes are similar and comparable with earlier studies [1-9, 19]. The similar displacement patterns of the FEA and polymeric model testing, together

with the comparability with earlier studies [6-9, 36-38], show that our study was conducted correctly.

The outcomes of the 3D simulation software programs were similar and comparable (Table 1 and 2) including stress and displacement patterns (Figure 6 and 7). This indicates that the FEA setup and outcomes are reproducible and correct. The minor differences in the Solidworks and Comsol outcome values are caused by the inherent differences in the computational calculations in the 3D simulation environments of both software.

Currently we are working on improving our current mandible model by developing a 3D computer model based on the exact geometrical shape of the mandible instead of using a simplified version, as we did in this study. An approachable method for 3D mandible modelling is being designed based on CT images. We believe that the FEA approach could significantly help the surgeon by giving a better understanding of the preferred fracture management regime via creating a 3D visualisation of the fracture, guiding towards an optimal reposition approach and enabling the selection of the most suitable fixation technique. Regarding complex fracture cases (e.g. comminuted or atrophic mandibles), FEA could be applied to design a patient-specific osteosynthesis system. To achieve this, we are analysing other types of mandibular fractures (e.g. angle, symphysis or parasymphysis) based on the FEA simulation and polymeric model testing validation. The model should help the surgeon to optimise mandibular fracture treatment, thereby improving the surgical practice and the clinical outcome. It is possible the same FEA methodology ap-

Table 3. Polymeric model testing displacement at 200 N compared to FEA displacement

Mandibular body height [mm]	Test number	Displacement [mm]		
		Polymeric model Testing	Solidworks (FEA)	Comsol (FEA)
18	I	3.85		
	II	3.46		
	III	3.28		
	<i>Mean</i>	<i>3.53</i>	<i>4.30</i>	<i>4.31</i>
14	I	4.26		
	II	3.74		
	III	5.09		
	<i>Mean</i>	<i>4.36</i>	<i>5.12</i>	<i>5.16</i>
10	I	4.49		
	II	5.68		
	III	5.93		
	<i>Mean</i>	<i>5.37</i>	<i>8.76</i>	<i>8.85</i>

All the test numbers (Test Number I-III) were done under the same conditions as miniplate located on the mandibular upper border. Italics: the mean polymeric model displacement (average test I-III) compared to the FEA study's displacement values.

proach can be used for optimisation of other bone fractures. However, extensive model testing is necessary to validate whether FEA can be used to test other kinds of fracture management. Such studies could determine whether FEA alone is sufficient to optimise surgical fracture management.

This is achieved by evaluating the biomechanical behaviour between the plate and the fracture (e.g. stress, displacement, and forces). Further, FEA provides a clear visualisation of what could be expected in terms of fracture stability.

Conclusions

This study illustrates that FEA is a promising applicable tool for simulating various types of fractures and fixation systems in OMF surgery. It can be applied in the clinical setting for fracture management. FEA can provide clinicians with a lot of information regarding the selection of suitable osteosynthesis and the positioning of the plate concerning fracture fixation stability.

Funding

None.

Conflicts of interest

None.

References

1. Gareb B, Roossien CC, van Bakelen NB, Verkerke GJ, Vissink A, Bos RRM, et al. Comparison of the mechanical properties of bio-degradable and titanium osteosynthesis systems used in oral and maxillofacial surgery. *Sci Rep*. 2020;10(1):18143. Available from: <http://www.ncbi.nlm.nih.gov/pubmed/33097757>
2. Payan Y, Chabanas M, Pelorson X, Vilain C, Levy P, Luboz V, et al. Biomechanical models to simulate consequences of maxillofacial surgery. *C R Biol*. 2002;325(4):407-17. Available from: <https://linkinghub.elsevier.com/retrieve/pii/S1631069102014439>
3. Wong RCW, Tideman H, Merckx MAW, Jansen J, Goh SM, Liao K. Review of biomechanical models used in studying the biomechanics of reconstructed mandibles. *Int J Oral Maxillofac Surg*. 2011;40(4):393-400. Available from: <https://linkinghub.elsevier.com/retrieve/pii/S0901502710005217>
4. Buijs GJ, van Bakelen NB, Jansma J, de Visscher JGAM, Hoppenreijts TJM, Bergsma JE, et al. A randomized clinical trial of bio-degradable and titanium fixation systems in maxillofacial surgery. *J Dent Res*. 2012;91(3):299-304. Available from: <http://journals.sagepub.com/doi/10.1177/0022034511434353>
5. Bohner L, Beiglböck F, Schwipper S, Lustosa R, Pieirna Marino Segura C, Kleinheinz J, et al. Treatment of mandible fractures using a miniplate system: a retrospective analysis. *J Clin Med*. 2020;9(9):2922. Available from: <https://www.mdpi.com/2077-0383/9/9/2922>
6. Haerle F, Champy M, Terry BC. Atlas of craniomaxillofacial osteosynthesis. Second. Haerle F, Champy M, Terry BC, Reinhardt A, editors. Stuttgart: Georg Thieme Verlag; 2009. Available from: <http://www.thieme-connect.de/products/ebooks/book/10.1055/b-002-72255>
7. Prein J, Ehrenfeld M, Manson PN. Principles of internal fixation of the craniomaxillofacial skeleton. Ehrenfeld M, Manson PN, Prein J, editors. Stuttgart: Georg Thieme Verlag; 2012. Available from: <http://www.thieme-connect.de/products/ebooks/book/10.1055/b-002-85491>
8. Champy M, Lodde JP. [Mandibular synthesis. Placement of the synthesis as a function of mandibular stress]. *Rev Stomatol Chir Maxillofac*. 1976;77(8):971-6. Available from: <http://www.ncbi.nlm.nih.gov/pubmed/1071237>
9. Tams J, van Loon J-P, Otten E, Rozema FR, Bos RRM. A three-dimensional study of bending and torsion moments for different fracture sites in the mandible: an in vitro study. *Int J Oral Maxillofac Surg*. 1997;26(5):383-8. Available from: <https://linkinghub.elsevier.com/retrieve/pii/S090150279780803X>
10. Franciosi E, Mazzaro E, Larranaga J, Rios A, Picco P, Figari M. Treatment of edentulous mandibular fractures with rigid internal fixation: case series and literature review. *Craniomaxillofac Trauma Reconstr*. 2014;7(1):35-41. Available from: <http://journals.sagepub.com/doi/10.1055/s-0033-1364195>
11. Batbayar EO, Bos RRM, van Minnen B. A treatment protocol for fractures of the edentulous mandible. *J Oral Maxillofac Surg*. 2018;76(10):2151-60. Available from: <https://linkinghub.elsevier.com/retrieve/pii/S027823911830329X>

12. Brucoli M, Boffano P, Romeo I, Corio C, Benech A, Ruslin M, et al. Surgical management of unilateral body fractures of the edentulous atrophic mandible. *Oral Maxillofac Surg.* 2020;24(1):65-71. Available from: <http://link.springer.com/10.1007/s10006-019-00824-8>
13. Goh BT, Lee S, Tideman H, Stoelinga PJW. Mandibular reconstruction in adults: a review. *Int J Oral Maxillofac Surg.* 2008;37(7):597-605. Available from: <https://linkinghub.elsevier.com/retrieve/pii/S0901502708000933>
14. Emam HA, Ferguson HW, Jatana CA. Management of atrophic mandible fractures: an updated comprehensive review. *Oral Surg.* 2018;11(1):79-87. Available from: <https://onlinelibrary.wiley.com/doi/10.1111/ors.12300>
15. Sukegawa S, Kanno T, Masui M, Sukegawa-Takahashi Y, Kishimoto T, Sato A, et al. A retrospective comparative study of mandibular fracture treatment with internal fixation using reconstruction plate versus miniplates. *J Cranio-Maxillofac Surg.* 2019;47(8):1175-80. Available from: <https://linkinghub.elsevier.com/retrieve/pii/S101051821830204X>
16. Sittitavornwong S, Denson D, Ashley D, Walma DC, Potter S, Freind J. Integrity of a single superior border plate repair in mandibular angle fracture: a novel cadaveric human mandible model. *J Oral Maxillofac Surg.* 2018;76(12):2611.e1-2611.e8. Available from: <https://linkinghub.elsevier.com/retrieve/pii/S0278239118308504>
17. Huang CM, Chan MY, Hsu JT, Su KC. Biomechanical analysis of subcondylar fracture fixation using miniplates at different positions and of different lengths. *BMC Oral Health* 2021;21(1):543. Available from: <https://bmcoralhealth.biomedcentral.com/articles/10.1186/s12903-021-01905-5>
18. Trainotti S, Raith S, Kesting M, Eichhorn S, Bauer F, Kolk A, et al. Locking versus nonlocking plates in mandibular reconstruction with fibular graft – a biomechanical ex vivo study. *Clin Oral Investig.* 2014;18(4):1291-8. Available from: <http://link.springer.com/10.1007/s00784-013-1105-1>
19. Hart RT, Hennebel V V., Thongpreda N, Van Buskirk WC, Anderson RC. Modeling the biomechanics of the mandible: A three-dimensional finite element study. *J Biomech.* 1992 ;25(3):261-86. Available from: <https://linkinghub.elsevier.com/retrieve/pii/002192909290025V>
20. Anthrayose P, Nawal RR, Yadav S, Talwar S, Yadav S. Effect of revascularisation and apexification procedures on biomechanical behaviour of immature maxillary central incisor teeth: a three-dimensional finite element analysis study. *Clin Oral Investig.* 2021;25(12):6671-9. Available from: <https://link.springer.com/10.1007/s00784-021-03953-1>
21. Patussi C, Sassi LM, Cruz R, Klein Parise G, Costa D, Rebellato NLB. Evaluation of different stable internal fixation in unfavorable mandible fractures under finite element analysis. *Oral Maxillofac Surg.* 2019;23(3):317-24. Available from: <http://link.springer.com/10.1007/s10006-019-00774-1>
22. Limjeerajarus N, Dhammayannarangsri P, Phaniijiva A, Tangsripongkul P, Jearanaiphaisarn T, Pittayapat P, et al. Comparison of ultimate force revealed by compression tests on extracted first premolars and FEA with a true scale 3D multi-component tooth model based on a CBCT dataset. *Clin Oral Investig.* 2020;24(1):211-20. Available from: <http://link.springer.com/10.1007/s00784-019-02919-8>
23. Merema BBJ, Kraeima J, Glas HH, Spijkervet FKL, Witjes MJH. Patient – specific finite element models of the human mandible: Lack of consensus on current setups. *Oral Dis.* 2021;27(1):42-51. Available from: <https://onlinelibrary.wiley.com/doi/10.1111/odi.13381>
24. Lisiak-Myske M, Marciniak D, Bieliński M, Sobczak H, Garbacewicz Ł, Drogoszewska B. Application of finite element analysis in oral and maxillofacial surgery – a literature review. *Materials (Basel)* 2020;13(14):3063. Available from: <https://www.mdpi.com/1996-1944/13/14/3063>
25. Daas M, Dubois G, Bonnet AS, Lipinski P, Rignon-Bret C. A complete finite element model of a mandibular implant-retained overdenture with two implants: Comparison between rigid and resilient attachment configurations. *Med Eng Phys.* 2008;30(2):218-25. Available from: <https://linkinghub.elsevier.com/retrieve/pii/S1350453307000379>
26. Ammar HH, Ngan P, Crout RJ, Mucino VH, Mukdadi OM. Three-dimensional modeling and finite element analysis in treatment planning for orthodontic tooth movement. *Am J Orthod Dentofac Orthop.* 2011;139(1):e59-71. Available from: <https://linkinghub.elsevier.com/retrieve/pii/S0889540610008061>
27. Novelli G, Sconza C, Ardito E, Bozzetti A. surgical treatment of the atrophic mandibular fractures by locked plates systems: our experience and a literature review. *Cranio-maxillofac Trauma Reconstr.* 2012;5(2):65-74. Available from: <http://journals.sagepub.com/doi/10.1055/s-0031-1300961>
28. Schupp W, Arzdorf M, Linke B, Gutwald R. Biomechanical testing of different osteosynthesis systems for segmental resection of the mandible. *J Oral Maxillofac Surg.* 2007;65(5):924-30. Available from: <https://linkinghub.elsevier.com/retrieve/pii/S0278239107001279>

29. Kumar S, Sankhla B, Garg A, Dagli N, Gattumeedhi S, Ingle E. Comparative evaluation of bite forces in patients after treatment of mandibular fractures with miniplate osteosynthesis and internal locking miniplate osteosynthesis. *J Int Soc Prev Community Dent.* 2014;4(4):26. Available from: <http://www.ijspcd.org/text.asp?2014/4/4/26/144575>
30. Brown AD, Walters JB, Zhang YX, Saadatfar M, Escobedo-Diaz JP, Hazell PJ. The mechanical response of commercially available bone simulants for quasi-static and dynamic loading. *J Mech Behav Biomed Mater.* 2019;90:404-16. Available from: <https://linkinghub.elsevier.com/retrieve/pii/S1751616118307458>
31. Park Y-C, Chae D-S, Kang K-Y, Ding Y, Park S-J, Yoon J. Comparative pull-out performances of cephalomedullary nail with screw and helical blade according to femur bone densities. *Appl Sci.* 2021;11(2):496. Available from: <https://www.mdpi.com/2076-3417/11/2/496>
32. Haug RH, Peterson GP, Goltz M. A biomechanical evaluation of mandibular condyle fracture plating techniques. *J Oral Maxillofac Surg.* 2002;60(1):73-80. Available from: <https://linkinghub.elsevier.com/retrieve/pii/S0278239102346408>
33. Bredbenner TL, Haug RH. Substitutes for human cadaveric bone in maxillofacial rigid fixation research. *Oral Surgery, Oral Med Oral Pathol Oral Radiol Endodontology* 2000;90(5):574-80. Available from: <https://linkinghub.elsevier.com/retrieve/pii/S1079210400094610>
34. Aymach Z, Nei H, Kawamura H, Bell W. Biomechanical evaluation of a T-shaped miniplate fixation of a modified sagittal split ramus osteotomy with buccal step, a new technique for mandibular orthognathic surgery. *Oral Surgery, Oral Med Oral Pathol Oral Radiol Endodontology* 2011;111(1):58-63. Available from: <https://linkinghub.elsevier.com/retrieve/pii/S1079210410002052>
35. Park B, Jung BT, Kim WH, Lee J-H, Kim B, Lee J-H. The stability of hydroxyapatite/Poly-L-lactide fixation for unilateral angle fracture of the mandible assessed using a finite element analysis model. *Materials (Basel)* 2020;13(1):228. Available from: <https://www.mdpi.com/1996-1944/13/1/228>
36. Ellis E, Price C. Treatment protocol for fractures of the atrophic mandible. *J Oral Maxillofac Surg.* 2008;66(3):421-35. Available from: <https://linkinghub.elsevier.com/retrieve/pii/S0278239107019453>
37. Gerbino G, Cocis S, Roccia F, Novelli G, Canzi G, Sozzi D. Management of atrophic mandibular fractures: An Italian multicentric retrospective study. *J Cranio-Maxillofacial Surg [Internet].* 2018;46(12):2176-81. Available from: <https://linkinghub.elsevier.com/retrieve/pii/S1010518218301963>
38. Sugiura T, Yamamoto K, Murakami K, Kawakami M, Kang Y-B, Tsutsumi S, et al. Biomechanical Analysis of miniplate osteosynthesis for fractures of the atrophic mandible. *J Oral Maxillofac Surg.* 2009;67(11):2397-403. Available from: <https://linkinghub.elsevier.com/retrieve/pii/S0278239108015127>

An echocardiographic tool for the interatrial conduction disorders – old dog, new tricks?

Jacek Marcin Zawadzki¹ , Jacek Jerzy Gajek² , Agnieszka Sławuta³ ,
Dariusz Kozłowski⁴ , Gabriel Zaborniak⁵, Bartosz Kudliński¹ 

¹ Department of Anesthesia, Critical Care and Emergency Medicine, University of Zielona Góra, Poland

² Faculty of Medicine, Wrocław University of Science and Technology, Poland

³ Department of Cardiology, Kłodzko County Hospital, Kłodzko, Poland

⁴ Department of Cardiology and Electrotherapy, Medical University of Gdańsk, Poland

⁵ Faculty of Mathematics, Informatics and Econometrics, University of Zielona Góra, Poland

Abstract

Background: Bachmann's bundle plays a crucial role in the physiology of interatrial signal conduction. In the 1970s, Bayes de Luna introduced the definition of interatrial blocks (IABs), which negatively influence atrioventricular (AV) synchrony and left atrial (LA) activation. We aimed to assess the potential of LA strain technology in evaluating the mechanics of LA in patients with correct conduction and IABs. Additionally, we measured the parameters of regurgitation in pulmonary veins (PV), which depend on the type of interatrial conduction. **Material and methods:** The study group comprised 51 patients (26 male, 25 female) with symptomatic COVID-19 and sinus rhythm. Our study analyzed their medical history, electrocardiography (ECG) and echocardiography, including the LA strain parameters. **Results:** Global peak atrial longitudinal strain (PALS) depended on P-wave duration, LA volume, left ventricular ejection fraction (LVEF) and inferior pulmonary veins (PV) regurgitation parameters. Global peak atrial contractile strain (PACS) statistically depends on the LVEF, LA volume and the P-wave morphology. **Conclusions:** The presence of IABs negatively influences PACS and PALS. Examining LA strain is complementary to accurate ECG, which may be helpful in everyday clinical practice, particularly in diagnosing heart failure with preserved ejection fraction (HFpEF) and as a predictor of new episodes of atrial fibrillation (AF).

Keywords: Bachmann's bundle · LA strain · echocardiography · ECG · P-wave

Citation

Zawadzki JM, Gajek JJ, Sławuta A, Kozłowski D, Zaborniak G, Kudliński B. An echocardiographic tool for the interatrial conduction disorders – old dog, new tricks? Eur J Transl Clin Med. 2023;6(2):26-35.

DOI: [10.31373/ejtcmed/177894](https://doi.org/10.31373/ejtcmed/177894)

Corresponding author:

Jacek Marcin Zawadzki, Department of Anesthesia, Critical Care and Emergency Medicine, University of Zielona Góra, Poland

e-mail: jacekzawadzki@gumed.edu.pl

Available online: www.ejtcmed.gumed.edu.pl

Copyright © Medical University of Gdańsk

This is Open Access article distributed under the terms of the Creative Commons Attribution-ShareAlike 4.0 International.



Introduction

The activation of atria physiologically starts from the sinus node, then spreads across the right atrium (RA) and simultaneously turns to the left atrium (LA) [1]. Bachmann's bundle plays a crucial role in the interatrial conduction because it is the only physiological pathway of the impulse to the LA [2]. The correct LA activation is directly connected with its correct contraction profile, i.e. mechanical function. This fact is also of great importance in the efficient filling of LV [3]. When the atrium contracts, some blood volume naturally flows back into the pulmonary veins (PV) without valves as they enter LA. The natural way of reducing that regurgitant flow is the activity of the circular fibers around the PV inlets which clench with LA contraction, thus reducing their diameter [4]. The other significant problem is the impairment of atrioventricular synchrony, which may result in developing heart failure (HF), usually with preserved ejection fraction (HFpEF) [5]. This issue touches mainly the LV due to the higher pressure necessary for efficient filling [6]. In this regard, the most dangerous subtype of the IABs should be the advanced interatrial conduction block (A-IAB). Typically, in this case, the roof of the LA is blocked for the approaching impulses [7]. This means the impulses spread through alternative pathways that are also visible in the ECG recording (Figure 1-2). Our goal was to assess the potential of LA strain technology in evaluating the mechanics of the LA in patients with correct conduction and IABs. Additionally, we measured the parameters of PV, which depend on the type of interatrial conduction.

Material and methods

Our study group consisted of 51 unselected patients (26 male, 25 female) hospitalized due to COVID-19 in the University Hospital in Zielona Góra. The inclusion criterion for the study group was the presence of sinus rhythm at the moment of examination. In contrast, the exclusion criteria were: presence of any other rhythm, valvular heart disease, eGFR < 30 ml/min/1.73 m², malignant tumor, decreased hemoglobin level (< 11 mg/dL), autoimmune disease and thyroid disease. We assessed each patient's history, laboratory tests, electrocardiography (ECG) and echocardiography. The used the Tele ECG device (Biomedical Instruments Co., Ltd., Shenzhen, China) to record 12-lead ECGs at the paper speed of 200 mm/s, with an enhancement x256. Full-size vector graphics of the ECG recordings were used during the interpretation. The IABs were divided as suggested by Bayes de Luna: by the specific morphology of the P-wave in leads II, III and aVF (Figure 1) [8-9]. The first group of patients (Group 1) had ECG recordings with

regular and positive P-waves, with < 120 ms duration or the amplitude > 0,1 mV [10]. Group 2 had ECGs with prolonged and flattened P-waves, which seems to be typical for atria with damaged structure e.g. due to fibrotic changes. Group 3 had ECGs with positive/negative P-wave morphology. In groups 2 and 3 the duration of P-waves was > 120 ms.

We used the Arietta 65 ultrasound system (FujiFilm Corporation, Tokyo, Japan) to assess the LA volume, left ventricular ejection fraction (LVEF), mitral regurgitation (MR) and PALS in different phases. In addition, we evaluated the speed and pressure of the regurgitant flow through the PV.

We conducted the study from September 2021 to March 2022 and it was approved by the local Bioethical Committee in Zielona Góra (Number 17/153/2021).

Statistical analysis

The study depicted patient characteristics through box and mean plots, while the relationships between variables were illustrated in scatter plots with regression curves and confidence intervals. The quantitative analysis involved a regression model, Pearson's correlation coefficient, Fisher's exact test and Student's t-test for group mean comparisons. Additionally, relationships between variables were validated using the analysis of covariance.

Results

The baseline characteristics of the patients who qualified for our study group are presented in Figure 3. Among most common comorbidities were: arterial hypertension (n = 36; 70.6%), diabetes mellitus 2 (n = 21; 41.2%), heart failure (n = 12; 23.5%), ischemic heart disease (n = 12; 23.5%), paroxysmal atrial fibrillation (n = 11; 21.6%), chronic obstructive pulmonary disease (n = 7; 13.7%), obesity (n = 5; 9.8%), asthma (n = 3; 5.9%), chronic kidney disease (n = 2; 3.9%).

The statistically significant data in Table 1 are divided into groups depending on the P-wave morphology. There was a statistically significant correlation between age, LV ejection fraction, LA volume, PALS, PACS and the P-wave morphology. The rest of the data and correlations are presented in Figure 4. Statistical significance exists between PALS and the inferior PV regurgitation flow parameters. LV ejection fraction and LA volume are also directly dependent on PALS.

Figure 5 shows the Scatterplot of observed PALS values against the predicted values based on all independent parameters that are statistically significant. The scatterplot indicates a sufficiently good fit of the model to the meas-

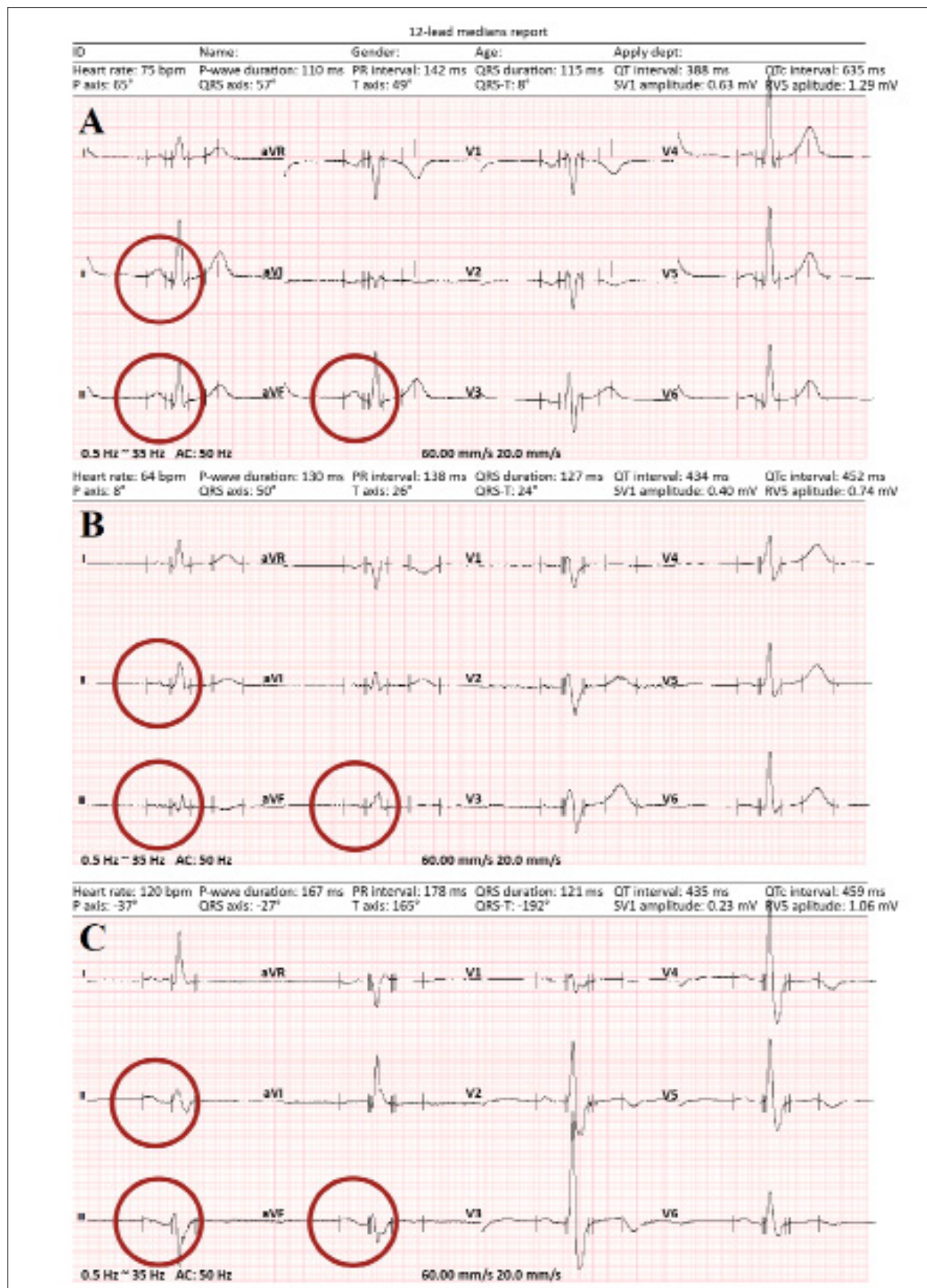


Figure 1. ECG recordings showing different P-wave morphologies

A – normal P-wave morphology; B – prolonged P-wave; C – the full Bachmann's bundle block reflected by positive/negative P-wave morphology. The recording was done by the means of raster graphics, with the following parameters: 60 mm/s and 20 mm/mV.

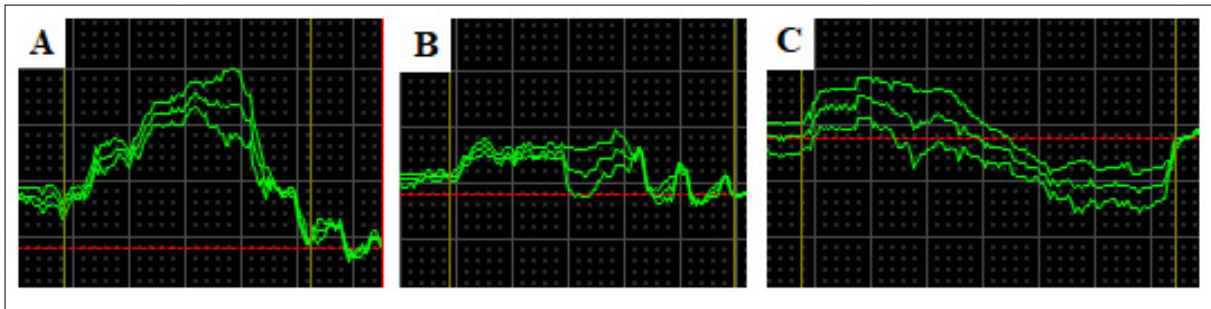


Figure 2. The same ECG recordings as in Figure 1 registered using fully scalable vector graphics. The accuracy of measurements is significantly higher than in Figure 1.

Table 1. Statistical significance of patients' characteristics depends on the P-wave morphology

Variable	P-wave morphology			P-value
	Normal	Prolonged	Bachmann's block	
P-wave duration (ms)	124.4 ± 15.2	138.5 ± 10.4	141.7 ± 19.7	0.007
Age (years)	63.8 ± 12.2	66.3 ± 14.2	73.6 ± 11.2	0.034
PALS (%)	12.5 ± 3.9	20.0 ± 12.2	19.6 ± 8.1	< 0.001
PACS (%)	16.9 ± 4.1	9.6 ± 6.0	9.3 ± 5.1	< 0.001
LVEF (%)	52.9 ± 9.6	43.4 ± 10.4	38.2 ± 10.9	< 0.001
LA volume (ml)	27 [19-31]	42 [34-45]	30 [21-45]	< 0.001

ured values. Similarly, Figure 6 shows the PACS scatterplot, independently correlated with LA volume.

An analysis of covariance, which was done based on nominal variables and quantitative variables in the presence of confounding variables, was another approach that shows exciting trends. We treated PALS as a dependent variable, while the presence of mitral regurgitation was an independent variable and LVEF was the confounding value. The results are presented in Table 2.

Based on Table 2, we state that at the $p = 0.001$ level, the null hypothesis (no significant effect of the LVEF variable on the PALS variable) should be rejected. In other words, the LVEF variable significantly affects the PALS variable. At the significance level of $p = 0.044$, the second null hypothesis (no effect of mitral regurgitation on PALS) should be rejected. Therefore, PALS depends significantly on the presence or absence of the mitral reverse flow, as supported by Figure 7.

Based on the presented results, we state that PALS is related to P-wave duration, LVEF and mitral reverse flow. Inter-

estingly, PACS seems to depend on the P-waves' morphology (Figure 8).

Abnormal P-wave indicated the presence of an A-IAB (advanced interatrial conduction block) or a P-IAB (partial interatrial conduction block). In the investigation of the correlation between hypertension and left atrial parameters (PALS and PACS), two-sample t-tests were employed. For PALS, the test yielded a non-significant result ($t = 0.39403$; $P\text{-value} = 0.6955$), suggesting a statistically not significant difference in the mean between groups with and without hypertension. Similarly, for PACS the t-test result ($t = -0.90182$; $P\text{-value} = 0.3722$) supports the absence of a significant difference in means between the two groups. Additionally, Fisher's exact test indicated a significant association between hypertension and interatrial block (IAB) ($P\text{-value} = 0.04098$, odds ratio = 4.43, 95% CI:0.93-25.13), highlighting a statistically relevant relationship, suggesting that individuals with hypertension are approximately 4.43 times more likely to have experienced an interatrial block (IAB).

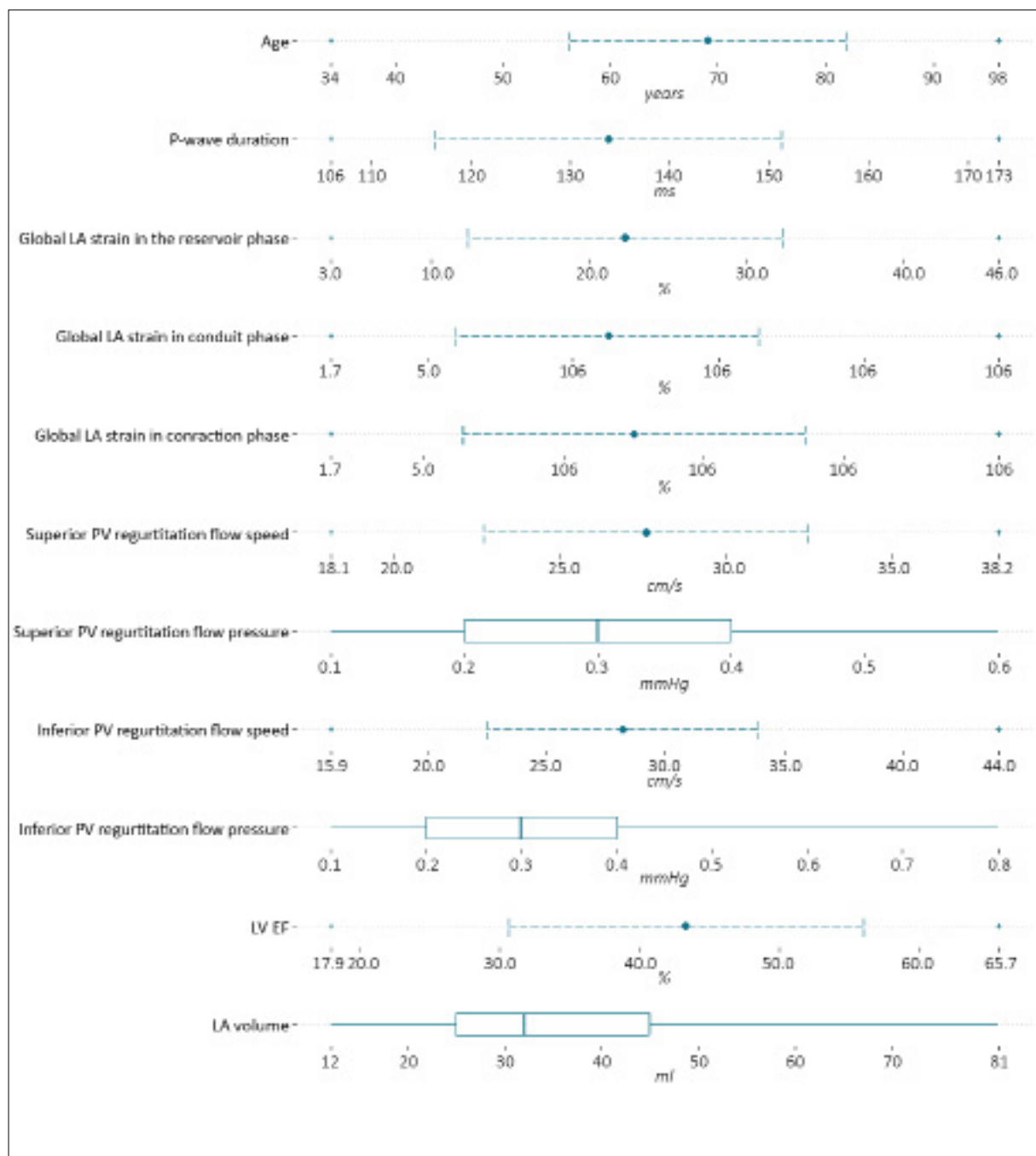


Figure. 3 The baseline characteristics of patients included in the study

Discussion

The critical material of our discussion should be focused on the fact that speckle tracking (LA strain) technology is complementary to accurate electrocardiographic assessment, which we proved in our research. Moreover, our results support the thesis that interatrial blocks affect interatrial synchrony and influence the mechanic synchrony of LA contraction.

Among the most critical correlations in our study, the parameters are directly dependent on the P-wave morphology (Table 1). P-wave morphology and LA volume (Figure 4) correlated with PALS. PALS is measured in LA early diastole, meaning that the diastolic function is worse in case of abnormal P-wave morphology. It is well-known that the structurally damaged atrium has poor signal conduction, resulting in altered P-wave morphology and a poor diastolic function. This correlation corresponds to the observations made by Kosma-

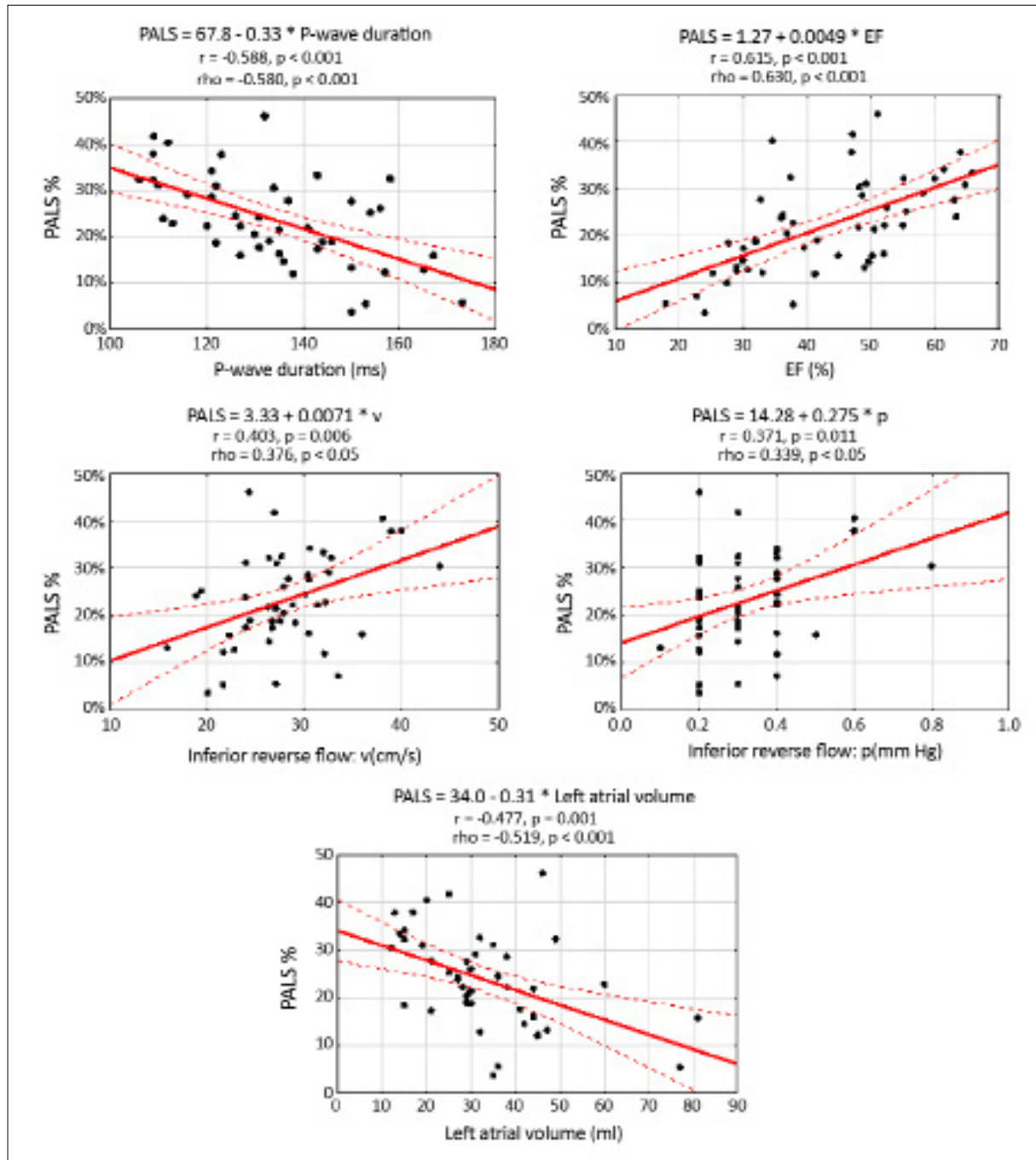


Figure 4. Graphs of PALS scattering depend on the P-wave duration, LVEF, velocity and pressure in the regurgitant flow in the inferior pulmonary veins (Pearson's correlation coefficients and the simple regression analysis)

la in his research published in 2020 [11]. The authors measured PALS, PACS and LA volume index (LAVI), which turned out to be the most predictive parameters for AF in the future. It was stated that the higher risk for AF was mainly connected to the lower LA strain values. The study was very interesting, showing the potential of echocardiographic tools. However, the authors didn't touch on the meaning of the P-wave morphologies, which prompted us to conduct our research.

The P-wave morphology is very important in this matter, as Bayes de Luna stated in his definition of "Bayes Syndrome" [12-13]. The point was that the presence of A-IAB is a strong predictor for new episodes of AF in patients with heart failure.

In our study, PALS and PACS correlated with the P-wave morphology, proving that the decreased atrial contraction is connected to the abnormal P-wave morphology. It should be remembered that the differences between PALS and PACS

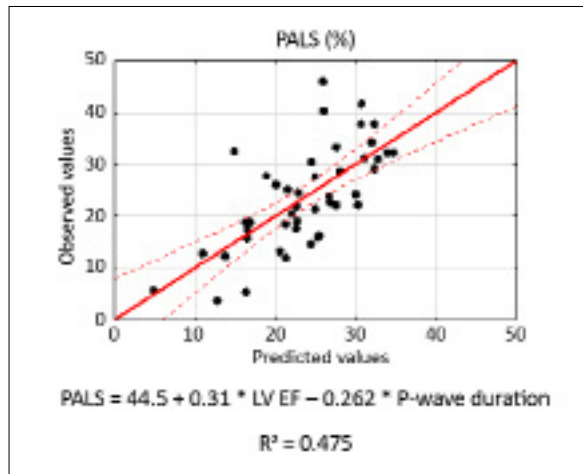


Figure 5. Scatterplot of observed PALS values against the predicted values

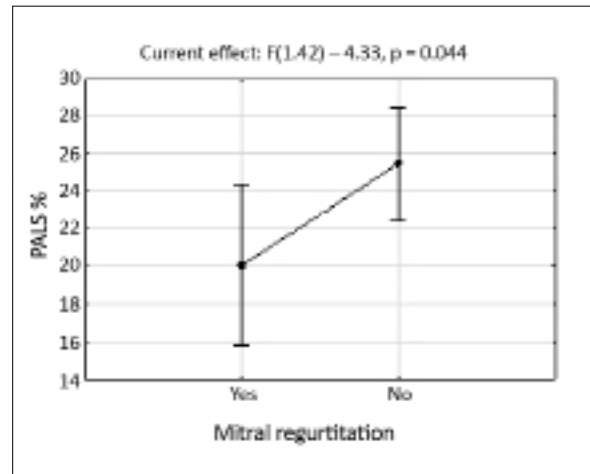


Figure 7. The graphic presentation of the results acquired from the analysis of covariance

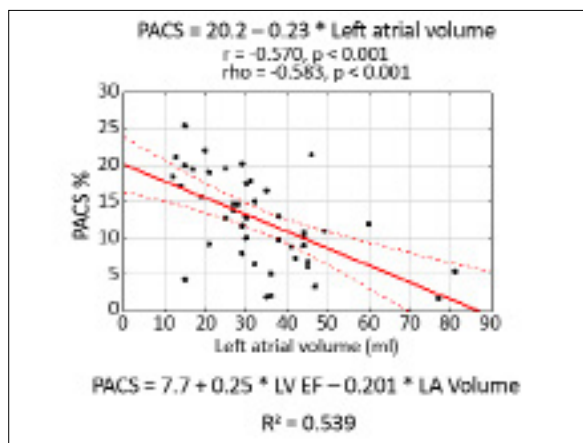


Figure 6. Scatterplot of PACS values against the LA volume

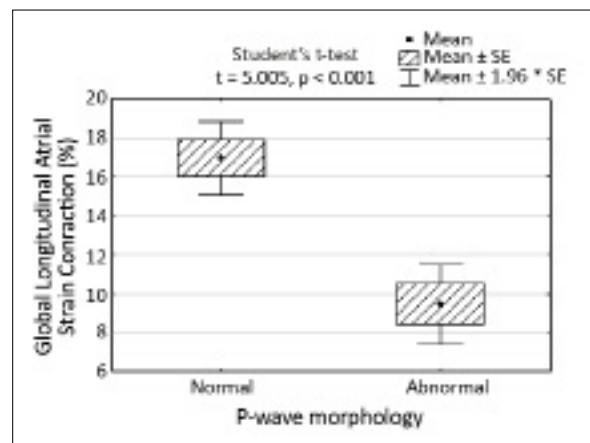


Figure 8. Correlation between PALS and the morphology of the P-wave regarding whether it is normal or abnormal

Table 2. The results of an analysis of covariance for PALS

Effect	SS	df	MS	F	P-value
Constant	67.5	1	67.5	1.03	0.315
EF	927.5	1	927.5	14.2	0.001
Mitral backflow	283.0	1	283.0	4.33	0.044
Error	2743.4	42	65.3		

Df – degrees of freedom (represent the number of independent values or observations available for estimating parameters or testing hypotheses; F – F-statistic (the ratio of variances used to test the hypothesis of equality among group means); MS – mean square (obtained by dividing the sum of squares by its corresponding degrees of freedom; p-value (indicates the probability of obtaining the observed F-statistic or a more extreme value if the null hypothesis is true); SS – sum of squares (represents the variability in the data)

versus P-wave morphology was significant only between normal and abnormal P-wave morphologies, i.e. normal P-wave versus any IAB (Figure 8). This tendency requires further research by quantitative LA regional strain.

Watanabe was close to this idea by presenting an exciting approach using the phenomenon of LA mechanic dispersion in his study in 2015 [14]. This term was defined as the SD of the time to the top of the regional strain curves. The measurements were corrected by RR interval. LA mechanical dispersion was supposed to determine the alterations in synchrony of LA contraction; however, similarly to Kosmala, the research did not mention the morphology of the P-wave and did not directly measure the order of the separate LA regions' contraction. This combined, complicated approach remains an open question for future research.

One of our aims was to examine the correlation between LA functional parameters and the parameters of PV regurgitant flow. Figure 4 shows there was a strong statistical dependence between PALS and the velocity and pressure in the inferior PV. Unfortunately, we haven't found any literature touching this problem, which makes our findings novel in this field and requires more detailed research. There was also another potential relation, which we had to analyze to remain as objective as possible: the connection between mitral regurgitation and the regurgitant flow in PV. It turned out there was no significant correlation between these two variables. We found more elaborate explanations for this fact in research published by Mark et al. [15]. The authors stated: "(...) it is unlikely that mitral regurgitation jet direction per se causes predictable and selective unilateral alteration in pulmonary vein flow patterns."

Focusing on PALS and PACS, we also defined the independent factors influencing these parameters. For example, as presented in Figure 5, PALS directly depends on LVEF and P-wave duration, with a sufficiently good coefficient R². When it comes to the analysis of covariance, it turned out that the presence of mitral regurgitation also correlated with PALS independently. In his study, Stassen found that PALS was associated with the severity of mitral regurgitation, which directly supports our findings [16]. The authors focused on patients with more than mild (grade ≥ 2) secondary MR.

PACS was also dependent on the LVEF and the other significant parameter was LA volume with a sufficiently good coefficient R². Most of the publications focus on the relationship between PALS and LV diastolic dysfunction in terms of HFpEF, which has been growing very popular. [17-19]. The reason for that is the assessment of LA enlargement, which is one of the diagnostic criteria in the definition of HF and LA strain turns out to be a promising new tool [20]. This means the discussion about PACS's meaning in patients with HFpEF and HFrEF is still open and requires more attention.

The IABs

To understand the complete perspective, we should discuss the phenomenon of interatrial blocks. Bayes de Luna first described and introduced the definition of interatrial blocks (IABs) in his research in 1979 [7-8]. The slowdown of the signal characterizes the partial block (P-IAB) of the Bachmann's bundle spread through the roof of the left atrium. It is problematic because the atria are physiologically connected by the Bachmann's bundle, which blends in with the muscular tissue of LA in the region of the LA roof [21-22]. This kind of block is observed in ECG as a prolonged, often double-peaked P-wave [23]. The peaks depict the activation of RA and LA, respectively, which means there is a delay between these activations. It is also common that the P-wave is flat in the case of P-IAB. The reasons for the low amplitude of the P-wave in P-IAB are the structural damage of atrial muscular tissue or the presence of additional activation connected with many electric currents spreading across LA. The multiple currents act against each other, resulting in a flat resultant of the P-wave [24]. The optional breakthrough spot between LA and RA may be located in the foramen ovale or the coronary sinus [25].

In the case of A-IAB, the roof of LA is blocked, which means that the impulses spread anteriorly and inferiorly around the blocked roof. This activation profile is followed by the caudocranial activation of the LA roof and the area between PV [26]. In ECG, this phenomenon is reflected by positive/negative P-wave morphology. The positive component reflects the contraction of RA, while the negative part depicts the caudocranial activation of LA.

Interestingly, the optional, pathologic ways of conduction may be present in both P-IAB and A-IAB. An argument supporting this statement is the fact that only normal vs. abnormal P-wave morphology was statistically significant regarding LA contraction strain. The subtypes of IAB aren't statistically significant between each other in this regard, according to the results of our research. The only important factor for PACS was the existence of any IAB (Figure 8). This fact requires further examination with an assessment of LA regional strain.

Clinical implications

Our findings may be clinically applied in improved diagnostics of the new onsets of AF in the future. The decreased LA strain in connection with abnormal P-wave morphology is evidence of asynchronous LA contraction, which increases the likelihood of AF in the future. Also, the decreased function of LA may be a component of HFpEF development and diagnosis.

Study limitations

Among significant study limitations, we enumerate a relatively small study group and the lack of other literature that could serve as a reference or a comparison. The acquired values were difficult to interpret or discuss without additional scientific support. This fact, however, makes our study one of the first to discuss this topic. The other limitation was the presence of acute COVID-19, the main comorbidity among patients in our study. We are unaware of how it influenced the results. Some publications indicate that COVID-19 per se could negatively affect the conduction and development of IABs [27]. It also means that the infection could have a negative impact on LA strain values. In future research, we plan to confront these findings with patients without COVID-19.

Conclusions

The presence of IABs influences PACS and PALS negatively, i.e., the mechanic function of LA is decreased. PALS statistically correlates with the P-wave duration, LVEF, LA volume and mitral regurgitation. At the same time, PACS is statistically dependent on the LVEF, LA volume and the P-wave morphology. Examining LA strain is complementary to an accurate ECG interpretation, which may be helpful in everyday clinical practice.

Conflicts of interest

None to report.

Funding

Not applicable.

References

1. Ramanathan C, Jia P, Ghanem R, Ryu K, Rudy Y. Activation and repolarization of the normal human heart under complete physiological conditions. *Proc Natl Acad Sci USA* [Internet]. 2006;103(16):6309-14. Available from: <http://www.ncbi.nlm.nih.gov/pubmed/16606830>
2. van Campenhout MJH, Yaksh A, Kik C, de Jaegere PP, Ho SY, Allessie MA, et al. Bachmann's Bundle. *Circ Arrhythmia Electrophysiol* [Internet]. 2013;6(5):1041-6. Available from: <https://www.ahajournals.org/doi/10.1161/CIRCEP.113.000758>
3. Pagel PS, Kehl F, Gare M, Hettrick DA, Kersten JR, Warltier DC. Mechanical function of the left atrium: new insights based on analysis of pressure-volume relations and Doppler echocardiography. *Anesthesiology* [Internet]. 2003;98(4):975-94. Available from: <http://www.ncbi.nlm.nih.gov/pubmed/12657862>
4. Aktan İkiz ZA, Üçerler H, Özgür T. Anatomic characteristics of left atrium and openings of pulmonary veins. *Anadolu Kardiyol Derg* [Internet]. 2014;14(8):674-8. Available from: <http://www.ncbi.nlm.nih.gov/pubmed/25188756>
5. Lavanya K, Mgbemena ON, Keim SG. Atrio-Ventricular Dyssynchrony After Cardiac Resynchronization Therapy: An Unusual Contributor to Heart Failure Symptoms. *Cureus* [Internet]. 2023;15(3): e35661. Available from: <https://www.cureus.com/articles/112036-atrio-ventricular-dyssynchrony-after-cardiac-resynchronization-therapy-an-unusual-contributor-to-heart-failure-symptoms>
6. Pasipoularides A. Right and left ventricular diastolic pressure-volume relations: a comprehensive review. *J Cardiovasc Transl Res* [Internet]. 2013;6(2):239-52. Available from: <http://www.ncbi.nlm.nih.gov/pubmed/23179133>
7. Bayes de Luna AJ. [Block at the auricular level]. *Rev Esp Cardiol* [Internet]. 1979;32(1):5-10. Available from: <http://www.ncbi.nlm.nih.gov/pubmed/441485>
8. Bayés de Luna A, Baranchuk A, Alberto Escobar Robledo L, Massó van Roessel A, Martínez-Sellés M. Diagnosis of interatrial block. *J Geriatr Cardiol* [Internet]. 2017;14(3):161-5. Available from: <http://www.ncbi.nlm.nih.gov/pubmed/28592957>
9. Bayés de Luna A, Platonov P, Cosio FG, Cygankiewicz I, Pastore C, Baranowski R, et al. Interatrial blocks. A separate entity from left atrial enlargement: a consensus report. *J Electrocardiol* [Internet]. 2012;45(5):445-51. Available from: <http://www.ncbi.nlm.nih.gov/pubmed/22920783>
10. Alexander B, Haseeb S, van Rooy H, Tse G, Hopman W, Martinez-Selles M, et al. Reduced P-wave Voltage in Lead I is Associated with Development of Atrial Fibrillation in Patients with Coronary Artery Disease. *J Atr Fibrillation* [Internet]. 2017;10(4):1657. Available from: <http://www.ncbi.nlm.nih.gov/pubmed/29487682>

11. Jasic-Szpak E, Marwick TH, Donal E, Przewlocka-Kosmala M, Huynh Q, Gozdzik A, et al. Prediction of AF in Heart Failure With Preserved Ejection Fraction: Incremental Value of Left Atrial Strain. *JACC Cardiovasc Imaging* [Internet]. 2021;14(1):131-44. Available from: <http://www.ncbi.nlm.nih.gov/pubmed/33413883>
12. Baranchuk A, Alexander B, Cinier G, Martinez-Selles M, Tekkesin AI, Elousa R, et al. Bayés' syndrome: Time to consider early anticoagulation? *North Clin Istanbul* [Internet]. 2018;5(4):370-8. Available from: <http://www.ncbi.nlm.nih.gov/pubmed/30815636>
13. Escobar-Robledo LA, Bayés-de-Luna A, Lupón J, Baranchuk A, Moliner P, Martínez-Sellés M, et al. Advanced interatrial block predicts new-onset atrial fibrillation and ischemic stroke in patients with heart failure: The "Bayes' Syndrome-HF" study. *Int J Cardiol* [Internet]. 2018;271:174-80. Available from: <https://linkinghub.elsevier.com/retrieve/pii/S0167527318310192>
14. Watanabe Y, Nakano Y, Hidaka T, Oda N, Kajihara K, Tokuyama T, et al. Mechanical and substrate abnormalities of the left atrium assessed by 3-dimensional speckle-tracking echocardiography and electroanatomic mapping system in patients with paroxysmal atrial fibrillation. *Hear Rhythm* [Internet]. 2015;12(3):490-7. Available from: <http://www.ncbi.nlm.nih.gov/pubmed/25485778>
15. Mark JB, Ahmed SU, Kluger R, Robinson SM. Influence of jet direction on pulmonary vein flow patterns in severe mitral regurgitation. *Anesth Analg* [Internet]. 1995;80(3):486-91. Available from: <http://www.ncbi.nlm.nih.gov/pubmed/7864412>
16. Stassen J, Namazi F, van der Bijl P, van Wijngaarden SE, Kamperidis V, Marsan NA, et al. Left Atrial Reservoir Function and Outcomes in Secondary Mitral Regurgitation. *J Am Soc Echocardiogr* [Internet]. 2022;35(5):477-485.e3. Available from: <http://www.ncbi.nlm.nih.gov/pubmed/35074443>
17. Nagueh SF, Smiseth OA, Appleton CP, Byrd BF, Dokainish H, Edvardsen T, et al. Recommendations for the Evaluation of Left Ventricular Diastolic Function by Echocardiography: An Update from the American Society of Echocardiography and the European Association of Cardiovascular Imaging. *J Am Soc Echocardiogr* [Internet]. 2016;29(4):277-314. Available from: <http://www.ncbi.nlm.nih.gov/pubmed/27037982>
18. Kapłon-Cieślicka A, Kupczyńska K, Dobrowolski P, Michalski B, Jaguszewski MJ, Banasiak W, et al. On the search for the right definition of heart failure with preserved ejection fraction. *Cardiol J* [Internet]. 2020;27(5):449-68. Available from: <http://www.ncbi.nlm.nih.gov/pubmed/32986238>
19. Santos ABS, Kraigher-Krainer E, Gupta DK, Claggett B, Zile MR, Pieske B, et al. Impaired left atrial function in heart failure with preserved ejection fraction. *Eur J Heart Fail* [Internet]. 2014;16(10):1096-103. Available from: <http://www.ncbi.nlm.nih.gov/pubmed/25138249>
20. Ponikowski P, Voors AA, Anker SD, Bueno H, Cleland JGF, Coats AJS, et al. 2016 ESC Guidelines for the diagnosis and treatment of acute and chronic heart failure: The Task Force for the diagnosis and treatment of acute and chronic heart failure of the European Society of Cardiology (ESC) Developed with the special contribution of. *Eur Heart J* [Internet]. 2016;37(27):2129-200. Available from: <http://www.ncbi.nlm.nih.gov/pubmed/27206819>
21. Platonov PG. Interatrial conduction in the mechanisms of atrial fibrillation: from anatomy to cardiac signals and new treatment modalities. *Europace* [Internet]. 2007;9 Suppl 6:vi10-6. Available from: <http://www.ncbi.nlm.nih.gov/pubmed/17959684>
22. Cabrera JA, Sánchez-Quintana D. Cardiac anatomy: what the electrophysiologist needs to know. *Heart* [Internet]. 2013;99(6):417-31. Available from: <https://heart.bmj.com/lookup/doi/10.1136/heartjnl-2011-301154>
23. de Luna AB, Massó-van Roessel A, Robledo LAE. The Diagnosis and Clinical Implications of Interatrial Block. *Eur Cardiol* [Internet]. 2015;10(1):54-9. Available from: <http://www.ncbi.nlm.nih.gov/pubmed/30310424>
24. Frydas A, Morris DA, Belyavskiy E, Radhakrishnan A-K, Kropf M, Tadic M, et al. Left atrial strain as sensitive marker of left ventricular diastolic dysfunction in heart failure. *ESC Hear Fail* [Internet]. 2020;7(4):1956-65. Available from: <http://www.ncbi.nlm.nih.gov/pubmed/32613770>
25. Chhabra L, Devadoss R, Chaubey VK, Spodick DH. Interatrial block in the modern era. *Curr Cardiol Rev* [Internet]. 2014;10(3):181-9. Available from: <http://www.ncbi.nlm.nih.gov/pubmed/24827803>
26. Ramdat Misier NL, van Schie MS, Li C, Oei FBS, van Schaagen FRN, Knops P, et al. Epicardial high-resolution mapping of advanced interatrial block: Relating ECG, conduction abnormalities and excitation patterns. *Front Cardiovasc Med* [Internet]. 2023;9. Available from: <https://www.frontiersin.org/articles/10.3389/fcvm.2022.1031365/full>
27. Russo V, Marano M, Nigro G. Watch the P wave in COVID-19 patients: the interatrial block. *J Cardiovasc Med (Hagerstown)* [Internet]. 2021;22(12):e51. Available from: <http://www.ncbi.nlm.nih.gov/pubmed/33534300>

Prevalence of tuberculosis and drug-resistant tuberculosis in tertiary care rural hospital in Gujarat, India: a retrospective study

Reena Ughreja¹, Vaibhav Bhatt¹, Sunny Shah² , Devang Boxa³

¹ Gujarat Technological University, Ahmedabad, Gujarat, India

² B. K. Mody Government Pharmacy College, Rajkot, Gujarat, India

³ Pandit Dindayal Upadhyay Medical College, Rajkot, Gujarat, India

Abstract

Background: *Mycobacterium tuberculosis* causes tuberculosis (TB), the most lethal infectious disease in the world that affects people of all ages. The aim of our study was to estimate the prevalence of TB in the Gujarat state (India). **Material and methods:** This was a retrospective study conducted at the Pandit Dindayal Upadhyay Government Medical Hospital (PDUGMH) in Gujarat between 2018 and 2022. **Results:** A total of 5624 TB notification records were reviewed from the TB & Chest Department of the PDUGMH. 5207 of them reported TB-positive results, majority of which concerned pulmonary TB (57.27%, n = 2982). 3586 (68.87%) of the TB-positive patients were male and 1621 (31.13%) were female. The most group most affected by TB was 15-29 years of age, with a high peak in 2019. Amongst the TB-positive patients, 215 suffered from diabetes and 454 were HIV-positive. Majority of patients with an infected lymph node suffered from extrapulmonary TB. Rifampicin-resistant TB was observed in 0.8% (n = 42) of patients and 3 patients were treated with the longer oral regimen for fluoroquinolone-resistant multi-drug resistant TB (0.1%). **Conclusions:** Our findings indicate that during 2018-2022, patients treated at PDUGMH had a TB prevalence of 92.59%, with a corresponding rate of multidrug-resistant TB standing at 1.48%. A comprehensive study is required to accurately assess the TB burden in India and to guide national strategies for TB eradication.

Keywords: tuberculosis • prevalence • drug resistance • retrospective studies

Citation

Ughreja R, Bhatt V, Shah S, Boxa D. Prevalence of tuberculosis and drug-resistant tuberculosis in tertiary care rural hospital in Gujarat, India: a retrospective study. Eur J Transl Clin Med. 2023;6(2):36-44

DOI: 10.31373/ejtcml/175674

Corresponding author:

Sunny Shah, B. K. Mody Government Pharmacy College, Rajkot, Gujarat, India

e-mail: shah_sunny@gtu.edu.in

Available online: www.ejtcml.gumed.edu.pl

Copyright © Medical University of Gdańsk

This is Open Access article distributed under the terms of the Creative Commons Attribution-ShareAlike 4.0 International.



Introduction

Mycobacterium tuberculosis, an infectious bacterial disease that most frequently affects the lungs but can harm other tissue, is the cause of tuberculosis. *M. tuberculosis* spreads between people through the respiratory system [1]. The global incidence of tuberculosis was 127 per 100000 people [2]. Tuberculosis (TB) is a leading cause of mortality and a global health issue among several mycobacterial illnesses. Based on the World Health Organization's (WHO) annual TB report for 2021, around 9.9 million people are ill with TB, with an anticipated 1.3 million deaths. It necessitates the development of new medicines, as well as improved diagnostics and health-care coverage. The WHO internationally endorsed the directly observed treatment, short course (DOTS) strategy in 1970. It has been acknowledged as a highly efficient and cost-effective technique for tuberculosis control [3]. Furthermore, the End TB strategy by WHO aims for a 95% reduction in TB mortality by the year 2035 [4].

M. tuberculosis is a sessile, noncapsulated, nonspore-forming bacterium which although acid-fast staining, it requires an additional stain (Ziehl Neelsen, ZN). It is because of mycolic acid, which is an unsaponifiable wax. It creates a semipermeable wall surrounding the cell, making it acid-fast. Children are immunized with the Bacillus Calmette-Guerin (BCG) vaccine to protect them from severe forms of TB. Sometimes BCG is advised for adults with drug-resistant TB [5]. Numerous diagnostic techniques are available now for identifying TB, but sputum smear microscopy still is the most common, which is ineffective in cases of medication resistance [6-8].

M. tuberculosis is transmitted via mucous droplets during activities such as coughing, laughing, sneezing, spitting, and even breathing. The infected airborne droplets make their way through the oral and nasal passages, eventually infecting the alveoli of the lungs [9]. Although *M. tuberculosis* typ-

ically infects the lungs and causes pulmonary TB, it can also spread to other bodily areas, including the kidney, spine, and brain, where it can cause extrapulmonary TB [10]. Samples from the respiratory system (e.g. sputum, induced sputum, bronchoalveolar lavage or lung biopsy) are typically analyzed to diagnose pulmonary TB, which is more prevalent. Whereas the extrapulmonary TB can be detected through various samples, including biopsies, urine, pus, aspirates and sterile body fluids (e.g. pleural, abdominal, cerebrospinal, synovial, genitourinary, pericardial and peritoneal fluids). For HIV-positive patients, the diagnosis of extrapulmonary TB will depend on the site of infection. For that, the stool sample is examined for intestinal TB to detect *M. avium* [11-12].

India is among the countries with high burden of TB [13-14]. Whereas the Gujarat state has a moderate case notification rate and in 2021 it achieved a > 20% reduction in TB incidence (received "Bronze" category award). As shown in Figure 1, the data released by TB India revealed that Nikshay-Gujarat stands third in contributing to total TB notification in April, 2020 [15]. TB burden estimation must be carried out annually in order to re-calibrate the state- and district-wide TB strategies.

As a Tertiary Care Institute, the TB and Chest Department of the PDUGMH receives sputum and other body fluid samples from the Rajkot district and 11 other districts to investigate cases of TB infections. The aim of our study was to estimate the prevalence of TB in the Gujarat state (India).

Material and methods

This study was conducted at the PDUGMH in, from where the notification records were collected between January 2018 to December 2022.

Data collection

From TB & Chest Department at PDUGMH (a Tertiary Care Teaching Institute in Rajkot), the TB notification records were gathered. These included patient demographic information such as age, sex, weight, HIV status, diabetes and drug susceptibility test results. The number of patients who died during the treatment was also noted.

Patients

Participants who reported cough lasting 2 weeks or longer, fever, weight loss or night sweats of any duration were catego-

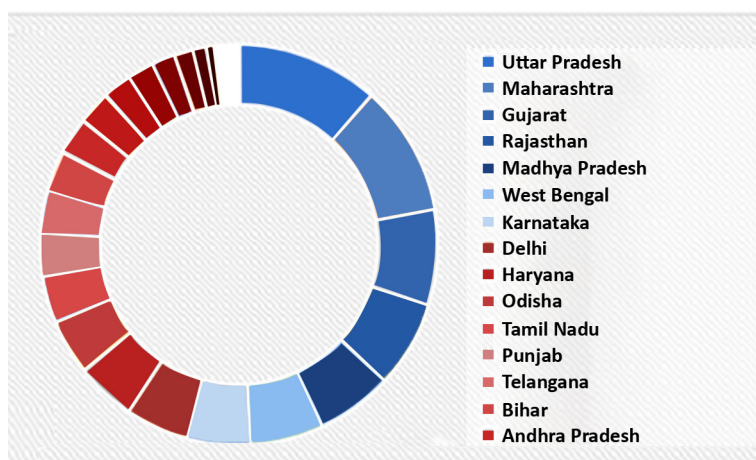


Figure 1. Nikshay-Gujarat stands third in contributing to the total TB notifications in April, 2020

rized as having TB symptoms and their sputum samples were collected. Two sputum samples were gathered: one immediately upon admission and the second on the following morning. The sputum samples were collected in sterile, single-use disposable containers within the PDUGMH laboratory in Rajkot on the same day for testing. The sputum from patients underwent testing for acid fast bacilli (AFB) through smear microscopy using a fluorescent stain. Patients were diagnosed with smear-positive TB if at least one sputum sample tested positive for AFB. The microscopic test employs an exceptionally sensitive microscope, capable of detecting individual live bacilli. The sputum was cultured on Lowenstein-Jensen medium and examined for *M. tuberculosis* growth once a week for eight weeks. A patient was diagnosed with sputum-positive pulmonary TB if found positive through smear and/or culture.

Patients underwent chest X-rays, chest ultrasonography, brain magnetic resonance imaging (MRI) and Cartridge Based Nucleic Acid Amplification Test (CBNAAT) based on their current condition and diagnostic results. For CBNAAT, specimens were transported at 2-8°C to the nearest diagnostic site using

triple packaging. Extrapulmonary TB symptomatic patients had their body fluids (e.g. abdominal fluids, pleural fluids, milary fluids, cerebrospinal fluid, pericardial fluids, genitourinary fluids) examined. Drug susceptibility tests were conducted, categorizing patients into H mono-resistant, H poly-resistant, rifampicin-resistant (RR) TB and longer multidrug-resistant (MDR) regimen cases.

Statistical analysis

The data were analyzed using Excel software (Microsoft, Redmond, WA, USA) and exported to IBM SPSS Statistics, Version 19 (IBM, Armonk, USA) for the descriptive statistics e.g. mean, total, and percent distribution. A Chi-Square statistic was applied to calculate the difference between variables like subject sex and age. The P-value of < 0.05 determined statistical significance. The percentage of resistance was estimated by dividing the total number of resistant isolates detected for a single drug or a combination by the total number of positive TB patients examined.

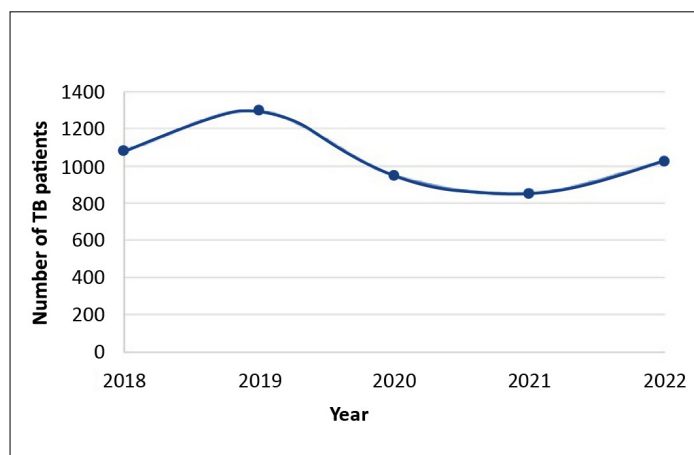


Figure 2. Number of positive TB cases

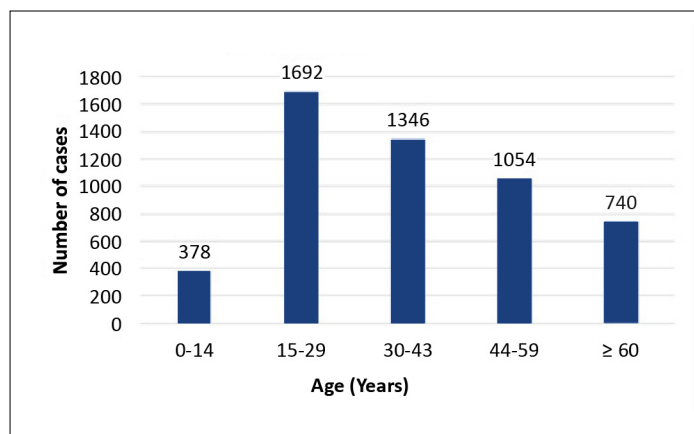


Figure 3. Age-wise distribution of TB-positive cases

Results

A total of 5624 records from January 1st 2018 and December 31st 2022 were examined, with an annual range of 954-1389. Majority of these, (92.58%, n = 5207) contained TB-positive results, with the annual positive rate fluctuating between 89.31% and 96.61%. Notably, there was a dip in the annual rate in 2021, reaching 89.31%. The year 2019 exhibited the highest case count (n = 1297), as visualized in Figure 2. Among the 5207 TB-positive patients, 3,586 (68.87%) were identified as males, while 1621 (31.13%) were females. Within this TB-positive group, 215 (4.13%) patients (mostly male) were diagnosed with diabetes and 454 (8.72%) were HIV-positive. The distribution of patient ages is illustrated in Table 1. When segmented by age, the group of patients were 15-29 years of age (n = 1692), while the lowest number of patients were in the 0-14 age bracket (n = 378), as portrayed in Figure 3.

Among the 5207 TB-positive patients, majority (n = 2982, 57.27%) were pulmonary TB-positive, and 2225 (42.73%) were extrapulmonary TB-positive. Majority of these patients were male, cases, A high prevalence of pulmonary TB and extrapulmonary TB was found in males: n = 2193 and n = 1393, respectively [13], as shown in Figure 4.

Table 1. Age distribution of TB-positive patients of the Pandit Dindayal Upadhyay Government Medical Hospital during 2018-2022

	Number of records (Year)					Total
Age (Years)	2018	2019	2020	2021	2022	
0-14	114	89	63	59	53	
15-29	345	396	345	273	333	
30-43	295	364	249	206	233	
44-59	200	255	183	182	234	
≥ 60	131	196	109	132	172	
Total	1122	1389	1037	954	1122	5624
Positive cases	1084	1297	949	852	1025	5207
Pulmonary tuberculosis						2982 (57.27%)
Extrapulmonary tuberculosis						2225 (42.73%)
Diabetes						215 (4.13%)
HIV-positive						454 (8.72%)

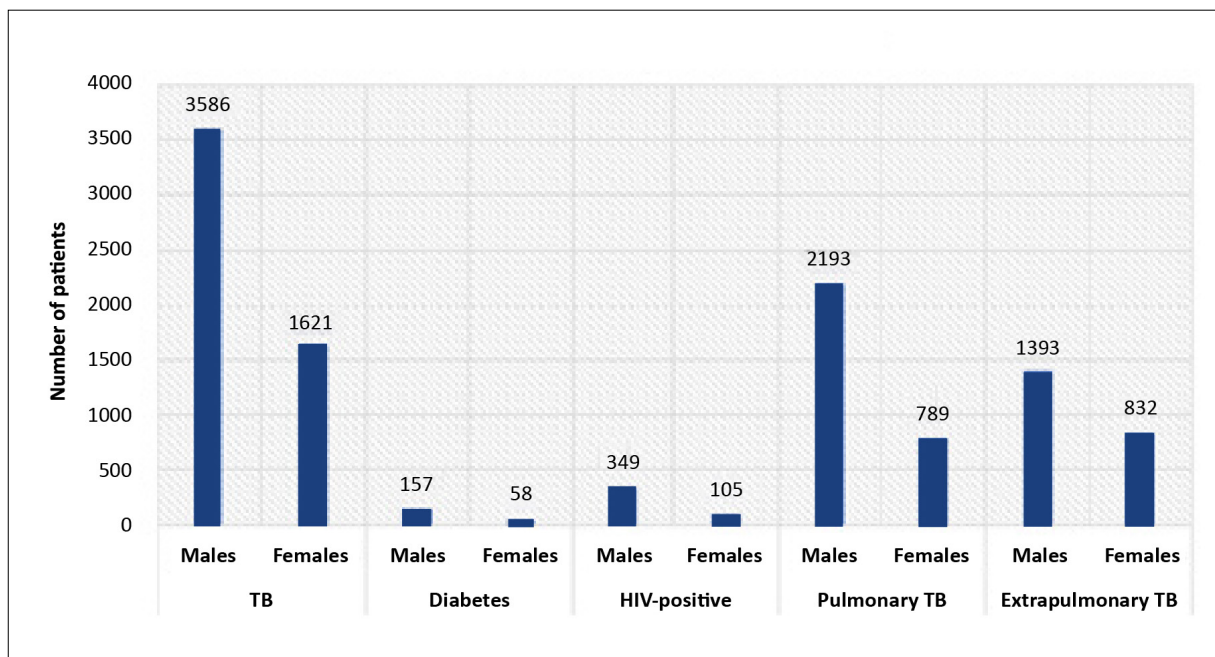


Figure 4. Specific diagnoses of TB-positive patients

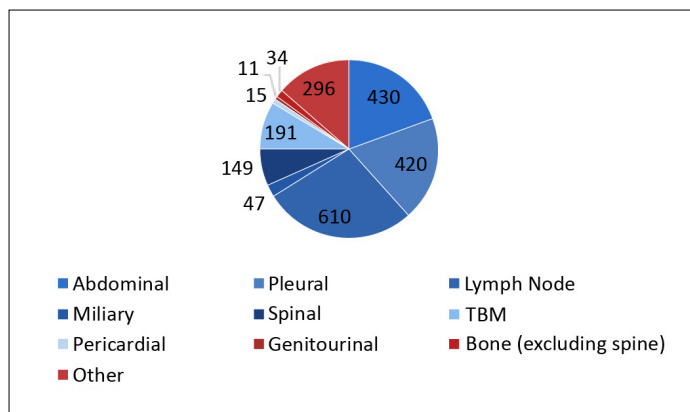


Figure 5. Distribution of extrapulmonary TB cases

Positive pulmonary TB cases were detected through sputum analysis by fluorescent stain microscopy [16]. Positive extrapulmonary TB cases were detected in the abdominal fluid, pleural fluid, lymph node, miliary, spinal fluid, genitourinary fluid, pericardial fluid, TBM, and bone (excluding spine). Apart from these sites, the positive extrapulmonary TB patients were classified as “others”. The highest number of extrapulmonary TB cases were detected through the lymph nodes ($n = 610$) and the least with genitourinary fluid ($n = 11$), as shown in Figure 5.

Among the 5207 TB-positive cultures, 5130 (98.52%) were susceptible to all the TB medications, while 77 (1.48%) were resistant to at least one drug. Of the 77 drug-resistant cultures, most ($n = 42$) were RR-TB cases (Figure 6).

The total of 683 deaths occurred while undergoing treatment, with the lowest count observed in the year 2022 ($n = 97$).

Discussion

This retrospective study aimed to determine the prevalence of TB in a particular region of India and to gauge the incidence of drug-resistant tuberculosis. We found that during the 5-year period (2018-2022), the prevalence of TB among the patients treated at this institute was 92.59%. 2019 was the year with the most remarkable rate of TB positive cases, probably due to the hospital laboratory receiving samples from various districts throughout the year.

Our results also showed males were more frequently infected with TB ($p < 0.05$), both the pulmonary and extrapulmonary presentation, as reported in the WHO's global surveillance report [17] and also seen in other studies [18-19]. The reasons behind this gender difference are behavioural (e.g. the patient's activities, tobacco smoking and alcohol use) and physiological e.g. sex hormones might modulate the immune response required for defending against TB and other infections [20-22].

In some of the published studies pulmonary TB and extrapulmonary TB were found equally often with

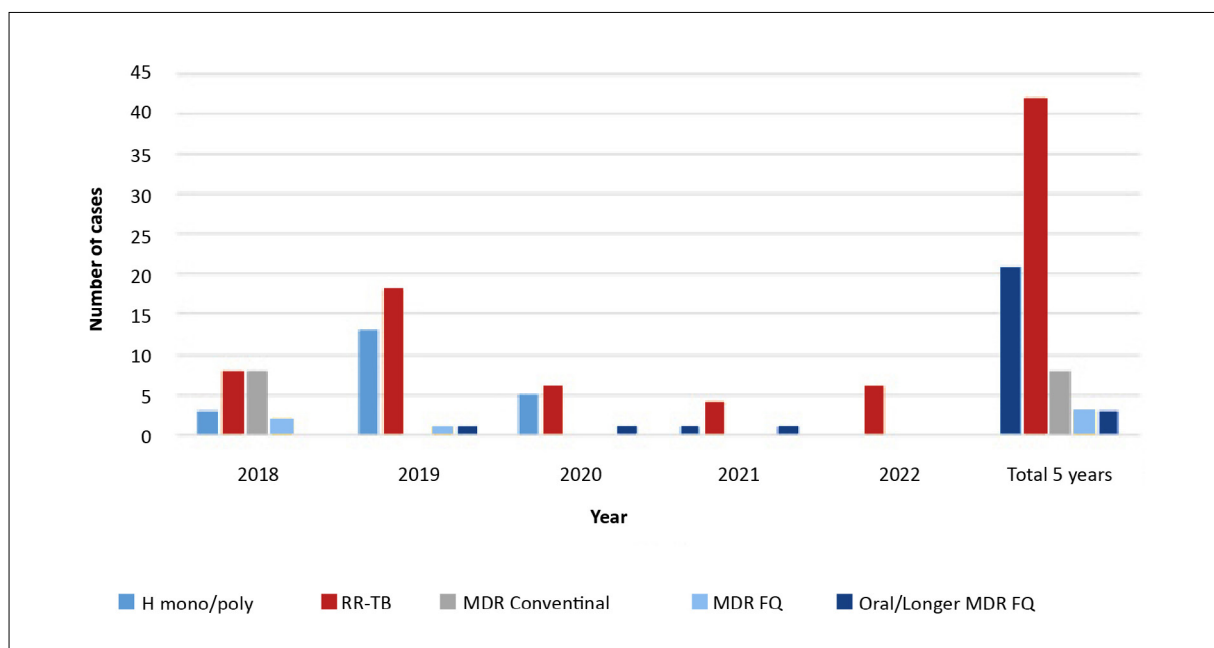


Figure 6. Distribution of drug resistant cases

FQ – fluoroquinolone-resistant, MDR – multidrug-resistant, RR – rifampicin-resistant, TB – tuberculosis

no significant difference ($p > 0.05$) [23-24], which is so seen in the results of the current study. We noted that the majority of pulmonary TB cases were confirmed with microscopy tests, whereas lymph node specimens were the major site for extrapulmonary TB.

A high score of positive TB infection is seen in the group 15-29 years of age ($p < 0.05$). The cause could be attributed to either disregarding the symptoms or delaying the seeking of medical attention upon their emergence. There might be a lack of awareness regarding the high transmission rate of the disease within the patients' own family [25]. The rise in co-morbidities or immunosenescence may also be one of the reasons for the reactivation of latent *M. tuberculosis* infection and the increase in susceptibility to TB disease in older people [26-27].

The rates of drug resistant TB in other regions of India is the subject of several studies [14, 28]. Similar studies are carried out which involved the estimation of trends in TB prevalence in different communities in south India [29-30] and north India [31]. The study conducted in Chennai [30] revealed a high prevalence among individuals aged 55-64 years, whereas we found a high prevalence among those aged 15-29 years which is consistent with the report from the Thiruvallur district of the Tamil Nadu state [32]. A study conducted in northern Indian districts [31] reported a high male representation among the TB-positive cases, which aligns with our own study's findings. Another study showed high TB burden in the states of Delhi and Tamil Nadu [33]. Also a 2005 study showed a comparative TB prevalence in India focusing rural and urban areas [34]. Following these studies, including the current one, there is a significant difference in rates of drug-resistant TB in India.

Furthermore, a study compared TB data from India with the WHO report where there was a decline in TB incidence which were close to estimates published in the recent Global TB report 2022 [35].

Since our study period includes the COVID-19 outbreak (2019), the TB incidence might be affected by the COVID positive cases. The data we collected did not include the COVID-19 results, therefore a correlation cannot be made on the TB positive and COVID positive cases. However, another study reports that there was a rise in May 2020 with peak in August and a decline in October 2020 [36]. Following our data from Table 1, it can be seen that there was a rise in TB positive cases from 2018 to 2019. Then it declined which might be due to the lock-down period from April to July 2020, as seen in a modelling study [35].

As seen in our results and in the literature, the drug resistance rate at the PDUGMH has dramatically decreased over the past five years ($p < 0.05$) [13, 37-39]. Improved compliance brought on by direct witnessed therapy and advancements in TB diagnosis and resistance testing may be responsible for the decline in antibiotic resistance. Among all the TB-positive

resistant cases, the majority of cases were attributed to RR-TB cases.

Limitations

Our study has several limitations, including the fact that we analyzed data from only one center, which does not accurately reflect the demographic structure of the entire nation. The TB notification records do not include data on previous history of TB, therefore we were not able to assess the risk factors for drug-resistant TB. This analysis excluded second-line anti-TB medications and patients for whom complete data were unavailable.

Future perspectives

The overall prevalence of TB in the Gujarat state is low. Still, to understand the deadliness of TB, the pattern of the disease must be monitored periodically to do appropriate planning. Also, details of the patient's history must be recorded, such as the spread of TB, sufficient and balanced nutrition, and cautious handling of ill family members. Healthcare providers must look into the information of patients' close contacts and perform screening, particularly for those having cough, fever, and weight loss and treat them if required.

Conclusion

Among PDUGMH patients, the prevalence of tuberculosis, particularly MDR-TB, is still low. Adult male patients are more likely to contract *M. tuberculosis*. Our findings indicate that men and people over 60 are more likely to have active TB illness. Investigations into India's nation-wide TB prevalence and antibiotic resistance are still needed. More emphasis must be placed on the importance of thorough national and international studies of the risk factors for the emergence of active TB and the treatment of its drug-resistance.

Acknowledgements

The authors thank the Superintendent of the Pandit Dindayal Upadhyay Government Medical Hospital in Rajkot for permitting the collection of data from TB and Chest Department.

Funding

This research did not receive any grant from institutions in the public, commercial or not-for-profit sectors.

Ethical considerations

The study was conducted following the principles described in the Declaration of Helsinki and was approved with a waiver of consent.

Conflicts of interest

None to report.

References

1. Bloom BR, Atun R, Cohen T, Dye C, Fraser H, Gomez GB, et al. Tuberculosis. In: Major Infectious Diseases [Internet]. 3rd ed. World Bank Group; 2017. p. 233-313. Available from: <https://openknowledge.worldbank.org/entities/publication/4699c-561-3dfb-5fad-a3c4-54893fa47014>
2. World health statistics 2022: monitoring health for the SDGs, sustainable development goals [Internet]. World Health Organization. 2022 [cited 2023 Dec 4]. Available from: <https://www.who.int/publications/i/item/9789240051157>
3. Global tuberculosis report 2021 [Internet]. 2021 [cited 2023 Dec 4]. Available from: <https://www.who.int/publications/i/item/9789240037021>
4. Conradie F, Diacon AH, Ngubane N, Howell P, Everitt D, Crook AM, et al. Treatment of Highly Drug-Resistant Pulmonary Tuberculosis. *N Engl J Med* [Internet]. 2020;382(10):893-902. Available from: <https://doi.org/10.1056/NEJMoa1901814>
5. Andersen P, Doherty TM. The success and failure of BCG – implications for a novel tuberculosis vaccine. *Nat Rev Microbiol* [Internet]. 2005;3(8):656-62. Available from: <https://doi.org/10.1038/nrmicro1211>
6. Kik S V, Denkinger CM, Chedore P, Pai M. Replacing smear microscopy for the diagnosis of tuberculosis: what is the market potential? *Eur Respir J* [Internet]. 2014;43(6):1793 LP-1796. Available from: <http://erj.ersjournals.com/content/43/6/1793.abstract>
7. Schumacher SG, Sohn H, Qin ZZ, Gore G, Davis JL, Denkinger CM, et al. Impact of Molecular Diagnostics for Tuberculosis on Patient-Important Outcomes: A Systematic Review of Study Methodologies. Goletti D, editor. *PLoS One* [Internet]. 2016;11(3):e0151073. Available from: <https://dx.plos.org/10.1371/journal.pone.0151073>
8. Lam E, Nateniyom S, Whitehead S, Anuwatnonthakate A, Monkongdee P, Kanphukiew A, et al. Use of drug-susceptibility testing for management of drug-resistant tuberculosis, Thailand, 2004–2008. *Emerg Infect Dis* [Internet]. 2014;20(3):400. Available from: https://wwwnc.cdc.gov/eid/article/20/3/13-0951_article
9. Zevallos M, Justman JE. Tuberculosis in the elderly. *Clin Geriatr Med* [Internet]. 2003;19(1):121-38. Available from: <https://www.sciencedirect.com/science/article/pii/S0749069002000575>
10. Rodriguez-Takeuchi SY, Renjifo ME, Medina FJ. Extrapulmonary Tuberculosis: Pathophysiology and Imaging Findings. *RadioGraphics* [Internet]. 2019;39(7):2023-37. Available from: <https://doi.org/10.1148/rg.2019190109>
11. Drobniewski FA, Caws M, Gibson A, Young D. Modern laboratory diagnosis of tuberculosis. *Lancet Infect Dis* [Internet]. 2003;3(3):141-7. Available from: <https://www.sciencedirect.com/science/article/pii/S1473309903005449>
12. Singh P, Saket VK, Kachhi R. Demethoxycurcumin ameliorates rotenone-induced toxicity in rats. *FBE*. 2019;11(1):38-60.
13. Dhamnetiya D, Patel P, Jha RP, Shri N, Singh M, Bhattacharyya K. Trends in incidence and mortality of tuberculosis in India over past three decades: a joinpoint and age–period–cohort analysis. *BMC Pulm Med* [Internet]. 2021;21(1):375. Available from: <https://doi.org/10.1186/s12890-021-01740-y>
14. Isaakidis P, Das M, Kumar AM V, Peskett C, Khetarpal M, Bamne A, et al. Alarming Levels of Drug-Resistant Tuberculosis in HIV-Infected Patients in Metropolitan Mumbai, India. Tyagi AK, editor. *PLoS One* [Internet]. 2014;9(10):e110461. Available from: <https://dx.plos.org/10.1371/journal.pone.0110461>
15. Ministry of Health and Family Welfare CTD. India TB Report 2023 [Internet]. 2023. Available from: <https://tbcindia.gov.in/showfile.php?id=3680>
16. Masali HT, Takpere A, Shahapur P. A Comparative Study of Ziehl-Neelsen Stain and Fluorescent Stain Microscopy in the Diagnosis of Pulmonary Tuberculosis. *J Pure Appl Microbiol*. 15 (4): 2027-2033, 2021. 2021; Available from: http://103.139.156.196/jspui/bitstream/123456789/4119/1/119_2021.pdf
17. Global Tuberculosis Report 2022 [Internet]. [cited 2023 Dec 4]. Available from: <https://www.who.int/teams/global-tuberculosis-programme/tb-reports/global-tuberculosis-report-2022>
18. Marçõa R, Ribeiro AI, Zão I, Duarte R. Tuberculosis and gender – Factors influencing the risk of tuberculosis among men and women by age group. *Pulmonology* [Internet]. 2018;24(3):199-202. Available from: <https://www.sciencedirect.com/science/article/pii/S2531043718300667>

19. Rhines AS. The role of sex differences in the prevalence and transmission of tuberculosis. *Tuberculosis* [Internet]. 2013;93(1):104-7. Available from: <https://linkinghub.elsevier.com/retrieve/pii/S1472979212001990>
20. Watkins RE, Plant AJ. Does smoking explain sex differences in the global tuberculosis epidemic? *Epidemiol Infect* [Internet]. 2005/08/19.2006;134(2):333-9. Available from: <https://www.cambridge.org/core/article/does-smoking-explain-sex-differences-in-the-global-tuberculosis-epidemic/D87B9C5AE7F2B623225919286C803887>
21. Randall D. Responses of fish to hypoxia. *Comp Biochem Physiol Part C Toxicol Pharmacol* [Internet]. 2008;148(4):461-2. Available from: <https://www.sciencedirect.com/science/article/pii/S1532045608002469>
22. Nhamoyebonde S, Leslie A. Biological Differences Between the Sexes and Susceptibility to Tuberculosis. *J Infect Dis* [Internet]. 2014;209(suppl_3):S100-6. Available from: <https://doi.org/10.1093/infdis/jiu147>
23. Alateah SM, Othman MW, Ahmed M, Al Amro MS, Al Sherbini N, Ajlan HH. A retrospective study of tuberculosis prevalence amongst patients attending a tertiary hospital in Riyadh, Saudi Arabia. *J Clin Tuberc Other Mycobact Dis* [Internet]. 2020;21:100185. Available from: <https://www.sciencedirect.com/science/article/pii/S2405579420300498>
24. Sunnetcioglu A, Sunnetcioglu M, Binici I, Baran AI, Karahocagil MK, Saydan MR. Comparative analysis of pulmonary and extrapulmonary tuberculosis of 411 cases. *Ann Clin Microbiol Antimicrob* [Internet]. 2015;14(1):34. Available from: <https://doi.org/10.1186/s12941-015-0092-2>
25. de Andrade HLP, Gomes D, Ramos ACV, Arroyo LH, Santos-Neto M, Palha PF, et al. Tuberculosis forecasting and temporal trends by sex and age in a high endemic city in northeastern Brazil: where were we before the Covid-19 pandemic? *BMC Infect Dis* [Internet]. 2021;21(1):1260. Available from: <https://doi.org/10.1186/s12879-021-06978-9>
26. Byng-Maddick R, Noursadeghi M. Does tuberculosis threaten our ageing populations? *BMC Infect Dis* [Internet]. 2016;16(1):119. Available from: <https://doi.org/10.1186/s12879-016-1451-0>
27. Murali S, Krishnamoorthy Y, Knudsen S, Roy G, Ellner J, Horsburgh CR, et al. Comparison of profile and treatment outcomes between elderly and non-elderly tuberculosis patients in Puducherry and Tamil Nadu, South India. Quinn F, editor. *PLoS One* [Internet]. 2021;16(8):e0256773. Available from: <https://dx.plos.org/10.1371/journal.pone.0256773>
28. Ramachandran R, Nalini S, Chandrasekar V, Dave P V, Sanghvi AS, Wares F, et al. Surveillance of drug-resistant tuberculosis in the state of Gujarat, India. *Int J Tuberc Lung Dis* [Internet]. 2009;13(9):1154-60. Available from: <http://www.ncbi.nlm.nih.gov/pubmed/19723407>
29. Kolappan C, Subramani R, Radhakrishna S, Santha T, Wares F, Baskaran D, et al. Trends in the prevalence of pulmonary tuberculosis over a period of seven and half years in a rural community in south India with DOTS. *Indian J Tuberc* [Internet]. 2013;60(3):168-76. Available from: <http://www.ncbi.nlm.nih.gov/pubmed/24000495>
30. Dhanaraj B, Papanna MK, Adinarayanan S, Vedachalam C, Sundaram V, Shanmugam S, et al. Prevalence and Risk Factors for Adult Pulmonary Tuberculosis in a Metropolitan City of South India. Tyagi AK, editor. *PLoS One* [Internet]. 2015;10(4):e0124260. Available from: <https://dx.plos.org/10.1371/journal.pone.0124260>
31. Aggarwal AN, Gupta D, Agarwal R, Sethi S, Thakur JS, Anjinappa SM, et al. Prevalence of Pulmonary Tuberculosis among Adults in a North Indian District. Herrmann JL, editor. *PLoS One* [Internet]. 2015;10(2):e0117363. Available from: <https://dx.plos.org/10.1371/journal.pone.0117363>
32. Chadha VK, Kumar P, Anjinappa SM, Singh S, Narasimhaiah S, Joshi M V., et al. Prevalence of Pulmonary Tuberculosis among Adults in a Rural Sub-District of South India. Pai M, editor. *PLoS One* [Internet]. 2012;7(8):e42625. Available from: <https://dx.plos.org/10.1371/journal.pone.0042625>
33. Chauhan A, Parmar M, Dash GC, Solanki H, Chauhan S, Sharma J, et al. The prevalence of tuberculosis infection in India: A systematic review and meta-analysis. *Indian J Med Res* [Internet]. 2023;157(2&3). Available from: https://journals.lww.com/ijmr/fulltext/2023/02000/the_prevalence_of_tuberculosis_infection_in_india_6.aspx
34. Paralkar V. Worlds Apart — Tuberculosis in India and the United States. *N Engl J Med* [Internet]. 2008 Mar 13;358(11):1092-5. Available from: <https://doi.org/10.1056/NEJMp0707933>
35. Mandal S, Rao R, Joshi R. Estimating the Burden of Tuberculosis in India: A Modelling Study. *Indian J Community Med* [Internet]. 2023;48(3). Available from: https://journals.lww.com/ijcm/fulltext/2023/48030/estimating_the_burden_of_tuberculosis_in_india_a.11.aspx
36. Parikh H, Savani N. Effect of COVID-19 on Tuberculosis Care in a District of Western Gujarat. *Indian J Respir Care* [Internet]. 2022;11(4):369-72. Available from: https://www.ijrc.in/doi/10.4103/ijrc.ijrc_105_22
37. Al-Tawfiq JA, Al-Muraikhy AA, Abed MS. Susceptibility Pattern and Epidemiology of Mycobacterium tuberculosis in a Saudi Arabian Hospital: A 15-Year Study From 1989 to 2003. *Chest* [Internet]. 2005;128(5):3229-32. Available from: <https://www.sciencedirect.com/science/article/pii/S0012369215528821>

38. Al-Awaidy ST, Al-Hamdan N. Drug-susceptibility pattern of mycobacterium tuberculosis among pulmonary tuberculosis patients in riyadh, saudi arabia. J Family Community Med [Internet]. 1997;4(2):65-9. Available from: <http://www.ncbi.nlm.nih.gov/pubmed/23008575>
39. Alrajhi AA, Al-Barrak AM. Mycobacterium tuberculosis susceptibility in Saudi Arabia. Saudi Med J [Internet]. 2002;23(10):1227-31. Available from: <http://www.ncbi.nlm.nih.gov/pubmed/12436127>

His bundle pacing in patients with permanent atrial fibrillation and heart failure with non-reduced ejection fraction – retrospective study

Bartosz Skonieczny¹, Agnieszka Sławuta² , Jadwiga Radziejewska³,
Dariusz Jagielski^{1, 4} , Jacek Gajek⁴ , Dariusz Kozłowski⁵ 

¹ Department of Cardiology, Centre for Heart Diseases, 4th Military Hospital, Wrocław, Poland

² Department of Cardiology, Kłodzko County Hospital, Kłodzko, Poland

³ Kłodzko County Hospital, Kłodzko, Poland

⁴ Faculty of Medicine, Wrocław University of Science and Technology, Poland

⁵ Division of Medical Rescue, Institute of Health Sciences, Pomeranian University in Słupsk, Poland

Abstract

Background: Heart failure (HF) constitutes a complex clinical entity and often coexists with atrial fibrillation (AF). There is a scarcity of evidence-based therapies for those with ejection fraction (EF) $\geq 40\%$. The effect restoring regular ventricular response in patients with HF with EF $\geq 40\%$ and concomitant permanent AF is unknown. **Methods:** This was a retrospective case-series study. 14 patients with symptomatic HF with EF $\geq 40\%$ and permanent AF who had undergone permanent His bundle pacing (pHBP) were identified and enrolled. For 9 patients pHBP was a primary strategy, for the remaining patients it was an upgrade from right single chamber ventricular pacing. All patients underwent a follow-up visit 3 months after the procedure. **Results:** The severity of HF based on the New York Heart Association (NYHA) class was significantly reduced post-pHBP (mean 2.5 vs. 1.0, p-value < 0.001). Left ventricular ejection fraction significantly increased (mean increase 8.5%, p < 0.001). Similarly, significant decrease in the left ventricular end-diastolic diameter was observed after pHBP (mean decrease 5.4 mm, p < 0.001). The degree of mitral regurgitation after three months was lower (mean grade 2.4 vs. 1.2, p < 0.001). **Conclusions:** Permanent HBP might be beneficial in the setting of permanent AF and HF with EF $\geq 40\%$.

Keywords: permanent atrial fibrillation • heart failure • His bundle pacing

Citation

Skonieczny B, Sławuta A, Radziejewska J, Jagielski D, Gajek J, Kozłowski D. His bundle pacing in patients with permanent atrial fibrillation and heart failure with non-reduced ejection fraction – retrospective study. Eur J Transl Clin Med. 2023;6(2):45-50

DOI: [10.31373/ejtcmm/177892](https://doi.org/10.31373/ejtcmm/177892)

Corresponding author:

Bartosz Skonieczny, Department of Cardiology, Centre for Heart Diseases, 4th Military Hospital, Wrocław, Poland

e-mail: bartosz.skon@gmail.com

Available online: www.ejtcmm.gumed.edu.pl

Copyright © Medical University of Gdańsk

This is Open Access article distributed under the terms of the Creative Commons Attribution-ShareAlike 4.0 International.



NO APC OA



Introduction

Heart failure (HF) constitutes a complex clinical entity. While there are many drugs and devices with proven benefit for HF with reduced ejection fraction (EF) < 40%, there is a scarcity of evidence for beneficial therapies for those with EF ≥ 40%. European Society of Cardiology (ESC) 2021 guidelines for HF with their 2023 Focused Update contain only one class I recommendation for drug therapy with proven benefit on prognosis: SGLT2 inhibitors [1-2]. As such, treatment of HF with mildly reduced or preserved ejection fraction remains difficult.

Numerous pathophysiological processes can lead to impaired left ventricular (LV) filling, with increased pressure in the pulmonary vascular bed and symptoms of HF regardless of preserved or mildly reduced left ventricular systolic function [3]. The clinical course of HF with preserved EF is commonly further complicated by coexistence of atrial fibrillation (AF). The lack of mechanical function of the atria, in particular of the left atrium, influences negatively the filling of the ventricles increasing the pressure in both venous vascular beds thus contributing to the symptoms of HF. AF contributes furthermore to the development of mitral regurgitation (MR) or exacerbation of the present one which facilitates HF symptoms.

The aim of our study was to assess the influence of permanent His bundle pacing (pHBP) in patients with permanent AF (PAF) and concomitant symptomatic HF with EF ≥ 40%.

Material and methods

Patients were selected and the data were gathered retrospectively from the medical records of the Kłodzko County Hospital. Baseline characteristics were extracted from admission clinical data collected prior to the procedure. Outcomes assessment was based on data collected during first follow-up visit after the device implantation, scheduled 3 months after the implantation.

The study group consisted of 14 patients who have undergone pHBP device implantation due to PAF with slow ventricular conduction or were upgraded from single chamber right ventricular pacing to pHBP. The inclusion criteria were as follows: age >18 years, symptomatic HF with NYHA class II-III, EF ≥ 40%, concomitant PAF, pHBP as part of treatment. All identified eligible patients were enrolled into the study. Written informed consent was given by every patient prior to the device implantation. Local institutional review board approved the study protocol.

Devices and pacing

All patients were provided with pHBP in the course of their therapy. Intrinsic QRS complexes were narrow in all of their electrocardiograms. For 9 patients, a pacemaker (PM) with the pHBP lead was the primary treatment strategy. One received single chamber pacemaker with pHBP lead only. The rest underwent dual chamber PM implantation with the HBP lead connected to atrial channel and RV lead connected to ventricular channel serving as a back-up in case of failure of HBP lead. Five patients had pre-existing single chamber VVI device with RV lead. They underwent an upgrade procedure – implantation of pHBP lead connected to atrial channel. The devices were set into the DDD (VVI in the single case with single chamber device) mode with very low atrial sensitivity level to functionally blind the atrial channel, so that the actual programmed functional mode was DVI. In 9 of them selective HBP was achieved. Whereas in the rest of the patients myocardial activation via nonselective HBP was also noted.

Statistical analysis

Continuous variables were compared with Student's t-test. Ordinal variables, such as mitral regurgitation, were compared with the Wilcoxon signed ranks test. Pearson correlation coefficient was used to assess changes in the left ventricular end-diastolic diameter (LVEDD) and EF values at baseline and after pHBP. All calculations and data analysis were performed using the JASP software (Version 0.13.1, JASP Team, University of Amsterdam). P-value < 0.05 was considered to be statistically significant and all tests were two-tailed.

Results

Baseline characteristics of patients are shown in Table 1. The follow-up visit took place 14.1 ± 4.6 (mean ± standard deviation) weeks after the procedure.

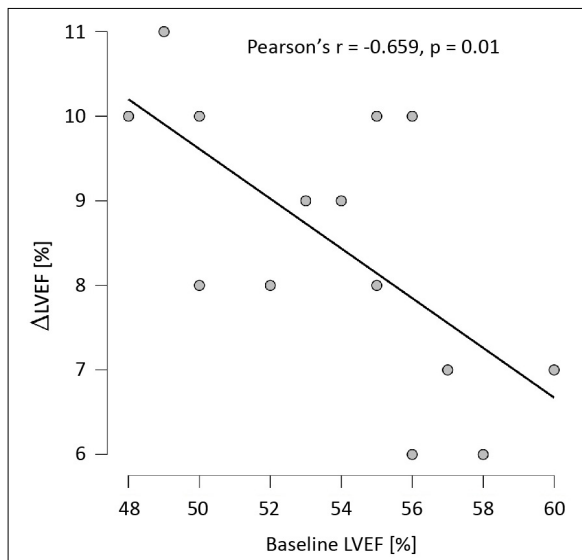
Procedure and pacing details

In 10 patients selective pHBP was achieved and nonselective pHBP in the remaining 4. The mean pHBP percentage, as assessed during the device follow-up, was 82.1% (minimum 66% – maximum 99%).

Table 1. Baseline characteristics

Sex [male:female]	4:10 [ratio]
Age [years]	69 ± 6.2 [mean ± SD]
NYHA [class II:III]	7:7
LVEF [%]	53.8 ± 3.6 (mean ± SD)
LVEDD [mm]	54.4 ± 2.3 (mean ± SD)
Metoprolol equivalent dose [mg]	39.3 ± 16.2 (mean ±)

NYHA – New York Heart Association; LVEF – left ventricular ejection fraction; LVEDD – left ventricular end diastolic diameter

**Figure 1. Scatter plot of baseline LVEF and difference in LVEF at follow-up.**

Outcomes

LVEF significantly increased from the mean 53.8% at baseline to 62.3% at follow-up (mean increase by 8.5%, 95% confidence interval 7.7-9.2, $p < 0.001$). Increase in EF was negatively correlated with the baseline values, as shown in Figure 1. Similarly, significant decrease in LVEDD was observed – from mean 54.4 mm at baseline to 49.6 mm at follow-up (mean decrease by 5.4 mm, 95% confidence interval 5.0-5.8, $p < 0.001$). However, in this case, no correlation between the baseline values and degree of diameter's reduction was observed (Pearson's $r = -0.306$, $p = 0.287$). The degree of MR after three months was lower (mean

grade at the baseline 2.4 vs. 1.2 at follow-up, $p < 0.001$). NYHA class was significantly reduced (mean class 2.5 vs. 1.0 $p < 0.001$). All of these findings are summarized in Table 2. Moreover, at follow-up prescribed doses of beta blocker were higher by 69.6 ± 29.7 (mean ± standard deviation) mg in metoprolol equivalents.

Discussion

AF and HF commonly coexist. This is no surprise as they share the same risk factors. Moreover, they influence each other so one can precede another. HF is the strongest predictor of AF in the future [4]. AF is precipitated by HF in many ways. AF can also affect HF and worsen LV function making this two conditions a vicious circle [5]. Clearly, the loss of atrial contractile function leads to a decrease in global heart contractile function. However, peculiar ventricular response in AF causes some unfavorable phenomena. Tachycardia-induced cardiomyopathy (TCM) is the long recognized clinical entity which was depicted in the setting of AF over 100 years ago [6]. Recently new clinical concept started to emerge: AF induced cardiomyopathy (AFCM) [7]. Basic assumption is that AF can lead to cardiomyopathy and worsening of LV function not only by rapid ventricular response, but due to the irregular rhythm. Clark et al. elegantly showed that irregularity of ventricular rhythm has an adverse impact on hemodynamics, irrespectively of the heart rate [8]. Similar results were observed in a study of patients with HF with reduced EF during biventricular pacing. However, detrimental effects of irregularity were seen only at higher heart rates [9]. Far bigger and clinically more important was the APAF-CRT trial. It involved patients with AF, symptomatic HF and narrow QRS. Patients were randomly assigned to the AV node ablation and biventricular pacing or to the optimal pharmacological rate-control therapy. Most of the trial participants were patients with HF and EF > 35%. That trial demonstrated the superiority of the AV node ablation and BiV pacing over the rate-control approach in matters of combined primary endpoint of death due to HF or hospitalization for HF or worsening of HF. This statistically significant effect was seen also among the patients with EF > 35% [10].

In recent years a few trials demonstrated that sinus rhythm restoration by pulmonary vein isolation (PVI) might be beneficial in HF patients. In 2013 a small, observational study showed augmentation of LV dysfunction following AF ablation, despite optimal medical therapy and well controlled ventricular rate [11]. The CASTLE-AF randomized controlled trial involving HF patients with EF ≤ 35% and AF,

Table 2. Outcomes

	Before pHBP	After pHBP	P-value
LVEF [%]	53.8 (95% CI 52-55.6)	62.3 (95% CI 60.9-63.7)	< 0.001
LVEDD [mm]	54.4 (95% CI 53.3-55.5)	49.6 (95% CI 48.5-50.7)	< 0.001
NYHA class	mean 2.5	mean 1.0	< 0.001
I	0	100% (14/14)	
II	50% (7/14)	0	
III	50% (7/14)	0	
IV	0	0	
MR grade	mean 2.4	mean 1.2	< 0.001
mild	0	80% (11/14)	
moderate	60% (9/14)	20% (3/14)	
severe	40% (5/14)	0	

CI – confidence interval; LVEF – left ventricular ejection fraction; LVEDD – left ventricular end diastolic diameter; MR – mitral regurgitation; NYHA – New York Heart Association; pHBP – permanent His bundle pacing

showed that PVI lowers risk of death and hospitalization for worsening HF compared to the rate control strategy [12]. These two trials were conducted among patients with severely reduced LVEF, however the benefit of PVI in patients with HF and EF > 40% was noted in the post-hoc analysis of the CABANA-AF trial. In the subgroup of patients with an established HF, PVI resulted in improved survival, freedom from AF recurrence and higher quality of life. Most importantly, only 11.7% of population had EF < 40% [13].

As expected, shift in management of AF in HF patients can be seen and in the recent ESC guidelines gave PVI in patients with AF and HF with reduced LVEF has a class IIa recommendation [1]. PVI might be beneficial for patients with HF due to the restoration of atrial contractility, of regular ventricular rhythm or both. Some insights came from the PABA-CHF trial. In this randomized clinical trial, PVI was compared with AV node ablation and biventricular pacing (BiV) in patients with AF and concomitant HF. Results favoured PVI owing to the fact that at follow-up the patients in the PVI arm presented with higher EF and lower Minnesota Living with Heart Failure questionnaire scores [14]. While achieving regularity of ventricular rhythm by means of pacing clearly lacks the potential benefit of restoring

atrial contractile function, nearly half of AF patients have PAF, therefore restoring the sinus rhythm is no longer considered suitable [15]. Moreover, nowadays a revolution in pacing is unfolding – conduction system pacing. Two studies published in 2017 explored role of pHBP in patients with AF and HF who had undergone AV node ablation. Vijayaraman et al. proved pHBP to be feasible in the context of AV node ablation due to symptomatic AF. Echocardiographic improvement was also noted, however driven mainly by the EF < 40% subgroup. Unfortunately, little data on baseline characteristics (e.g. prior rate control) were provided [16]. Huang et al. published the results of a prospective registry in which patients with HF (regardless of EF) and permanent AF with satisfying rate control (mean 83 beats per minute) underwent pHBP and AV node ablation [17]. During follow-up the authors noted improvements in EF, NYHA class and diuretic use in patients with EF ≤ 40% as well as EF > 40% [17]. In accordance with our results, the improvement in EF noted in both aforementioned studies was correlated with baseline EF.

We hypothesize that irregular ventricular response facilitates the worsening of heart function which might be reversed by physiological ventricular pacing achieved by

pHBP. Our results provide further data to support that thesis.

However, we identify serious limitations of our study, e.g. it was a retrospective study on a small population. Data collection was conducted in a non-blinded, unsystematic manner. We couldn't identify data neither on prior rate control nor on QRS duration after pHBP. Percentage of pHBP pacing was far from recommended for BiV percentage.

Conclusions

Our study has shown that patients with HF with EF \geq 40% and concomitant PAF may benefit from restoring regular heart rate with pHBP. All patients had significant clinical

improvement as shown by lower NYHA class. Moreover, LVEF increase in every case, (at least by 7%) and a decrease in LVEDD suggests that the restoration of a regular heart rhythm with narrow QRS reverses adverse LV remodeling. Due to the limitations of our study, more research is needed to draw firm conclusions.

Conflicts of interest

None to report.

Funding

Not applicable.

References

- McDonagh TA, Metra M, Adamo M, Gardner RS, Baumbach A, Böhm M, et al. 2021 ESC Guidelines for the diagnosis and treatment of acute and chronic heart failure: Developed by the Task Force for the diagnosis and treatment of acute and chronic heart failure of the European Society of Cardiology (ESC) With the special contribution. *Eur Heart J* [Internet]. 2021;42(36):3599-726. Available from: <https://doi.org/10.1093/eurheartj/ehab368>
- McDonagh TA, Metra M, Adamo M, Gardner RS, Baumbach A, Böhm M, et al. 2023 Focused Update of the 2021 ESC Guidelines for the diagnosis and treatment of acute and chronic heart failure. *Eur Heart J* [Internet]. 2023;44(37):3627-39. Available from: <https://academic.oup.com/eurheartj/article/44/37/3627/7246292>
- Borlaug BA, Paulus WJ. Heart failure with preserved ejection fraction: pathophysiology, diagnosis, and treatment. *Eur Heart J* [Internet]. 2011;32(6):670-9. Available from: <https://doi.org/10.1093/eurheartj/ehq426>
- Benjamin EJ. Independent Risk Factors for Atrial Fibrillation in a Population-Based Cohort. *JAMA* [Internet]. 1994;271(11):840. Available from: <http://jama.jamanetwork.com/article.aspx?doi=10.1001/jama.1994.03510350050036>
- Maisel WH, Stevenson LW. Atrial fibrillation in heart failure: epidemiology, pathophysiology, and rationale for therapy. *Am J Cardiol* [Internet]. 2003;91(6):2-8. Available from: <https://linkinghub.elsevier.com/retrieve/pii/S0002914902033738>
- Gossage AM, Braxton Hicks JA. On auricular fibrillation. *QJM An Int J Med* [Internet]. 1913;6:435-40. Available from: <https://academic.oup.com/qjmed/article/os6/4/435/1579375/ON-AURICULAR-FIBRILLATION>
- Huizar J, Ellenbogen K, Tan A, Kaszala K. Arrhythmia-Induced Cardiomyopathy. *J Am Coll Cardiol* [Internet]. 2019;73(18):2328-44. Available from: <https://doi.org/10.1016/j.jacc.2019.02.045>
- Clark D, Plumb V, Epstein A, Kay, GN. Hemodynamic Effects of an Irregular Sequence of Ventricular Cycle Lengths During Atrial Fibrillation. *J Am Coll Cardiol* [Internet]. 1997;30(4):1039-45. Available from: [https://doi.org/10.1016/S0735-1097\(97\)00254-4](https://doi.org/10.1016/S0735-1097(97)00254-4)
- Melenovsky V, Hay I, Fetics BJ, Borlaug BA, Kramer A, Pastore JM, et al. Functional impact of rate irregularity in patients with heart failure and atrial fibrillation receiving cardiac resynchronization therapy. *Eur Heart J* [Internet]. 2005;26(7):705-11. Available from: <https://doi.org/10.1093/eurheartj/ehi066>
- Brignole M, Pokushalov E, Pentimalli F, Palmisano P, Chieffo E, Occhetta E, et al. A randomized controlled trial of atrioventricular junction ablation and cardiac resynchronization therapy in patients with permanent atrial fibrillation and narrow QRS. *Eur Heart J* [Internet]. 2018;39(45):3999-4008. Available from: <https://doi.org/10.1093/eurheartj/ehy555>
- Ling L-H, Taylor AJ, Ellims AH, Iles LM, McLellan AJA, Lee G, et al. Sinus rhythm restores ventricular function in patients with cardiomyopathy and no late gadolinium enhancement on cardiac magnetic resonance imaging who undergo catheter ablation for atrial fibrillation. *Hear Rhythm* [Internet]. 2013;10(9):1334-9. Available from: <https://www.sciencedirect.com/science/article/pii/S1547527113006607>

12. Marrouche NF, Brachmann J, Andresen D, Siebels J, Boersma L, Jordaens L, et al. Catheter Ablation for Atrial Fibrillation with Heart Failure. *N Engl J Med* [Internet]. 2018;378(5):417-27. Available from: <https://doi.org/10.1056/NEJMoa1707855>
13. Packer DL, Piccini JP, Monahan KH, Al-Khalidi HR, Silverstein AP, Noseworthy PA, et al. Ablation Versus Drug Therapy for Atrial Fibrillation in Heart Failure. *Circulation* [Internet]. 2021;143(14):1377-90. Available from: <https://doi.org/10.1161/CIRCULATIONAHA.120.050991>
14. Khan MN, Jaïs P, Cummings J, Di Biase L, Sanders P, Martin DO, et al. Pulmonary-Vein Isolation for Atrial Fibrillation in Patients with Heart Failure. *N Engl J Med* [Internet]. 2008;359(17):1778-85. Available from: <https://doi.org/10.1056/NEJMoa0708234>
15. Chiang C-E, Naditch-Brûlé L, Murin J, Goethals M, Inoue H, O'Neill J, et al. Distribution and Risk Profile of Paroxysmal, Persistent, and Permanent Atrial Fibrillation in Routine Clinical Practice. *Circ Arrhythmia Electrophysiol* [Internet]. 2012;5(4):632-9. Available from: <https://doi.org/10.1161/CIRCEP.112.970749>
16. Vijayaraman P, Subzposh FA, Naperkowski A. Atrioventricular node ablation and His bundle pacing. *EP Eur* [Internet]. 2017;19(suppl_4):iv10-6. Available from: <https://doi.org/10.1093/europace/eux263>
17. Huang W, Su L, Wu S, Xu L, Xiao F, Zhou X, et al. Benefits of Permanent His Bundle Pacing Combined With Atrioventricular Node Ablation in Atrial Fibrillation Patients With Heart Failure With Both Preserved and Reduced Left Ventricular Ejection Fraction. *J Am Heart Assoc* [Internet]. 2023;6(4):e005309. Available from: <https://doi.org/10.1161/JAHA.116.005309>

The impact of ginger and curcumin on diabetic nephropathy induced by streptozotocin in rats

Alaa Taha¹, Hanaa Ashour¹ , Manar Reffat²,

Omali Yousef Elkhawaga² 

¹ Chemistry Department, Faculty of Science, Suez Canal University, Ismailia, Egypt

² Biochemistry Division, Chemistry Department, Faculty of Science, Mansoura University, Mansoura, Egypt

Abstract

Background: Diabetes mellitus is a global health concern affecting 173 million adults annually that requires effective treatment. Medicinal plants such as ginger and curcumin, rich in bioactive compounds, have therapeutic potential. The aim of this study was to evaluate the therapeutic potential of ginger and curcumin extracts in diabetic nephropathy in the rat model. **Material and methods:** High-performance liquid chromatography was used to examine ginger and curcumin extracts. Fifty male Sprague Dawley rats were divided into five groups: control, untreated diabetic, ginger-treated diabetic, curcumin-treated diabetic, and a ginger + curcumin combination group. Diabetes was induced with a single intraperitoneal dose of streptozotocin. Rats received daily oral doses of ginger, curcumin or the combination of both. After sixteen weeks, rats were anesthetized and various tests were conducted to evaluate treatment outcomes. **Results:** The rats treated with combined ginger and curcumin extracts had superior outcome in terms of more antioxidant activity, better glycemia management and less DN-related kidney damage (reduced albuminuria and less histological changes). **Conclusions:** Our findings indicate that ginger and curcumin extracts have therapeutic potential in mitigating functional and structural alterations in the kidneys of diabetic rats, possibly due to their anti-diabetic and anti-inflammatory properties.

Keywords: oxidative stress · ginger · curcumin · anti-inflammatory · diabetic nephropathy

Citation

Taha A, Ashour H, Reffat M, Elkhawaga OY. Impact of ginger and curcumin on diabetic nephropathy induced by streptozotocin in rats. Eur J Transl Clin Med. 2023;6(2):51-65.

DOI: [10.31373/ejtcmm/172884](https://doi.org/10.31373/ejtcmm/172884)

Corresponding author:

Omali Yousef Elkhawaga, Biochemistry Division, Chemistry Department, Faculty of Science, Mansoura University, Mansoura, Egypt
e-mail: elkhawaga70s@mans.edu.eg

Available online: www.ejtcmm.gumed.edu.pl

Copyright © Medical University of Gdańsk

This is Open Access article distributed under the terms of the Creative Commons Attribution-ShareAlike 4.0 International.



Abbreviations

- ALT – alanine aminotransferase
- AST – aspartate aminotransferase
- AOA – anti-oxidant activity
- BUN – blood urea nitrogen
- CAT – catalase
- DAB – 3,3'-diaminobenzidine tetrachloride
- DM – diabetes mellitus
- DN – diabetic nephropathy
- DPPH – 2,2-diphenyl-1-picrylhydrazyl
- GSH – reduced glutathione
- IL-6 – interleukin- 6
- MDA – malondialdehyde
- NF-κB – nuclear factor kappa B
- OS – oxidative stress
- PKC – protein kinase C
- ROS – reactive oxygen species
- SOD – superoxide dismutase
- STZ – streptozotocin

Introduction

Diabetes mellitus (DM), affecting 8.8% of people globally in 2017 and expected to rise to 9.9% by 2045 [1], often leads to diabetic nephropathy (DN) in 30-40% of individuals. DN is linked to improper glycemia management, glycosylated proteins, and renal tissue abnormalities. Researchers emphasize the role of reactive oxygen species (ROS) and oxidative stress (OS) in DN pathophysiology [2-3]. Despite recent medical trials, addressing vascular issues and poor glucose control remains a challenge [4]. Early detection and understanding the complex interplay of metabolic factors are crucial to managing this chronic kidney disease [5].

Despite therapies with anti-hyperglycemic and renin-angiotensin system blocking drugs, DN development persists. Exploring new treatment options is essential. Studies investigating the potential benefits of nutritional antioxidants in diabetes patients have been conducted. Additionally, there's a growing demand for herbal medications derived from medicinal plants [6].

The ginger plant (*Zingiber officinale* Roscoe) belongs to the Zingiberaceae family, renowned for its medicinal significance and wide distribution. This family encompasses 53 genera and over 1200 medicinal plants, primarily found in tropical regions with large rhizomes. Ginger is cultivated in Southeast Asia, Australia, Brazil, West Africa, and the United States [7-8]. Its chemical analysis reveals more than 400 compounds, including phenolic and terpene compounds like gingerol, shogaol, and paradols, which contribute to its diverse biological activities. Ginger is widely used as a con-

diment in various cuisines around the world [9-10]. Ginger's phytochemical composition underscores its health-enhancing properties [11]. It serves as an antioxidant, protecting the body from oxidative stress and DNA damage while counteracting free radicals [12]. Ginger's therapeutic effect in managing diabetic complications is believed to involve reducing oxidative stress and inflammation, partly through inhibiting the NF-κB signaling pathway [13]. Studies indicate that ginger, containing compounds like Zerumbone, alleviates renal damage in diabetic rats. Thanks to its anti-inflammatory benefits, ginger can be helpful in conditions such as gout, osteoarthritis and rheumatoid arthritis. Ginger's functions include regulating blood glucose levels, pain relief, cardiac stimulation, antiemetic, antimicrobial, and antifungal actions [14]. Ginger exhibits protective effects on diabetic liver, kidney, eye, and nervous system complications. Numerous experiments confirm ginger extract's ability to lower blood glucose levels in both diabetes types, demonstrating a dose-dependent pattern [15].

Curcumin, extracted from the rhizome of turmeric belongs to the *Zingiberaceae* family, grows predominantly in India, Southeast Asia and China. Curcumin is a potent component in herbal medicine and is extensively studied for various health conditions [16]. Its primary compound, polyphenol curcumin, exhibits powerful anti-inflammatory, antioxidant, and anticarcinogenic properties. In diabetes management, curcumin's effectiveness lies in its interaction with key molecules and pathways crucial in the disease's progression. Studies show curcumin's ability to alleviate insulin resistance, a factor in metabolic syndrome. Both ginger and curcumin contain antioxidants that activate redox-sensitive transcription factors, bolstering cellular antioxidant defenses [17-18]. Given the importance of dietary management in diabetes, interventions using natural substances like ginger and curcumin offer promising strategies to mitigate the renal complications of DM.

In this study we aimed to assess the impact of curcumin and ginger on kidney function, antioxidant activity (AOA) and lipid peroxidation in diabetic rats with DM induced by streptozotocin (STZ). We also explored the effects of ginger extract, curcumin extract, and their combination on treating DN in rat models with DM.

Material and methods

Chemicals and extraction

Acetonitrile and STZ were obtained from Sigma-Aldrich (St. Louis, USA). Superoxide dismutase was obtained from

Biodiagnostic Company, Egypt. The ginger and curcumin powders were obtained from the Imtenan Egypt Company. Methyl alcohol was obtained from El Nasr Pharmaceutical Chemicals Company in Egypt.

The ginger powder (500g) and curcumin powder (500 g) were soaked in pure methanol for 72 hours two times. Then, the extract was clarified, and the residue was rejected. Excess alcohol was eliminated from every extract using a rotary evaporator at 50 °C and afterwards dried in a freeze-dryer. The sticky extracts were collected and stored at -20 °C before the experiment [19].

Preliminary phytochemical investigation of the plants

The presence of carbohydrates was determined by the Molisch's test [20]. A few sodium hydroxide drops determined the presence of flavonoids according to the alkaline reagent test [21]. The presence of saponins was determined based on the presence of foam. The presence of tannins was tested using a 2% solution of FeCl₃ [22]. Additionally, the presence of glycoside content was detected according to the Wagner and Hager tests [23]. The reaction of Liebermann detected the presence of steroid content [24]. The presence of terpenoids was determined according to Salkowski's test (a reddish-brown tint appeared upon contact) [25]. The total flavonoids in each plant extract were determined by spectrophotometric analysis using the reference substances quercetin and gallic acid, respectively [26].

Analysis of the plant extracts' anti-oxidant activity (AOA)

The obtained extracts' ability to react with stable 2,2-diphenyl-1-picrylhydrazyl (DPPH) free radicals (measured by using a spectrophotometer at wavelength 517 nm) was used to determine the extracts' antioxidant activity (AOA) [27-28]. The total flavonoid content (extracted from ginger and curcumin) was calculated using a colorimetric assay. A freshly prepared extract (0.5 g) was put in a tube with 5 ml of methanol (80%) in this assay. The extracts were inverted and mixed after vortexing the tubes and letting them stand for 20 minutes. A clear micro-centrifuge tube was filled with 2 ml of each extract, and then the tubes underwent a 5-minute, 4 °C, 12000 rpm centrifugation. The supernatant was analyzed within two weeks after being stored at -20 °C in a clear microcentrifuge tube. A combination of 600 µl of distilled water and 45 µl of NaNO₂ was added with 150 µl of the methanol extract. After the incubation of the solution at room temperature for 5 minutes, 45 µl of AlCl₃ (10%) was added, and the combination was

then re-incubated for 1 minute. Finally, 300 µl of distilled water and 1M NaOH were added. In place of the extract, a blank containing 80% aqueous methanol was used to calculate the absorbance at 510 nm. Using catechin as the standard, the concentration was calculated using a calibration curve. Catechin equivalents (CE) were expressed as mg of CE/g fresh weight [29].

Spectroscopic Investigation

The ginger extracts were analyzed on a high-performance liquid chromatography (HPLC) instrument Agilent1260 (Agilent Technologies, Santa Clara, USA). The series column used was the Agilent C18 column (4.6 mm x 250 mm, i.e., 5µm). The mobile phase consisted of acetonitrile: 5% Acetic Acid (50:50, v/v). The sample solvent was methanol. The flow rate was set to 2 ml/min. The injection volume of the sample, which was dissolved in methanol, was 25 µm. The column's temperature was 25°C, the wavelength of detection was 280 nm, and the run was 20 min [30]. The curcumin extract was analyzed using the same HPLC instrument and mobile phase as the ginger extract. For each of the curcumin sample solutions, the injection volume of the sample dissolved in methanol in the column was 20 ml. At 425 nm, the multiple wavelength detector was adjusted. Finally, the column was stored at 40 °C [30].

Experimental Animals

Fifty male Sprague Dawley rats weighing between 180 and 200 g were selected. Before the experiment, the animals were given a week to get used to the lab environment in separate metal cages with five animals per cage. Clean and fresh water was made available at all times. Throughout the study, the nutritional status of the rats was monitored under standard environmental conditions (temperature 23-27 °C, 60% humidity). The animal experiment in this study were performed in compliance with the guidelines of the Guide for the Care and Use of Laboratory Animals and approved by the Suez Canal University Animal Care Committee (REC 26/2022).

Induction of T1DM

In order to induce DM, a single intraperitoneal injection of 60 mg STZ dissolved in citrate buffer (pH 4.5) / kg body weight was given to 40 of the 50 rats [31]. The glycemia of all rats was measured in blood samples obtained from the tail vein 72 hours following an overnight fast. After that, blood sugar levels were checked every three days using a GlucoDr Super Sensor glucometer (OneTouch Technology, All Medicus Co, Korea). The study comprised of 38 rats

who developed DM (chronic hyperglycemia ≥ 250 mg/dl) one week after the STZ injection [32].

Experimental Design and Groups

The 50 rats were divided into 5 groups. The control group ($n = 10$) received 0.25 ml of citrate buffer (pH 4.5) intravenously. As mentioned above, 40 rats that were injected with STZ and we subdivided them into 4 additional groups of 10 each: DM (not treated with any substance), DM-ginger (treated with 350 mg/kg/day of ginger extract), DM-curcumin (treated with 350 mg/kg/day of curcumin) and DM ginger + curcumin (treated with combination of both extracts). An intragastric tube was used to administer both extracts orally after dissolving in water. The conversion of drug dosages to human equivalent doses was used [33]. Drug treatment began 8 weeks after the STZ injection and continued for additional 8 weeks, making the total study duration 16 weeks. At the end of week 16 of the experiment, all the rats were sacrificed via cervical dislocation and tissue samples were obtained for analysis.

Urine Samples

Rats from each group were weighed every 2 weeks and kept apart in metabolic cages to enable 24-hour urine collection. The rodents' access to food and water remained unlimited. The total volume of urine output was measured. In addition, urine samples were collected every 24 hours, stored at -80°C and were used to calculate the excretion of urinary albumin.

Biochemical estimation and evaluation

Glucose levels, liver function (alanine aminotransferase, ALT; aspartate aminotransferase, AST), and kidney function (blood urea nitrogen and creatinine) were examined in the serum. Albuminuria changed due to the experiment's measurement of the inflammation markers IL6 and malondialdehyde (MDA) and the antioxidants; superoxide dismutase (SOD), reduced glutathione (GSH), and catalase (CAT).

To determine the amount of glucose in blood samples, glucose kits (Engineering Chemistry for Lab Technology, BioMed-Glucose L. S., Badr City, Egypt) were used [34]. Creatinine levels were measured using kits (Diamond Diagnostics Company Hannover, Germany) [35]. Berthelot enzymatic colorimetric method was used to measure blood urea nitrogen (BUN) (Diamond Diagnostics Company, Hannover, Germany) [36].

Utilizing micro-albuminuria kits from ABC Diagnostic in New Damietta, Egypt, urine samples were collected in

accordance with the manufacturer's instructions to test urinary albumin excretion ($\mu\text{g/ml}$) [37]. Using methods that considered the urine volume (ml) in 24 hours, albuminuria was computed as $\text{g}/24$ hours. ALT and AST were measured using the kits (Cat. No. 264001 and 260001) from Spectrum Diagnostics Company was used to detect ALT in serum. Additionally, AST was measured in serum according to the kit of aspartate aminotransferase from the Company of Spectrum Diagnostics (Cat. No. 260001).

Inflammatory Markers and Kidney Anti-oxidant Parameters

The right kidney of all rats was taken and homogenized in phosphate buffer to test the mean OS parameters, MDA, GSH, CAT, SOD, and IL-6 levels using specialized kits following the manufacturer's instructions. The following kits were used: a rat IL-6 ELISA kit from Bioassay Technology Laboratory Company (Shanghai, China) and MDA, GSH, CAT, and SOD kits from the Bio-Diagnostic Company (Dokki, Giza, Egypt; MD2529, CA2517 and SD2521, respectively).

Histopathology and immunohistochemistry

Neutral buffered formalin (10%) was perfused into the left kidneys of all rats, which were then processed into 5-mm paraffin sections for histological examination. Hematoxylin and eosin (H & E), Masson, periodic acid-Schiff (PAS), and immunostaining renal sections against NF- κB were used to stain all kidney tissues [6]. NF- κB expression was assessed through the immunostaining of deparaffinized samples slides using polyclonal NF- κB antibody (sc-59103) from Santa Cruz Biotechnology Inc., CA, USA) diluted 1:50.

Data analysis

After doing a one-way analysis of variance (ANOVA), the parametric data presented as mean \pm SD were examined using the post-hoc Scheffé test. The Kruskal-Wallis H, chi-square " χ^2 " or Fisher's exact test were applied to examine quantitative data. $P \leq 0.05$ served as the significance threshold.

Results

Ginger and curcumin extract contained the highest phytochemical content and AOA (Table 1). The two *Zingiberaceae* plant species were examined phytochemically to identify seven naturally occurring classes (carbohydrates,

Table 1. Phytochemistry of plant extracts

Plant/ test	Carbo- hydrates	Saponins	Flavonoid	Glycosides	Steroids	Alkaloids	Tannins	Terpenes
Curcumin	+++	-	+	++	-	++	++	+++
Ginger	++	+++	+++	-	-	+	+	+

The signs (-) and (+) denote a negative test, (+) a weakly positive test, (++) a moderately positive test, and (+++) a strongly positive test, respectively.

Table 2. Total flavonoid contents and DPPH scavenging activity

Plant	Part	Total flavonoid content (mg/g dry wt.)	DPPH (1%)
Curcumin	roots	175.667	89.632%
Ginger	roots	186.800	95.789%

Table 3. HPLC analysis of the ginger extract

Peak name	RT	Area	% Area	Height	Amount	Units
6-gingerol	2.386	7655845	51.64	2009871	957.578	ppm
8-gingerol	3.635	1494096	10.08	270289	181.579	ppm
6-shogaol	4.245	2534128	17.09	430806	266.302	ppm
10-gingerol	6.120	2184887	14.74	259930	333.790	ppm
8-shogaol	7.354	487584	3.29	50571	71.738	ppm
10-shogaol	12.289	469197	3.16	79936	76.559	ppm

saponins, glycosides, tannins, alkaloids, flavonoids, and steroids). It was found that ginger extract had a significant amount of phenolic (flavonoids). The high glycoside content was recorded in curcumin. The high saponins content was recorded in ginger. The high carbohydrate content was recorded in ginger. Furthermore, the high terpene content was recorded in curcumin extract. The highly alkaloid content was recorded in curcumin extract.

DPPH scavenging activity

Each extract underwent quantitative analysis to estimate the outcomes of the analysis of scavenging activity (2, 2-diphenyl-1-picrylhydrazyl, DPPH). It was found that the scavenging activity of ginger was more than that of curcumin (Table 2).

Total Flavonoids Contents

Each extract underwent quantitative analysis to determine its estimated total flavonoid concentration. The ginger extract had a greater total flavonoid content than the curcumin extract (Table 2).

HPLC Results

HPLC chromatogram results of ginger extract interpretation are shown in (Table 3, Figure 1). The peak identification of the ginger extract component depends on retention time, peak area, and height of the ginger extract compared with the standard. It was found that the detailed levels 6-gingerol was more abundant than 6-shogaol, 10-gingerol, and 8-gingerol. The lowest peak was 10-shogaol and 8-shogaol.

The sample performed in HPLC triplicate resulted in the identification of the curcumin extract. By dividing the overall area of peaks, which included the primary curcumin peak, demethoxycurcumin, and at least bisdemethoxycurcumin, one can determine the standard or curcumin extract ratio. By dividing the standard's ratio by the standard's ratio times the standard's potency, the amount of curcumin in curcumin extract was estimated (Table 4; Figures 2a and 2b).

Characterization of STZ-induced diabetes

Based on their fasting blood glucose levels, 96% of the rats developed DM one week following the STZ injection.

tion. Before the 16 week-long observation was completed, rats with DM who received no treatment had a mortality rate of 30% ($n = 3$). The same mortality rate was observed in the curcumin group (30 %, $n = 3$), whereas in the ginger group it was 20% ($n = 2$). No mortality was noted in the control group.

Glycemia, kidney function and liver function

We noted a significantly increased glycemia in the control group and the untreated diabetic group ($p < 0.05$). In contrast, glycemia was significantly lower after treatment with the extracts of ginger, curcumin or their combination ($p < 0.05$) (Table 5). It was found that there was a more significant increase in renal function parameters (creatinine and blood urea nitrogen) in the control group and untreated diabetic group ($p < 0.05$). However, there were significantly lower levels of creatinine and blood urea nitrogen after treatment with either of the extracts or their combination ($p < 0.05$). Combining ginger and curcumin extracts achieved reduced blood urea nitrogen and creatinine levels ($p < 0.05$) (Table 5). There was a highly significant increase in liver function parameters (ALT, AST and albumin levels) in the untreated diabetic group compared to the control group ($p < 0.05$). After the treatment of the diabetic group with ginger extract, curcumin extract, or their combination. (ALT, AST, and albumin levels) decreased significantly ($p < 0.05$), with a more pronounced decline in the group treated with combined ginger and curcumin ($p < 0.05$) (Table 5).

Body weight, kidney weight to body weight, IL-6, OS parameters and AOA

The treated groups' mean body weight increased after the treatment ($p < 0.05$). In the treated groups compared to the STZ-diabetic group, the mean kidney weight and the renal weight to body weight ratio decreased ($p < 0.05$), and OS and inflammation markers decreased ($p < 0.05$) after extract treatment compared to STZ diabetics that were not treated. Additionally, anti-oxidant levels were significantly higher ($p < 0.05$) in the treated groups (Table 6). The ratio of kidney weight to body weight significantly decreased following treatment with the extracts ($p < 0.05$) after treatment with ginger and curcumin extract. It was noted that the treatment using extracts of ginger and curcumin together reduced the kidney weight relative to body weight ($p < 0.05$) (Table 6).

Following treatment with ginger and curcumin extract, there was a significant ($p < 0.05$) decrease in IL6 and MDA. The treatment with combined ginger and curcumin extracts was produced a more significant reduction in IL6 and MDA levels ($p < 0.05$) (Table 6).

There was a significant decrease in glutathione, catalase and SOD levels in the control group compared to the untreated diabetic group ($p < 0.05$). In contrast, the levels of these antioxidants significantly increased after treatment with the extracts ($p < 0.05$), with greater increase more following treatment with combined extracts ($p < 0.05$) (Table 6).

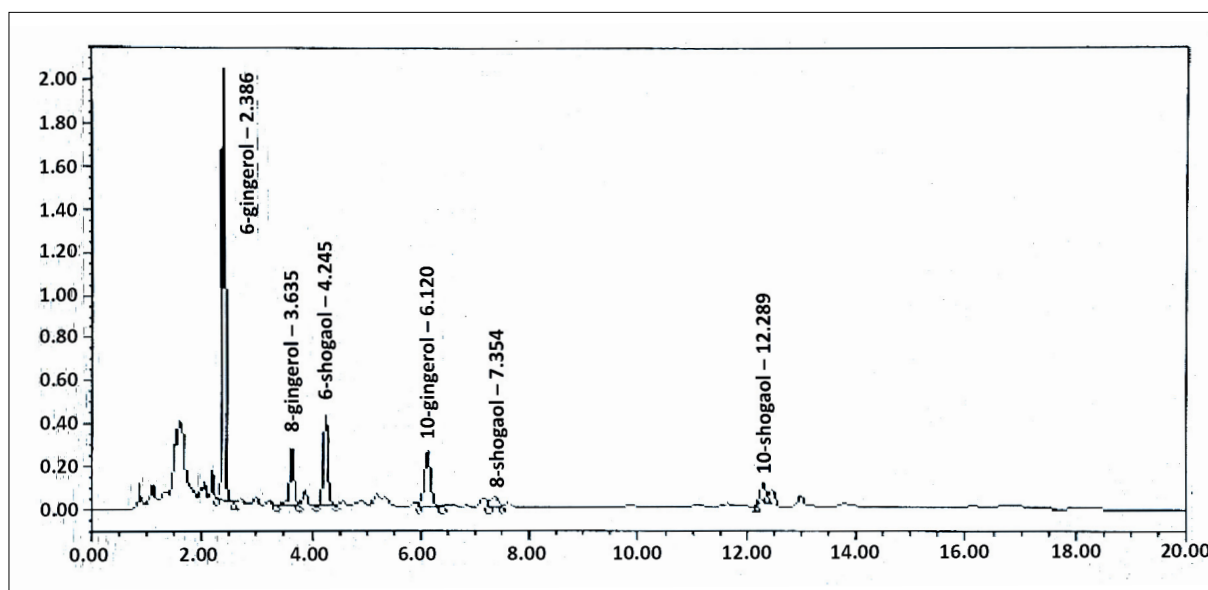


Figure 1. HPLC chromatogram of the ginger extract

Table 4. HPLC analysis of the curcumin extract

Peak name	RT	Type	Width	Area	% Area
Standard curcumin	4.7	BB	0.181	1197.24	100%
Bisdemethoxycurcumin	3.7	BV	0.1724	413.2	19.864%
Demethoxycurcumin	4.23	VV	0.1763	533.2	25.63%
Curcumin	4.77	MM	0.1978	1133.9	54.505%

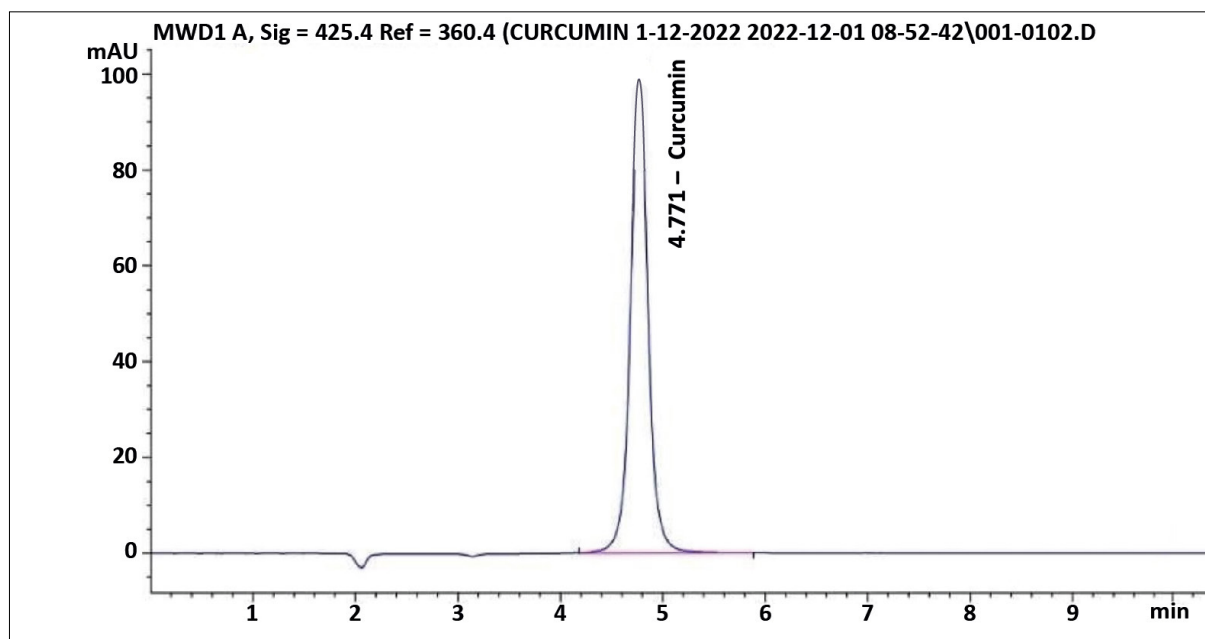


Figure 2a. HPLC chromatogram of a standard (Curcumin)

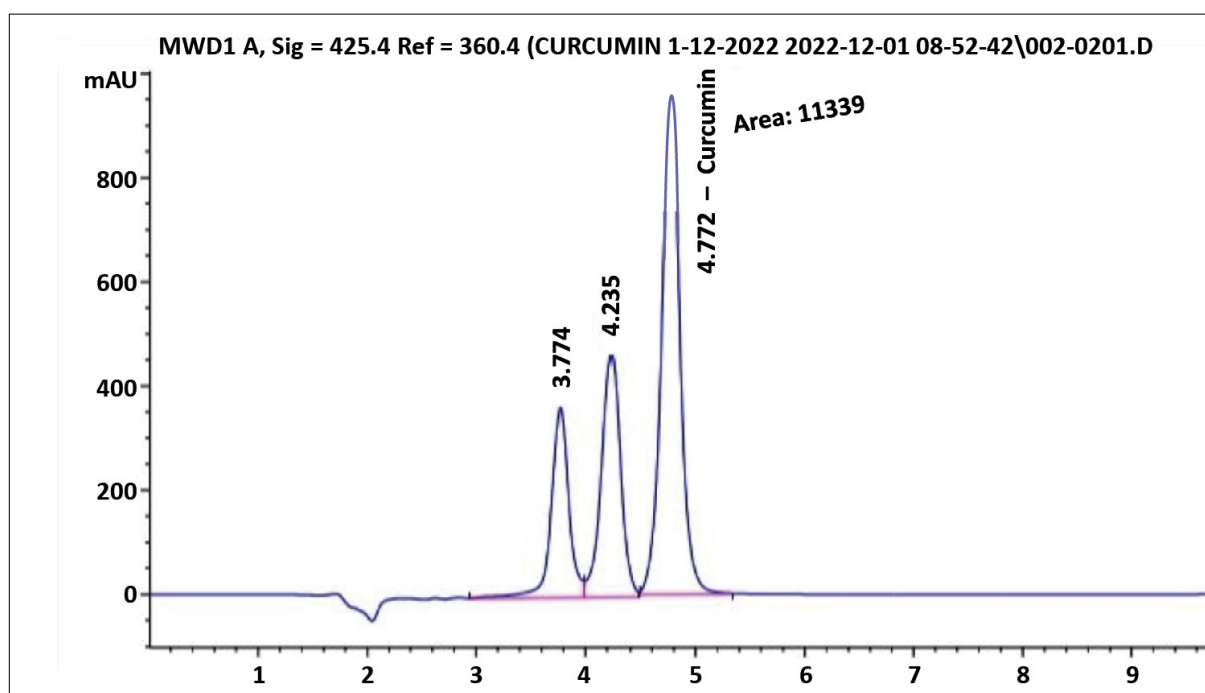


Figure 2b. HPLC chromatogram of Curcumin extract

Table 5. Blood glucose levels, kidney function and liver function tests

	Control	DM untreated	DM ginger	DM curcumin	DM ginger + curcumin	P-value
Creatinine (mg/dl)	0.764 ± 0.06 ^a	2.171 ± 0.30 ^b	0.9438 ± 0.13 ^{ac}	1.104 ± 0.08 ^c	0.9486 ± 0.10 ^{ac}	0.0001 ***
Urea (mg/dl)	28.4 ± 6.50 ^a	75.75 ± 7.88 ^b	39.25 ± 5.8 ^c	40.96 ± 3.85 ^c	32.14 ± 4.48 ^{ac}	0.0001 ***
ALB (g/dl)	4.068 ± 0.09 ^a	3.413 ± 0.38 ^b	3.995 ± 0.28 ^a	4.013 ± 0.31 ^a	4.11 ± 0.19 ^a	0.0002 ***
ALT (U/l)	29 ± 2.55 ^{ac}	50.76 ± 4.505 ^b	33.81 ± 5.7 ^{ac}	35 ± 7.95 ^a	25.47 ± 2.55 ^c	0.0001 ***
AST (U/l)	23.6 ± 3.97 ^{ac}	47.94 ± 6.78 ^b	29.88 ± 4.35 ^{ac}	33.14 ± 9.28 ^a	23.15 ± 4.52 ^c	0.0001 ***
Glucose (mg/dl)	104.8 ± 15.22 ^a	451.9 ± 30.48 ^b	107.5 ± 11.1 ^a	119.1 ± 31.41 ^a	93.14 ± 11.62 ^a	0.0001 ***

The post-hoc Scheffé test ($p < 0.05$) was employed after one-way ANOVA was used to analyze the mean and standard deviation of the data. As a result, a < 0.05 p-value indicates that having numerous letters in the same column is significant.

Table 6. IL-6, OS parameters, AOA, body weight and kidney weight

Parameters	Control	DM untreated	DM ginger	DM curcumin	DM ginger + curcumin	P-value
BW (g)	243 ± 9.19 ^a	139.6 ± 7.67 ^b	226.1 ± 4.42 ^{ac}	202.1 ± 8.63 ^c	245.3 ± 35.08 ^a	0.0001***
KW (g)/BW (g)	4.664 ± 0.31 ^a	8.026 ± 0.66 ^b	6.069 ± 0.16 ^c	6.683 ± 0.09 ^d	5.882 ± 0.09 ^c	0.0001***
SOD (u/g)	719 ± 2.69 ^a	424.1 ± 4.52 ^b	521.1 ± 3.57 ^c	440.2 ± 5.62 ^d	729.2 ± 8.057 ^e	0.0001***
MDA (nmol/g)	106.5 ± 1.35 ^a	328.9 ± 6.81 ^b	134.5 ± 3.08 ^c	212.9 ± 4.10 ^d	125.2 ± 3.002 ^e	0.0001***
CAT (u/g)	3.584 ± 0.08 ^{ad}	1.221 ± 0.23 ^b	3.223 ± 0.29 ^a	2.72 ± 0.12 ^c	3.913 ± 0.27 ^d	0.0001***
GSH (mg/g)	21.82 ± 4.10 ^a	10.2 ± 2.24 ^b	21.08 ± 1.9 ^a	21.82 ± 2.62 ^a	24.76 ± 2.12 ^a	0.0001***
IL6 (Pgm/ml)	21.64 ± 3.52 ^a	111.5 ± 9.23 ^b	60.27 ± 7.84 ^c	56.29 ± 12.9 ^c	36.92 ± 4.1 ^d	0.0001***

BW - body weight, KW - kidney weight

The mean +SD data were analyzed using one-way ANOVA, and the post-hoc Scheffé test was run ($p < 0.05$). This means various letters in the same column are significant at $p < 0.05$.

Albuminuria

There were variations in albuminuria (mg/24 h) in all the groups of rats we observed. The rats treated with ginger, curcumin or a combination of the two extracts all had a significant increase in 24-hour urine volume and protein excretion. Starting from the 10th week of treatment, albuminuria decreased in the groups receiving the extracts, with the best effect in rats treated with a combination of ginger and curcumin extracts ($p < 0.05$) (Table 7).

Histopathology

The kidney sections obtained from the control group revealed no collagen accumulation, interstitial tissue or abnormal glycogen (Figures 3-B, 3-C, and 3-D). Conversely, sections of kidney samples from DM rats sections displayed significant blue collagen (Figure 3-H) and tubular dilation with glycogen buildup (blue arrows). Kidney sections obtained from rats treated with ginger contained glycogen-free areas, reduced collagen (blue arrows), and milder

Table 7. Changes in albuminuria during the study

	Control	DM untreated	DM ginger	DM curcumin	DM ginger + curcumin	P value
W0	179.8 ± 7.94	174.4 ± 4.44	175.2 ± 9.44	175.2 ± 6.41	173.2 ± 2.86	0.65 NS
W2	196.94 ± 7.835	504.8 ± 6.37	486.4 ± 14.32	496.2 ± 11.60	479 ± 12.26	0.0001 ***
W4	215.66 ± 6.97	760.16 ± 4.70	776.6 ± 14.31	775 ± 19.46	780.6 ± 14.8	0.001 ***
W6	237.5 ± 6.96	996.16 ± 4.70	991.2 ± 10.77	996.2 ± 6.76	954.4 ± 62.2	0.0001 ***
W8	260.966 ± 6.85	1402.106 ± 8.55	1391 ± 5.43	1397.6 ± 3.91	1396.2 ± 6.90	0.001 ***
W10	284.66 ± 6.33	1795.288 ± 25.42	1490.8 ± 5.26	1491.2 ± 8.84	1488 ± 12.56	0.001 ***
W12	307.46 ± 7.91	2224.976 ± 70.51	1558 ± 14.94	1563.2 ± 15.69	1567 ± 19.68	0.0001 ***
W14	364.466 ± 7.74	2501.2 ± 9.52	1323 ± 16.38	1326.4 ± 17.31	1307 ± 14.43	0.0001 ***
W16	398.466 ± 8.47	2859.6 ± 25.97	918.2 ± 27.44	923.2 ± 27.84	874.4 ± 43.8	0.0001

Albuminuria (mg / 24 hours) changes during the 16 weeks (W) of the experiment data are expressed as mean ± SD. An increase in 24-hour urine volume and an increase in urine protein excretion were seen in the diabetic control group. However, when diabetic rats were given the extract, they all decreased ($p < 0.05$).

tubular changes (Figure 3-L, 3-J, and 3-G). Kidney samples from curcumin-treated rats revealed reduced collagen and showed minimal tissue changes (Figure 3-N and 3-O). Finally, sections of kidneys of rats treated with combined ginger and curcumin extracts displayed no collagen, minimal tissue, and no glycogen deposition (Figure 3-R, 3-S, and 3-T).

Immunohistochemistry

Microscopic views of immunostained renal sections against NF- κ B in the control group showed negative expression, according to IHC counterstained with Mayer's hematoxylin (Figure 3-A). The diabetic group's brown tubular expression was positive in microscopic images of immunostained renal sections against NF- κ B (Figure 3-E): A very slight positive reaction was seen in the diabetic group treated with ginger in comparison to the curcumin-treated

diabetic group in microscopic images of immunostained renal sections against NF- κ B (Figure 3-M) (Figure 3-I). In the group treated with combined extracts, brown tubular expression (blue arrows) and negative expression are shown (Figure 3-Q).

Discussion

Insulin deficiency leads to persistent hyperglycemia and metabolic imbalances, making diabetes challenging to treat [38]. Diabetic nephropathy (DN) is a major cause of renal failure, affecting 15-25% of T1DM and 30-40% of T2DM patients [39]. STZ-induced diabetes mimics these conditions. In our study, prolonged hyperglycemia led to DN, evident in decreased antioxidant levels, intense ROS production, reduced kidney function and abnormal renal histology [40-41]. These findings emphasize the link be-

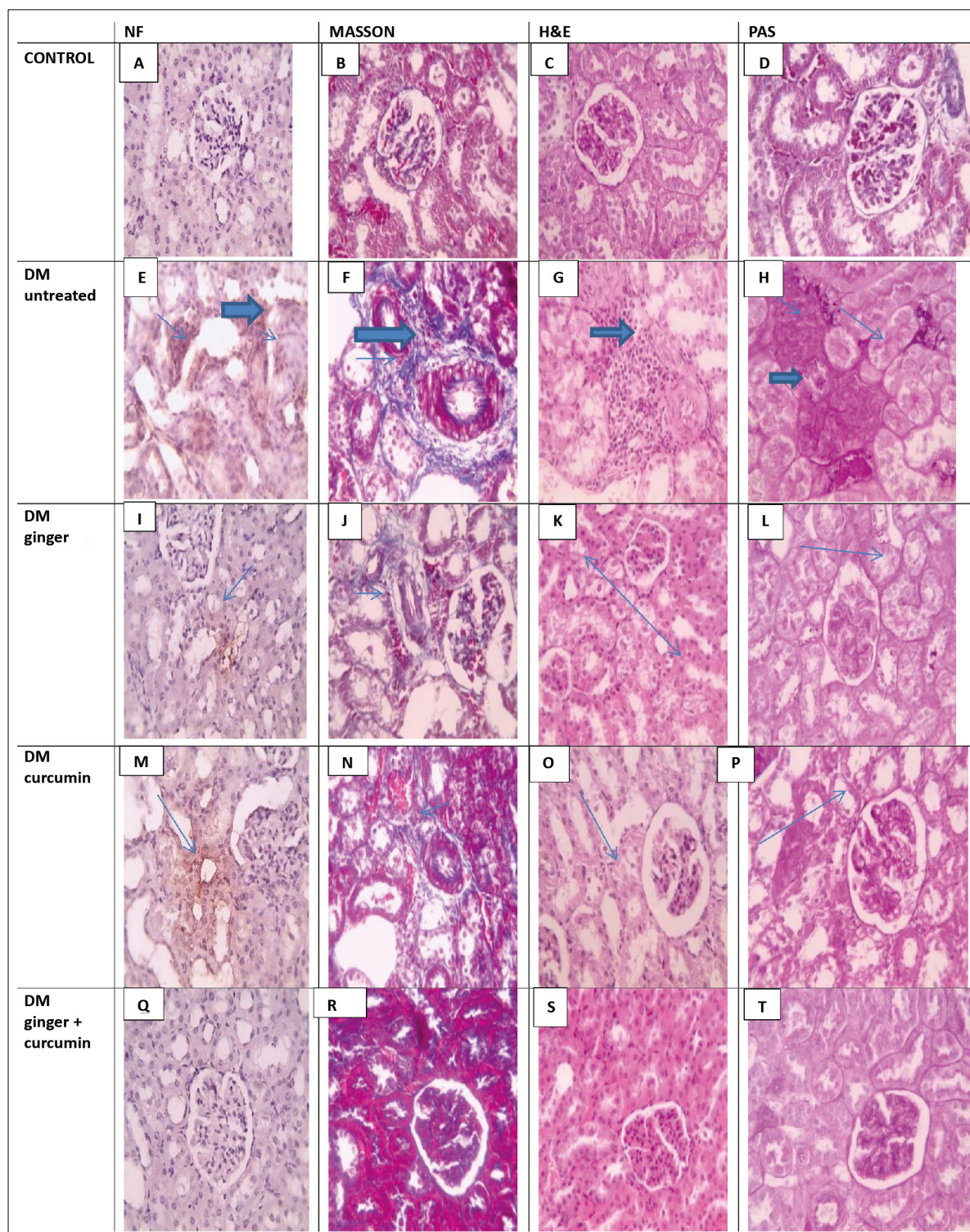


Figure 3. Histopathological and immunohistochemical assessments

tween sustained hyperglycemia, oxidative stress and DN progression.

The basis for the DM model in our study was the chemotherapy drug STZ, which damages pancreatic cells and reduces insulin production leading to chronic hyperglycemia

[42]. This study demonstrated how persistent hyperglycemia encouraged energy imbalances with strong lipolysis through increased feed intake and weight loss in animals [42-43]. Polydipsia, polyuria and decreased GFR were seen as a result of STZ's involvement in the hemodynamic al-

terations brought on by glomerular hyperfiltration [43]. Because systemic hyperglycemia negatively affects glomerular filtration, which leads to an excessive buildup of intracellular glucose, endothelial cells cannot manage glucose transport through the plasma membrane. The high intracellular glucose levels encourage manufacturing cytokines e.g. transforming and vascular endothelial growth factors. Through vasodilating prostanoids and nitric oxide, these substances cause macrovascular endothelial lesions and increase glomerular permeability. Additionally, these macromolecules change the hemodynamics of the glomerulus, intensifying vasodilation of the afferent arteriole compared to the efferent one. Glomerular hyperfiltration results from a final representation of artery imbalance [43-45]. An ongoing rise in hydrostatic pressure (intraglomerular pressure that forces fluid through capillaries while albumin is lost into the ultra-filtrate) is a sign of changes caused by glomerular dysfunction [44, 46]. Proteoglycans and collagen IV, which are in charge of thickening the basal glomerular membrane and altering the negative charge of the podocytes, are two molecules synthesized and catabolized during glomerular dysfunction. Protein loss in the urine and glomerulosclerosis with a reduced GFR are signs of glomerular dysfunction [46-47]. In our study, the characteristics of renal lesions linked to macrovascular changes of diabetic nephropathy were validated in animals that had undergone nephrectomy, demonstrated by the increased kidney and relative weight (kidney weight/body weight). The chronic hyperglycemia affected the glomerular basal membrane's structure. It promoted extracellular matrix growth in the mesangial area, which resulted in tubular area hyperplasia and hypertrophy [47]. The progression of kidney disease was hastened in diabetic animals that received left nephrectomy in this investigation using the STZ-induced DM model in rats. The signs of DN included increased urine albumin excretion and impaired renal function (elevation in plasma creatinine concentration and reduced GFR).

The main factor thought to contribute most significantly to intracellular ROS generation is chronic hyperglycemia. Significant amounts of glucose are transferred inside the glomerular endothelium, mesangial cells and tubular epithelium cells because some cells cannot maintain intracellular glucose homeostasis, thus speeding up glycolysis and releasing an excessive quantity of ROS [45, 48]. In addition to being mediated by hydrogen peroxide (H_2O_2), unattached iron, and the creation of additional free radicals such OH- and peroxynitrite, an oxidative lesion cascade is initiated by a chain reaction that breaks down lipids, proteins and nucleic acids by creating the (ONOO-) O_2 radical [45, 49]. The elevated levels of urine peroxides and thiobarbituric acid reactive substances (TBARS) in diabetic rats served as additional evidence of the importance

of ROS in the experimental model of DN. H_2O_2 is an extremely effective membrane-crosser and when its level is too high, it emits OH and TBARS are excreted in the urine, a clear sign of lipid peroxidation caused by unbound iron [48-49]. Due to changes in mitochondrial permeability, aberrant ATP synthesis, unbalanced intracellular calcium levels and other ROS-mediated disorders, the mitochondrial area was particularly vulnerable to cell death through necrosis and apoptosis [50]. Excessive ROS triggered the activation of numerous antioxidant mechanisms, including enzymatic systems and free radical scavengers. The anti-oxidant enzymes (e.g. reduced glutathione (GSH), catalase (CAT)) converted H_2O_2 into water [45, 48]. The unbalanced antioxidant enzymes utilized in hyperglycemia were SOD, GSH and CAT [45]. Thiol levels dropped in diabetic rats after nephrectomy, suggesting that the antioxidant enzyme is active. Much research supported the role of ROS in the diabetic nephropathy lesion mechanism. An in vivo investigation using mesangial cells exposed to high glucose concentrations demonstrated significant ROS production [51], using ginger and curcumin to treat diabetic nephropathy. Ginger and curcumin are two well-known functional foods from the Zingiberaceae family that have anti-inflammatory qualities [52-53]. Ginger is known for its anti-inflammatory properties attributed to its phenolic compounds, which include 6-gingerol (6-g) [54] and 6-shogaol (6-s) [55] as these are the main compounds involved in decreasing the main proinflammatory mediators, e.g., IL-6 and TNF [53]. Short pre-clinical and clinical studies on turmeric's anti-inflammatory effects were conducted [56-59].

In our study, we found that STZ diabetic rats had higher MDA levels, indicating increased production of free radicals and related lipid peroxidation. However, administering the ginger, curcumin or a combination of both extracts to diabetic rats significantly decreased the MDA level. Accordingly, we hypothesized that administering ginger extract, curcumin extract, or a combination of them for diabetic rats would reduce the generation of free radicals and the peroxidation of lipids, thereby preventing oxidative damage to cellular structures. Our results also showed that those extracts could increase the intracellular activity of SOD, CAT and GSH enzymes. In contrast, the activity of the above-mentioned enzymes all dramatically decreased in the diabetic rats not receiving treatment. This might highlight a weak antioxidant defense against damage caused by free radicals. We hypothesize that treatment with extracts reduced OS by scavenging free radicals and/or enhancing endogenous antioxidant activities, thereby improving diabetic condition, reducing inflammatory state and advancing the treatment of kidney functions and tissue. One treatment method for challenging diseases involving inflammation is combination therapy with a synergistic

approach [60]. In particular, the mechanical anti-inflammatory effects of ginger and curcumin share numerous molecular targets and signaling pathways, including Nrf2 activation [53, 61-63]. Despite research into the specific anti-inflammatory properties of ginger and curcumin, their usage is not widespread [53, 57-59]. In our study, the rats treated with combined ginger and curcumin extracts had superior outcome in terms of better glycemia management and less DN-related kidney damage.

Conclusions

Our results demonstrated the anti-inflammatory and the antioxidant effects of ginger and curcumin extracts, administered individually or in combination. Our data have also shown that ginger and curcumin extracts helped manage STZ-induced diabetic nephropathy and oxidative stress via significant suppression of the NF- κ B gene expression. These extracts possess anti-inflammatory potential by suppressing inflammatory cytokines and modulators through the suppression of redox-based NF- κ B activation.

References

1. Standl E, Khunti K, Hansen TB, Schnell O. The global epidemics of diabetes in the 21st century: Current situation and perspectives. *Eur J Prev Cardiol* [Internet]. 2019;26(2_suppl):7-14. Available from: <https://doi.org/10.1177/2047487319881021>
2. Schena FP, Gesualdo L. Pathogenetic Mechanisms of Diabetic Nephropathy. *J Am Soc Nephrol* [Internet]. 2005;16(3_suppl_1). Available from: https://journals.lww.com/jasn/fulltext/2005/03001/pathogenetic_mechanisms_of_diabetic_nephropathy.8.aspx
3. Tanios BY, Ziyadeh FN. Emerging Therapies for Diabetic Nephropathy Patients: Beyond Blockade of the Renin-Angiotensin System. *Nephron Extra* [Internet]. 2012;2(1):278-82. Available from: <https://doi.org/10.1159/000343312>
4. Papadopolou-Marketou N, Paschou SA, Marketos N, Adamidi S, Adamidis S, Kanaka-Gantenbein C. Diabetic nephropathy in type 1 diabetes. *Minerva Med* [Internet]. 2018;109(3):218-28. Available from: <http://europepmc.org/abstract/MED/29205998>
5. Tervaert TWC, Mooyaart AL, Amann K, Cohen AH, Cook HT, Drachenberg CB, et al. Pathologic Classification of Diabetic Nephropathy. *J Am Soc Nephrol* [Internet]. 2010;21(4):556-63. Available from: https://journals.lww.com/jasn/fulltext/2010/04000/pathologic_classification_of_diabetic_nephropathy.7.aspx
6. Fouda A-M, Ashour RH, El-Banna F, Saad MA, Mostafa FA, Fouda MI. Differential Effects of Low-Dose Erythropoietin in Rat Model of Diabetic Nephropathy. *Adv Med Med Res* [Internet]. 2018;1(1):25-33. Available from: https://www.researchgate.net/profile/Abdel-Motaal-Fouda/publication/325207039_Differential_Effects_of_Low-Dose_Erythropoietin_in_Rat_Model_of_Diabetic_Nephropathy/links/5e0c45e8a6fdcc28374d4555/Differential-Effects-of-Low-Dose-Erythropoietin-in-Rat-Model-of-Diabetic-Nephropathy.pdf
7. WHO monographs on selected medicinal plants. World Health Organization; 1999.
8. Zingiber officinale [Internet]. USDA. [cited 2023 Oct 26]. Available from: <https://plants.usda.gov/home/plantProfile?symbol=ZIOF>
9. Prasad S, Tyagi AK. Ginger and Its Constituents: Role in Prevention and Treatment of Gastrointestinal Cancer. Shaffer EA, editor. *Gastroenterol Res Pract* [Internet]. 2015;2015:142979. Available from: <https://doi.org/10.1155/2015/142979>
10. Mao Q-Q, Xu X-Y, Cao S-Y, Gan R-Y, Corke H, Beta T, et al. Bioactive Compounds and Bioactivities of Ginger (*Zingiber officinale* Roscoe). *Foods* [Internet]. 2019;8(6):185. Available from: <https://www.mdpi.com/2304-8158/8/6/185>

Acknowledgments

The authors are grateful to the Chemistry Department, Faculty of Science, Suez Canal University, and Mansoura University in Egypt for providing some of the resources required for this study.

Funding

The authors declare that no funds, grants, or other support forms were received during the preparation of this manuscript.

Conflict of interest

The authors declare no conflict of interest.

11. Zhang S, Kou X, Zhao H, Mak K-K, Balijepalli MK, Pichika MR. *Zingiber officinale* var. *rubrum*: Red Ginger' s Medicinal Uses. *Molecules* [Internet]. 2022;27(3):775. Available from: <https://www.mdpi.com/1420-3049/27/3/775>
12. Butt MS, Sultan MT. Ginger and its Health Claims: Molecular Aspects. *Crit Rev Food Sci Nutr* [Internet]. 2011;51(5):383-93. Available from: <https://doi.org/10.1080/10408391003624848>
13. Aktan F, Henness S, Tran V, Duke C, Roufogalis B, Ammit A. Gingerol Metabolite and a Synthetic Analogue CapsarolTM Inhibit Macrophage NF- κ B-Mediated iNOS Gene Expression and Enzyme Activity. *Planta Med* [Internet]. 2006;72(8):727-34. Available from: <http://www.thieme-connect.com/products/ejournals/abstract/10.1055/s-2006-931588>
14. Qian Q, Yue W, Wang Y, Yang Z, Liu Z, Chen W. Gingerol inhibits cisplatin-induced vomiting by down regulating 5-hydroxy-tryptamine, dopamine and substance P expression in minks. *Arch Pharm Res* [Internet]. 2009;32(4):565-73. Available from: <https://doi.org/10.1007/s12272-009-1413-9>
15. Lindstedt I. Ginger and diabetes: A mini-review. *Arch Gen Intern Med* [Internet]. 2018;2(2):29-33. Available from: <https://www.alliedacademies.org/articles/ginger-and-diabetes-a-minireview-9959.html>
16. Ching W-Y, Bin-Yusoff Y, Wan-Amarina W-NB. Extraction of essential oil from *Curcuma longa*. *J Food Chem Nutr* [Internet]. 2014;2(1):1-10. Available from: <https://esciencepress.net/journals/index.php/JFCN/article/view/310>
17. Mashhadi NS, Ghiasvand R, Askari G, Hariri M, Darvishi L, Mofid MR. Anti-oxidative and anti-inflammatory effects of ginger in health and physical activity: review of current evidence. *Int J Prev Med* [Internet]. 2013;4(Suppl 1):S36-42. Available from: <http://www.ncbi.nlm.nih.gov/pubmed/23717767>
18. Nishikawa S, Kato M, Ikehata A, Dochi K, Tani T, Takahashi T, et al. Curcumin improves glucose tolerance via stimulation of glucagon-like peptide-1 secretion. *Mol Nutr Food Res* [Internet]. 2017;61(3):1600471. Available from: <https://doi.org/10.1002/mnfr.201600471>
19. Mostafa M, Amer N, Serag M, Khedr AH, Abdel-Mogib M. Phytochemical constituents and antibacterial activity of the medicinal herb *Deverra tortuosa* (Desf.) DC. *Res J Pharm Biol Chem Sci* [Internet]. 2020;11(2):108-15. Available from: https://www.researchgate.net/publication/343999329_Phytochemical_Constituents_and_Antibacterial_Activity_of_the_Medicinal_Herb_Deverra_tortuosa_Desf_DC
20. Khalid S, Shahzad A, Basharat N, Abubakar M, Anwar P. Phytochemical screening and analysis of selected medicinal plants in Gujrat. *J Phytochem Biochem* [Internet]. 2018;2(1):1-3. Available from: <https://www.omicsonline.org/open-access/phytochemical-screening-and-analysis-of-selected-medicinal-plants-in-gujrat-100085.html>
21. Bansode TS, Salalkar BK. Phytochemical analysis of some selected Indian medicinal plants. *Int J Pharm Bio Sci* [Internet]. 2015;6(1):550-6. Available from: https://www.researchgate.net/publication/281690290_Phytochemical_analysis_of_some_selected_Indian_medicinal_plants
22. Abdel Wahab F. Preliminary phytochemical screening, quantitative estimation of total flavonoids, total phenols and antioxidant activity of *ephedra alata* decne [Internet]. 2015 [cited 2023 Oct 26]. Available from: <https://repository.najah.edu/items/4bd621a8-3369-46cd-a8b7-7678862c0c1e/full>
23. Tiwari P, Kumar B, Kaur M, Kaur G, Kaur H. Phytochemical screening and extraction: a review. *Int Pharm Sci* [Internet]. 2011;1(1):98-106. Available from: <https://www.researchgate.net/profile/Chukwuebuka-Egbuna/post/Why-does-petroleum-ether-solvent-yield-more-alkaloids-and-polyphenols-and-why-does-aqueous-extraction-yield-more-flavonoids/attachment/59d650a779197b80779a968f/AS%3A504112410497024%401497201172241/download/Phytochemical+screening+and+extraction+-+A+review.pdf>
24. Zohra SF, Meriem B, Samira S, Muneer MA. Phytochemical screening and identification of some compounds from mallow. *J Nat Prod Plant Resour* [Internet]. 2012;2(4):512-6. Available from: <https://www.scholarsresearchlibrary.com/articles/phytochemical-screening-and-identification-of-some-compoundsfrom-mallow.pdf>
25. Fesseha YA. Phytochemical Screening of Some Selected Home Garden Plants in Amhara Region, North Gondar, Gondar [Internet]. *Semantic Scholar*; 2020 [cited 2023 Oct 26]. Available from: <https://api.semanticscholar.org/CorpusID:212552297>
26. Saied S, Begum S. Phytochemical Studies of *Berberis vulgaris*. *Chem Nat Compd* [Internet]. 2004;40(2):137-40. Available from: <https://doi.org/10.1023/B:CONC.0000033929.60336.bb>
27. Wood LG, Gibson PG, Garg ML. A review of the methodology for assessing in vivo antioxidant capacity. *J Sci Food Agric* [Internet]. 2006 86(13):2057-66. Available from: <https://doi.org/10.1002/jsfa.2604>
28. Moon J-K, Shibamoto T. Antioxidant Assays for Plant and Food Components. *J Agric Food Chem* [Internet]. 2009;57(5):1655-66. Available from: <https://doi.org/10.1021/jf803537k>
29. Albahlol F, Khalil M, Ghoniem G, Aboulnaga E. Evaluation of pan bread fortified with sunflower seeds powder. *J Food Dairy Sci* [Internet]. 2022;13(10):139-47. Available from: https://jfds.journals.ekb.eg/article_267528.html

30. Lee M-J, Prabhu S, Meng X, Li C, Yang CS. An Improved Method for the Determination of Green and Black Tea Polyphenols in Biomatrices by High-Performance Liquid Chromatography with Coulometric Array Detection. *Anal Biochem* [Internet]. 2000;279(2):164-9. Available from: <https://doi.org/10.1006/abio.2000.4487>
31. Wahl PR, Hir MLE, Voetseder A, Arcaro A, Strake A, Waekerle-Men Y, et al. Mitotic activation of Akt signalling pathway in Han:SPRD rats with polycystic kidney disease. *Nephrology* [Internet]. 2007;12(4):357-63. Available from: <https://doi.org/10.1111/j.1440-1797.2007.00811.x>
32. Furman BL. Streptozotocin-Induced Diabetic Models in Mice and Rats. *Curr Protoc Pharmacol* [Internet]. 2015;70(1):5.47.1-5.47.20. Available from: <https://doi.org/10.1002/0471141755.ph0547s70>
33. Shin J-W, Seol I-C, Son C-G. Interpretation of animal dose and human equivalent dose for drug development. *J Korean Orient Med*. 2010;31(3):1-7. Available from: [http://www.jkom.org/upload/31-3%2001%20\[01-07\].pdf](http://www.jkom.org/upload/31-3%2001%20[01-07].pdf)
34. Trinder P. Determination of Glucose in Blood Using Glucose Oxidase with an Alternative Oxygen Acceptor. *Ann Clin Biochem Int J Lab Med* [Internet]. 1969;6(1):24-7. Available from: <http://journals.sagepub.com/doi/10.1177/000456326900600108>
35. Young DS, Friedman RB. Effects of disease on clinical laboratory tests. 2001.
36. Tabacco A, Meiattini F, Moda E, Tarli P. Simplified enzymic/colorimetric serum urea nitrogen determination. *Clin Chem* [Internet]. 1979;25(2):336-7. Available from: <http://www.ncbi.nlm.nih.gov/pubmed/759035>
37. Schosinsky KH, Vargas M, Luz Esquivel A, Chavarria MA. Simple spectrophotometric determination of urinary albumin by dye-binding with use of bromphenol blue. *Clin Chem* [Internet]. 1987;33(2):223-6. Available from: <https://doi.org/10.1093/clinchem/33.2.223>
38. Bastaki S. Diabetes mellitus and its treatment. *Int J Diabetes Metab* [Internet]. 2019;13(3):111-34. Available from: <https://doi.org/10.1159/000497580>
39. Gheith O, Farouk N, Nampoory N, Halim MA, Al-Otaibi T. Diabetic kidney disease: world wide difference of prevalence and risk factors. *J nephropharmacology* [Internet]. 2016;5(1):49-56. Available from: <http://www.ncbi.nlm.nih.gov/pubmed/28197499>
40. Fırat U, Kaya S, Çim A, Büyükbayram H, Gökalp O, Dal MS, et al. Increased Caspase-3 Immunoreactivity of Erythrocytes in STZ Diabetic Rats. Galassetti P, editor. *Exp Diabetes Res* [Internet]. 2012;2012:316384. Available from: <https://doi.org/10.1155/2012/316384>
41. Padil VVT, Senan C, Wacławek S, LERNÍK M. Electrospun fibers based on Arabic, karaya and kondagogu gums. *Int J Biol Macromol* [Internet]. 2016;91:299-309. Available from: <https://doi.org/10.1016/j.ijbiomac.2016.05.064>
42. Badal SS, Danesh FR. New Insights Into Molecular Mechanisms of Diabetic Kidney Disease. *Am J Kidney Dis* [Internet]. 2014;63(2, Supplement 2):S63-83. Available from: <https://doi.org/10.1053/j.ajkd.2013.10.047>
43. Vallon V, Thomson SC. Renal Function in Diabetic Disease Models: The Tubular System in the Pathophysiology of the Diabetic Kidney. *Annu Rev Physiol* [Internet]. 2012;74(1):351-75. Available from: <https://www.annualreviews.org/doi/10.1146/annurev-physiol-020911-153333>
44. Lopes GS, Lemos CCS, Mandarim-de-Lacerda CA, Bregman R. Effect of unilateral nephrectomy on renal function of diabetic rats. *Histol Histopathol* [Internet]. 2004; Available from: <https://digitum.um.es/digitum/handle/10201/21618>
45. Forbes JM, Cooper ME. Mechanisms of Diabetic Complications. *Physiol Rev* [Internet]. 2013;93(1):137-88. Available from: <https://doi.org/10.1152/physrev.00045.2011>
46. O' Bryan GT, Hostetter TH. The renal hemodynamic basis of diabetic nephropathy. *Semin Nephrol* [Internet]. 1997;17(2):93-100. Available from: <http://europepmc.org/abstract/MED/9148381>
47. Vallon V, Blantz RC, Thomson S. Glomerular Hyperfiltration and the Salt Paradox in Early Type 1 Diabetes Mellitus: A Tubulo-Centric View. *J Am Soc Nephrol* [Internet]. 2003;14(2):530-37. Available from: https://journals.lww.com/jasn/full-text/2003/02000/glomerular_hyperfiltration_and_the_salt_paradox_in.30.aspx
48. Nath KA, Norby SM. Reactive oxygen species and acute renal failure. *Am J Med* [Internet]. 2000;109(8):665-78. Available from: [https://doi.org/10.1016/S0002-9343\(00\)00612-4](https://doi.org/10.1016/S0002-9343(00)00612-4)
49. Jomova K, Valko M. Advances in metal-induced oxidative stress and human disease. *Toxicology* [Internet]. 2011;283(2):65-87. Available from: <https://doi.org/10.1016/j.tox.2011.03.001>
50. Pingle SC, Mishra S, Marcuzzi A, Bhat SG, Sekino Y, Rybak LP, et al. Osmotic Diuretics Induce Adenosine A1 Receptor Expression and Protect Renal Proximal Tubular Epithelial Cells against Cisplatin-mediated Apoptosis. *J Biol Chem* [Internet]. 2004;279(41):43157-67. Available from: <https://linkinghub.elsevier.com/retrieve/pii/S0021925820770717>
51. Heilig CW, Concepcion LA, Riser BL, Freytag SO, Zhu M, Cortes P. Overexpression of glucose transporters in rat mesangial cells cultured in a normal glucose milieu mimics the diabetic phenotype. *J Clin Invest* [Internet]. 1995;96(4):1802-14. Available from: <http://www.jci.org/articles/view/118226>

52. Lantz RC, Chen GJ, Sarihan M, Sólyom AM, Jolad SD, Timmermann BN. The effect of extracts from ginger rhizome on inflammatory mediator production. *Phytomedicine* [Internet]. 2007;14(2):123-8. Available from: <https://www.sciencedirect.com/science/article/pii/S0944711306000493>
53. Kota N, Krishna P, Polasa K. Alterations in antioxidant status of rats following intake of ginger through diet. *Food Chem* [Internet]. 2008;106(3):991-6. Available from: <https://doi.org/10.1016/j.foodchem.2007.07.073>
54. Panchatcharam M, Miriyala S, Gayathri VS, Suguna L. Curcumin improves wound healing by modulating collagen and decreasing reactive oxygen species. *Mol Cell Biochem* [Internet]. 2006;290(1):87-96. Available from: <https://doi.org/10.1007/s11010-006-9170-2>
55. Shishodia S, Sethi G, Aggarwal BB. Curcumin: Getting Back to the Roots. *Ann N Y Acad Sci* [Internet]. 2005;1056(1):206-17. Available from: <https://doi.org/10.1196/annals.1352.010>
56. Swarnakar S, Ganguly K, Kundu P, Banerjee A, Maity P, Sharma A V. Curcumin Regulates Expression and Activity of Matrix Metalloproteinases 9 and 2 during Prevention and Healing of Indomethacin-induced Gastric Ulcer. *J Biol Chem* [Internet]. 2005;280(10):9409-15. Available from: <https://linkinghub.elsevier.com/retrieve/pii/S0021925819629583>
57. Mani H, Sidhu GS, Kumari R, Gaddipati JP, Seth P, Maheshwari RK. Curcumin differentially regulates TGF- β 1, its receptors and nitric oxide synthase during impaired wound healing. *BioFactors*. 2002;16(1-2):29-43. Available from: <https://content.iospress.com/articles/biofactors/bio00478>
58. Chattopadhyay I, Biswas K, Bandyopadhyay U, Banerjee RK. Turmeric and curcumin: Biological actions and medicinal applications. *Curr Sci* [Internet]. 2004;87(1):44-53. Available from: <http://www.jstor.org/stable/24107978>
59. Horie S, Yamamoto H, Michael GJ, Uchida M, Belai A, Watanabe K, et al. Protective role of vanilloid receptor type 1 in HCl-induced gastric mucosal lesions in rats. *Scand J Gastroenterol* [Internet]. 2004 1;39(4):303-12. Available from: <https://doi.org/10.1080/00365520310008647>
60. el Gammal C, Kligman AM. Pretreatment of Photodamaged Forearm Skin with Topical Tretinoin Accelerates Healing of Full-Thickness Wounds BT - Wound Healing and Skin Physiology. In: Altmeyer P, Hoffmann K, el Gammal S, Hutchinson J, editors. Berlin, Heidelberg: Springer Berlin Heidelberg; 1995. p. 617-30.
61. Sidhu GS, Mani H, Gaddipati JP, Singh AK, Seth P, Banaudha KK, et al. Curcumin enhances wound healing in streptozotocin induced diabetic rats and genetically diabetic mice. *Wound Repair Regen* [Internet]. 1999;7(5):362-74. Available from: <https://doi.org/10.1046/j.1524-475X.1999.00362.x>
62. Jagetia GC, Rajanikant GK. Curcumin Treatment Enhances the Repair and Regeneration of Wounds in Mice Exposed to Hemibody γ -Irradiation. *Plast Reconstr Surg* [Internet]. 2005;115(2):515-28. Available from: https://journals.lww.com/plasrecon-surg/fulltext/2005/02000/curcumin_treatment_enhances_the_repair_and.21.aspx
63. Singer AJ, McClain SA, Romanov A, Rooney J, Zimmerman T. Curcumin Reduces Burn Progression in Rats. *Acad Emerg Med* [Internet]. 2007;14(12):1125-9. Available from: <https://doi.org/10.1197/j.aem.2007.07.012>

ST segment depression in atrioventricular reentrant tachycardia

Jakub Szymon Mercik¹ , Marcin Kuniewicz^{2,3} , Jadwiga

Radziejewska⁴ , Katarzyna Pach⁵ , Dorota Zyśko¹ , Jacek Gajek⁶ 

¹ Department of Emergency Medicine, Wrocław Medical University, Poland

² Department of Electrophysiology, Institute of Cardiology, John Paul II Hospital, Jagiellonian University Medical College, Kraków, Poland

³ Department of Anatomy, Jagiellonian University Medical College, Kraków, Poland

⁴ Kłodzko County Hospital, Kłodzko, Poland

⁵ Students' Scientific Association, Department of Emergency Medical Service, Wrocław Medical University, Poland

⁶ Department of Emergency Medical Service, Wrocław Medical University, Poland

Abstract

Background: ST segment deviation is common in patients with narrow QRS complex tachycardia. It mainly concerns young people in whom ischemic background is unlikely. In our work we would also like to propose another potential mechanism – the overlapping of individual components of the QRS complex. **Material and methods:** The study included 11 patients (7 women and 4 men) with paroxysmal narrow QRS complex tachycardia. An electrophysiological study was performed in all patients, the diagnosis of atrioventricular reentrant tachycardia was established and finally successful RF ablation was done. We measured the individual components of QRS QR, RS and RJ during sinus rhythm and during tachycardia. **Results:** The difference RJ-QR during tachycardia correlated negatively with tachycardia cycle length $T(r = -0.85, p = 0.000831)$. We also showed a significant difference between the amplitude of the RJ segment in tachycardia and during sinus rhythm ($p = 0.005$), at the same time we showed no differences between the amplitude of QR and RS. **Conclusions:** We showed a statistically significant difference in ST segment depression in correlation with the rate of tachycardia in patients with AVRT resulting mainly from the overlapping of individual components of the QRS complex.

Keywords: ST-segment depression • tachycardia with narrow QRS complex • AVRT

Citation

Mercik JS, Kuniewicz M, Radziejewska J, Pach K, Zyśko D, Gajek J. ST segment depression in atrioventricular reentrant tachycardia. Eur J Transl Clin Med. 2023;6(2):66-70.

DOI: [10.31373/ejtcml/172311](https://doi.org/10.31373/ejtcml/172311)

Corresponding author:

Jakub Mercik, Department of Emergency Medicine, Wrocław Medical University, Poland

e-mail: jakub.mercik@wp.pl

Updated: 2024-01-18

Available online: www.ejtcml.gumed.edu.pl

Copyright © Medical University of Gdańsk

This is Open Access article distributed under the terms of the Creative Commons Attribution-ShareAlike 4.0 International.



NO APC OA



Abbreviations

- AV – atrioventricular
- AVNRT – atrioventricular nodal reentry tachycardia
- AVRT – atrioventricular reentrant tachycardia
- ECG – electrocardiogram
- EPS – electrophysiological study

Introduction

ST segment changes are mainly associated with coronary artery disease (CAD). However, in supraventricular tachycardias (SVTs) ST segment changes are common and may affect to 50-60% of patients with atrioventricular nodal reentry tachycardia (AVNRT) and atrioventricular reentrant tachycardia (AVRT) [1]. In patients with AVNRT or AVRT, the change in the ST segment on the electrocardiogram (ECG) most often takes the form of downward oblique deviation [2]. Vast majority of these patients are healthy, young people in whom cardiac ischemia is unlikely [3]. The ST segment changes during episodes of SVT has been discussed many times, but none of these studies demonstrated a clear mechanism responsible for the ST segment deviations [4-5]. In this paper, we discuss the potential explanation of ST segment changes in AVRT. We also propose another potential mechanism – the overlapping of individual components of the QRS-T complex resulting in a change in the baseline reference point and a measurement artifact in the form of ST segment depression.

Materials and methods

11 patients (7 women and 4 men) took part in the study, their average age was about 28 years. All patients underwent an electrophysiological study (EPS), during which the diagnosis of AVRT was made, followed by successful radiofrequency ablation of the accessory pathway was performed. Detailed demographic, clinical, and laboratory data are described in Table 1.

We assessed the ECG analogously to our earlier work on AVNRT [6-7]. Figure 1 shows how the individual components of the QRS complex were measured. Due to the best visibility of the R wave, lead V5 was used for all measurements.

The statistical analysis was performed using the computer program Statistica v. 13.3 (StatSoft Inc., Tulsa, USA). The Shapiro-Wilk W test was used to calculate normality of distribution, we used the Wilcoxon test for dependent groups for comparisons, and the Spearman's test for correlation. The study was approved by the local Bioethical Committee at Wrocław Medical University number KB – 213/2020.

Table 1. Clinical characteristics of studied patients

	Total N = 11
Mean age (years)	28.06 ± 10.16
Male/female	4/7
Comorbidities:	–
HT	1 (9.1%)
DM	0 (0%)
IHD	0 (0%)
CKD	0 (0%)
Laboratory	–
Hemoglobin (mmol/L)	13.57 ± 1,20
K ⁺ (mmol/L)	4.21 ± 0.40
Glucose (mg/dL)	95.04 ± 12.3
Creatinine (mg/dL)	0.7 ± 0.10
TSH (mU/L)	1.75 ± 1.20

HT – arterial hypertension, DM – diabetes mellitus, CKD – chronic kidney disease, IHD – ischemic heart disease, HF – heart failure

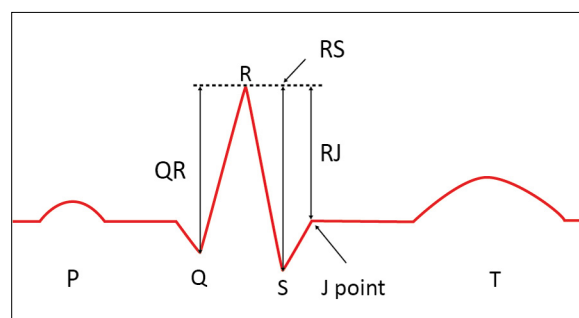


Figure 1. Individual components of the QRS complex

QR segment – the distance between the bottom of the Q wave and the peak of the R wave, RS segment – the distance between the peak of the R wave and the bottom of the S wave, RJ segment – the segment between the peak of the R wave and the J point

Results

ECG parameters are presented in Table 2 and Figure 2. We noted a significant difference between the amplitude of the RJ segment in tachycardia and during sinus rhythm ($p = 0.005$). At the same time we found no differences between the amplitude of QR and RS.

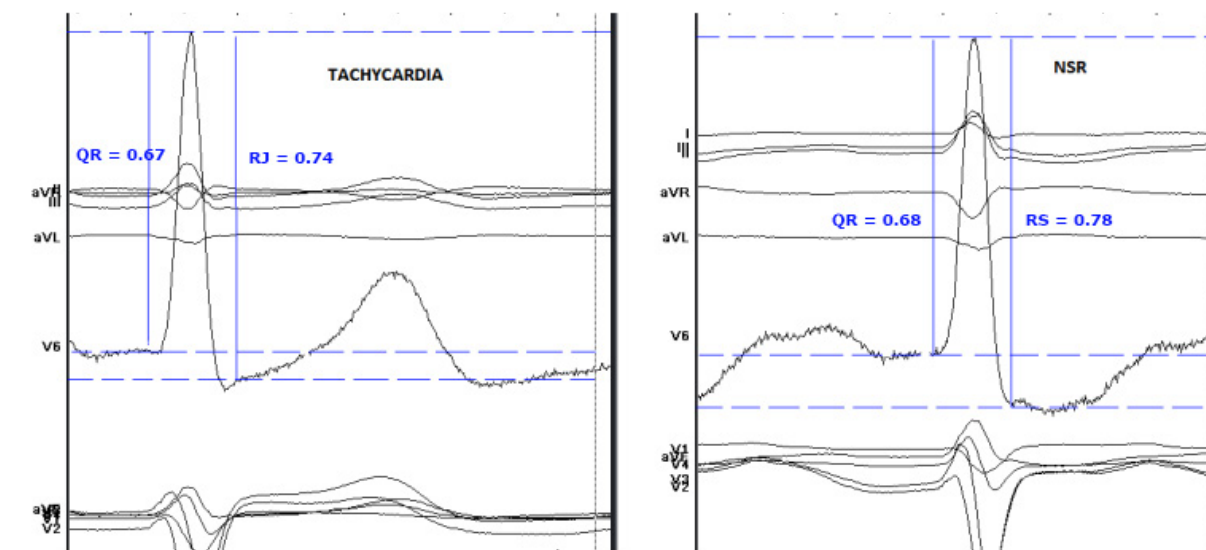


Figure 2. QR and RJ measurements during tachycardia (left panel) and during sinus rhythm (right panel)

NSR – normal sinus rhythm

Table 2. The basic electrocardiographic parameters measurements in sinus rhythm and tachycardia with according differences and statistical test results

	QR(mV)	RS(mV)	RJ(mV)	RJ – QR(mV)	Cycle length (ms)
Tachycardia	1.103 +/- 0.400	1.213 +/- 0.433	1.147 +/- 0.393	0.033 +/- 0.091	329.50 +/- 37.56
Sinus Rhythm	1.065 +/- 0.469	1.189 +/- 0.434	1.064 +/- 0.440	0.010 +/- 0.073	739.55 +/- 179.5
Difference	0.038	0.024	0.083	0.023	—
P	0.575	0.114	0.005	0.207	—

We also showed a significant negative correlation between the tachycardia cycle length and the RJ-QR difference – the faster the arrhythmia, the greater the ST segment denivulation ($r = -0.85$, $p = 0.000831$). During sinus rhythm, there were no significant changes in RJ-QR difference.

A graphical representation of the above-mentioned relationships is shown in Figure 3.

Discussion

In patients with AVRT, there is a phenomenon of ST segment depression. Because this tachycardia affects mainly young people in whom ischemic etiology is unlikely, the most probable cause is a measurement artefact – the overlapping

Table 3. The correlation of RJ-QR in tachycardia and sinus rhythm with tachycardia cycle length

Parameters	Heart rate in tachycardia Spearman correlation rank
RJ-QR Tachycardia	$r = -0,85$, $p = 0,000831^*$
RJ-QR Sinus Rhythm	$r = -0,50$, $p = 0,074$

In the graph on the left there is a strong dependence of RJ-QR on tachycardia, while during sinus rhythm (graph on the right) this relationship is not statistically significant (although its values are close to the level of statistical significance).

of individual components of the QRS complex and elevation of the baseline, a retrograde P wave or QRS alternans [1].

ST segment depression during SVT is well-documented in the literature [4-5]. These changes usually resolve when

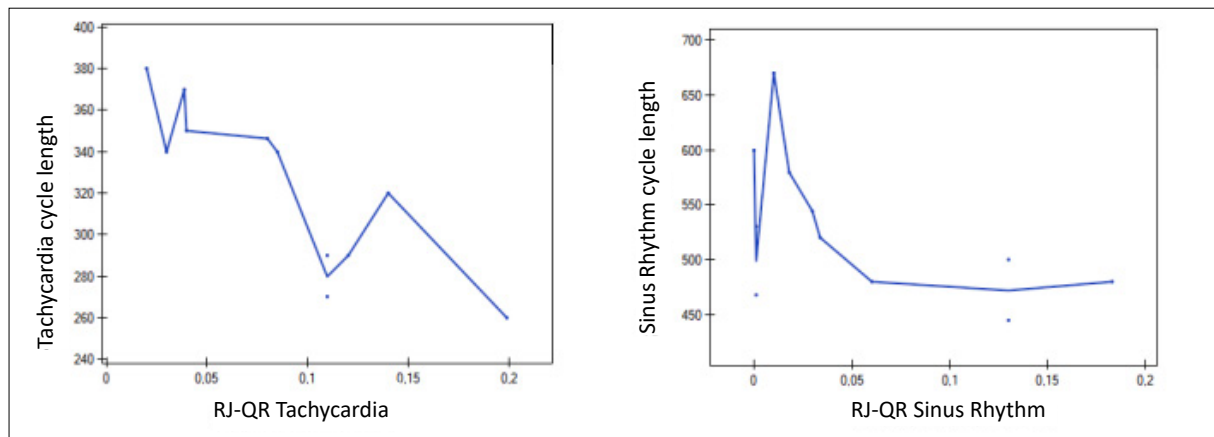


Figure 3. A graphical representation of the above-mentioned dependencies: RJ-QR (mV) during tachycardia (ms) (left panel) and during sinus rhythm (ms) (right panel)

sinus rhythm is restored, although it has been reported that ST-segment depression may persist and is not associated with CAD-related myocardial damage [3].

Dorenkamp et al. concluded that there is no correlation between the presence of CAD and ST segment depression in ECG of patients with paroxysmal SVT [1]. The same percentage of people with ST segment depression was observed both among patients with significant narrowing in the coronary vessels and in patients with normal coronary angiography results.

In our study, we demonstrated a positive correlation between ST segment depression and arrhythmia rate. The shorter the arrhythmia cycle, the greater the overlap of the T wave of the previous QRS complex with the next QRS complex, which causes a rise the baseline and may give the impression of ST segment depression. We proposed a similar explanation for the AVNRT in another article [6].

During fast AVRT, in some patients there is an QRS alternans. Due to the dynamic change in the amplitude of all components of the QRS complex (QR, RS, RJ) from beat to beat, there is a change in the baseline, which may look like a depression of the ST segment. The QRS alternans in AVRT has not been explained, some studies suggest intraventricular conduction disturbances as the cause of this phenomenon [6]. In our study, unfortunately, we did not have patients with QRS alternans during orthodromic tachycardia.

A retrograde P wave occurs during AVRT. In orthodromic AVRT, the interval between the QRS complex and the retrograde P wave should be at least 70 ms, depending on the electrophysiological properties of the accessory pathway and the location between pathway and AV node [7]. For this reason, the retrograde P wave is projected onto the ST segment or the T wave. This may cause ST segment depression, which looks like its denivelations, likewise to myocardial ischemia. Riviera et al reached similar conclusions [8].

When considering the spatiotemporal relationships of retrograde atrial activation during AVRT, the possible locations of accessory pathways should be considered [9]. Viewed from the V5 lead, the left-sided accessory pathways generate retrograde P waves that will be negative, inducing a lowering of the J point and ST-segment in this lead. Right lateral pathways cause opposite changes inducing the relative elevation of the J point and the ST segment of the electrocardiogram in lead V5. Septal tracts induce similar changes, as activation of the left atrium electrically prevails over activation of the right atrium, but in this location the retrograde P wave is exceptionally short, which means that, depending on the speed of retrograde conduction, the change in a targeted manner may influence the J point or a fragment of the ST segment. Posterior pathways, depending on the location, can affect the described phenomenon in different ways. Therefore, in the case of our results, obtained in a relatively small study group, the relationships described do not have to be unambiguous. A probabilistic conclusion may be that the relationship described earlier is true, modified only by the influence of the retrograde P wave depending on the location of the accessory pathway [10-11].

Limitations

This is a single-center study conducted in a small group of patients. Because AVRT is a rare arrhythmia, there are significant difficulties in gathering a larger group of patients. None of the patients had coronary angiography performed to completely exclude the ischemic cause of ST segment changes. In addition, there was no exercise test performed and no pacing with the arrhythmia rate during the EPS to reproduce the baseline conditions during arrhythmia.

Conclusions

The cause of ST-T segment changes during AVRT remains unexplained. In this paper we propose a fairly simple but important explanation. The concept of ST segment change as a measurement artifact resulting from the overlapping of individual components of the QRS-T complex in AVRT has not been described in the literature so far. More research is needed to confirm this concept and to search for other potential mechanisms.

Conflicts of interest

None to report.

Funding

Not applicable.

References

1. Dorenkamp M, Zabel M, Sticherling C. Role of coronary angiography before radiofrequency ablation in patients presenting with paroxysmal supraventricular tachycardia. *J Cardiovasc Pharmacol Ther* [Internet]. 2007;12(2):137-44. Available from: <https://doi.org/10.1177/10742484073007752>
2. Habash F, Albashaireh A, Madmani ME, Paydak H. ST segment elevation and depressions in supraventricular tachycardia without coronary artery disease. Rodriguez AE, editor. *Case Reports Cardiol* [Internet]. 2018;2716312. Available from: <https://doi.org/10.1155/2018/2716312>
3. Elikowski W, Baszko A, Wróblewski D, Słomczyński M, Małek M. [Supraventricular tachycardia as a cause of elevated troponin I in a patient with normal coronary arteries]. *Pol Merkuriusz Lekarski* [Internet]. 2005;18(108):696-9. Available from: <http://www.ncbi.nlm.nih.gov/pubmed/16124386>
4. Nelson SD, Kou WH, Annesley T, de Buitelir M, Morady F. Significance of ST segment depression during paroxysmal supraventricular tachycardia. *J Am Coll Cardiol* [Internet]. 1988;12(2):383-7. Available from: <http://www.ncbi.nlm.nih.gov/pubmed/3392331>
5. Habash F, Albashaireh A, Madmani ME, Paydak H. ST segment elevation and depressions in supraventricular tachycardia without coronary artery disease. *Case reports Cardiol* [Internet]. 2018;2716312. Available from: <http://www.ncbi.nlm.nih.gov/pubmed/30647973>
6. Mercik J, Radziejewska J, Pach K, Zawadzki G, Zyśko D, Gajek J. ST-segment depression in atrioventricular nodal reentrant tachycardia: Important finding or just an artifact? *Medicine (Baltimore)* [Internet]. 2022;101(49):e31806. Available from: <https://journals.lww.com/10.1097/MD.00000000000031806>
7. Mercik J, Radziejewska J, Pach K, Zyśko D, Gajek J. ST-segment depression in atrioventricular nodal reentrant tachycardia: Preliminary results. *Adv Clin Exp Med* [Internet]. 2021;30(12):1323-8. Available from: <https://advances.umw.edu.pl/en/article/2021/30/12/1323/>
8. Roten L, Delacrétaiz E. QRS alternans and cycle length oscillation during narrow QRS tachycardia. *EP Eur* [Internet]. 2008;10(6):778. Available from: <https://doi.org/10.1093/europace/eun116>
9. Obel OA, Camm AJ. Accessory pathway reciprocating tachycardia. *Eur Heart J* [Internet]. 1998;19 Suppl E:E13-24, E50-1. Available from: <http://www.ncbi.nlm.nih.gov/pubmed/9717020>
10. Rivera S, Paz Ricapito MD LA, Conde D, Verdu MB, Roux JF, Paredes FA. The retrograde p-wave theory: explaining ST segment depression in supraventricular tachycardia by retrograde AV node conduction. *Pacing Clin Electrophysiol* [Internet]. 2014;37(9):1100-5. Available from: <https://onlinelibrary.wiley.com/doi/10.1111/pace.12394>
11. Ching-Tai T, Shih-Ann C, Chern-En C, Shih-Huang L, Zu-Chi W, Chuen-Wang C, et al. A new electrocardiographic algorithm using retrograde p waves for differentiating atrioventricular node reentrant tachycardia from atrioventricular reciprocating tachycardia mediated by concealed accessory pathway. *J Am Coll Cardiol* [Internet]. 1997;29(2):394-402. Available from: [https://doi.org/10.1016/S0735-1097\(96\)00490-1](https://doi.org/10.1016/S0735-1097(96)00490-1)

Internet searching may predict novel symptoms, but not new outbreaks. A long-term evaluation of infoveillance in COVID-19

Jakub Aleksander Radziwon¹ , Maciej Lubiejewski² , Przemysław Waszak³ , Zbigniew Heleniak⁴ , Maria Alicja Dębska-Ślizień⁴ 

¹ Scientific Circle of Adult Neurology, Medical University of Gdańsk, Poland

² Student Scientific Group of Nephrology, Department of Nephrology, Transplantology and Internal Diseases, Medical University of Gdańsk, Poland

³ Department of Hygiene and Epidemiology, Medical University of Gdańsk, Poland

⁴ Department of Nephrology, Transplantology and Internal Diseases, Medical University of Gdańsk, Poland

Abstract

Background: At the beginning of COVID-19 pandemic authors in several countries reported the possibility of predicting disease outbreaks using internet analysis and search tools like GoogleTrends™. Our aim was to investigate the impact of changes in COVID-19 symptomatology and pandemic intensity on those predictions. **Material and methods:** GoogleTrends™ was utilized to track online searches for COVID-19 symptoms in Poland during two years of the pandemic. Search volumes were then assessed for correlation with daily cases in each wave of infection separately. **Results:** The symptoms that correlated strongly with new cases were anosmia and ageusia (Spearman's rho = 0.5230 and rho = 0.4483 respectively, $p < 0.01$). Searches for these symptoms preceded an outbreak by 12 days during the first wave of infections, but this gap was later shortened to five days. The frequency of searching for these symptoms markedly diminished during the last phase and was no longer adequate. Stronger correlations were then shown for fever, sore throat, and headache. **Conclusions:** In conclusion, COVID-19 case prediction using GoogleTrends™ did not remain possible later on in the pandemic course. However, noticeable changes reflecting novel features of emerging SARS-CoV-2 variants were observed. Therefore, monitoring symptom changes and virus evolution might be a promising application of internet search analysis in the future.

Keywords: prediction • COVID-19 • infodemiology

Corresponding author:

Jakub Aleksander Radziwon, Scientific Circle of Adult Neurology, Medical University of Gdańsk, Poland

e-mail: j.radziwon@gumed.edu.pl

Available online: www.ejtcgumed.edu.pl

Copyright © Medical University of Gdańsk

This is Open Access article distributed under the terms of the Creative Commons Attribution-ShareAlike 4.0 International.



Citation

Radziwon JA, Lubiejewski M, Waszak P, Heleniak Z, Dębska-Ślizień MA. Internet searching may predict novel symptoms, but not new outbreaks. A long-term evaluation of infoveillance in COVID-19. *Eur J Transl Clin Med*. 2023;6(2):71-77.

DOI: [10.31373/ejtc/173451](https://doi.org/10.31373/ejtc/173451)

Introduction

As an emerging field of science, infodemiology aims to analyze internet data in order to uncover useful information about public health [1]. Before the era of the Severe Acute Respiratory Syndrome Virus 2 (SARS-CoV-2) pandemic, infodemiology was predominantly involved in the fields of infectious diseases and mental health [2]. Implementation of novel techniques for the surveillance of contagious diseases seems extremely advantageous nowadays and such an approach is called infoveillance [3]. Recently, investigations early in the pandemic demonstrated the possibility of recognizing new Coronavirus Disease 2019 (COVID-19) symptoms [4] and pointed toward the possibility of monitoring the pandemic using the Google Trends™ (GT) web tool [5-6]. This method enables the monitoring of anonymized internet users' searches related to various public health issues. Searching for any selected term is divided by number of all searches in the area and presented as a relative number with its temporal variation [7]. Early escalation in those values, representing increased public interest in COVID-19-related topics was considered an early sign of a forthcoming outbreak [5]. However, the major part of these data are from the initial period of the pandemic, within the first year since the global outbreak [8]. Therefore, the aim of our study was to investigate whether this internet tool can still be useful, despite substantial changes of pandemic course and the evolution of the SARS-CoV-2 virus itself.

Methods

GT data are presented as a relative search volume (RSV) – a number from 0 to 100 representing the relative intensity of searching [1]. Absolute numbers of searches are not available, while RSVs are a fraction of selected phrase searching in all the searches recorded in the particular region. In GT one phrase could be searched as a topic (group of similar terms and translations predefined by the platform operator) or a term (an exact word or combination of words).

Relative search volumes have been acquired for 4 topics ("Coronavirus", "Coronavirus disease 2019", "COVID-19 testing", "COVID-19 vaccine") and 13 search terms describing the symptoms (fever, cough, dyspnea, fatigue, muscle aches, headache, loss of smell (anosmia), loss of taste (ageusia), sore throat, nasal congestion, rhinorrhea, nausea, diarrhea). All phrases were searched in the Polish language, the area of interest was set to Poland and "all categories" were selected. The interval in which the data are shown depends on the selected period of observation [1]. Therefore, to cover the 2 years of the pandemic in daily intervals, the extraction of data was divided into four periods (01.03 – 30.09.2020; 01.10.2020 – 30.04.2021; 01.05 – 30.11.2021; 01.12.2021 – 30.06.2022). One term was checked in each query for all four periods, which provided proportional values for comparison between periods, but not between terms. We followed the guidelines for reporting GT medical research [2]. Numbers of new cases, number of SARS-CoV-2 tests conducted and vaccination numbers were obtained from the 'Our World in Data' database, which contains data from the official government reports [9].

For analysis, the data was further divided into five periods, one for each "wave" of SARS-CoV-2 infection reported in Poland. We adopted the following numeration: wave "0" for the initial period of the COVID-19 pandemic in Poland (when the number of cases remained relatively low) and consecutive numbers for the major peaks of infection rates. The specific timeframes were: 01.03.2020 – 31.05.2020, 01.10.2020 – 31.01.2021, 01.02.2021 – 31.05.2021, 1.10.2021 – 31.12.2021, 01.01.2022 – 31.03.2022.

RSVs were tested for correlation with the daily number of cases diagnosed or tests and vaccinations performed. Models for 3, 5, 7, 9, 10, 12, and 14-day time lags between searching and diagnosis were tested to find the best-fitting model for each wave separately. Statistical analyses were conducted using the Statistica 13 Software (TIBCO Software Inc., CA, USA). The distribution of all data was assessed using the Kolmogorov-Smirnov test and further analyzed using the non-parametric Spearman's correlation test as RSVs generally follow a non-normal distribution. The significance level was set at $\alpha = 0.05$.

Only publicly available internet resources were used in this study. Individual patient data was not analyzed and therefore the Ethical Committee approval was not required.

Results

Searches for the topic 'COVID-19' closely correlated with the distribution of reported cases, while the topic 'Coronavirus' was prominent mostly during the first weeks

of the pandemic. Searching for 'COVID-19 testing' correlated very strongly with the number of SARS-CoV-2 tests conducted ($r_s = 0.9088$, $p < 0.01$) and RSV of 'COVID-19 vaccine' with the volume of new vaccinations ($r_s = 0.6644$, $p < 0.01$). A significant positive correlation between the RSV and the recorded new cases have been found regarding 0, 5, 7, 4 and 7 symptoms in each wave respectively, while the most distinguished pattern was presented by the symptoms anosmia and ageusia (Table 1). Correlation coefficients were highest in the model in which searching for

Table 1. Results of Spearman's rank-order correlation test between search volumes of symptoms and daily detected COVID-19 cases

Symptom	Entire study period 01.03.2020 – 31.03.2022	Wave 0 01.03.2020 – 31.05.2020	Wave 1 01.06.2020 – 31.01.2021	Wave 2 01.02.2021 – 31.05.2021	Wave 3 01.10.2021 – 31.12.2021	Wave 4 01.01.2022 – 30.06.2022
Fever	0.269	-0.683	0.354	0.361	0.255	0.531
Cough	0.375	-0.698	0.355	0.518	-0.492	0.354
Dyspnea	0.067	-0.002	0.008	0.036	0.036	0.036
Fatigue	0.097	-0.001	-0.042	0.016	-0.073	-0.007
Muscle aches	0.175	-0.162	0.020	0.115	0.053	0.174
Headache	0.450	-0.408	0.304	0.509	0.068	0.432
Ageusia	0.448	-0.106	0.425	0.314	0.474	0.233
Anosmia	0.523	0.116	0.398	0.579	0.515	0.195
Sore throat	0.198	-0.640	-0.043	0.295	0.075	0.484
Nasal congestion	0.371	-0.227	0.108	0.154	0.262	0.398
Coryza	0.277	-0.648	-0.039	0.087	-0.227	0.018
Nausea	0.153	-0.084	0.041	0.069	0.178	0.206
Diarrhea	0.194	-0.357	0.061	0.299	-0.004	0.290

Correlation coefficients were calculated for the whole observation period, as well as for each wave of infections separately. Statistically significant ($p < 0.05$) values are bolded.

Table 2. The best-fitted time lag models for prediction of wave outbreak

Symptom	Wave 0 01.03.2020– 31.05.2020	Wave 1 01.10.2020– 31.01.2021	Wave 2 01.02.2021 – 31.05.2021	Wave 3 01.10.2021 – 31.12.2021	Wave 4 01.01.2021 – 30.06.2022
Fever	12	12	5	12	5
Cough	14	12	12	12	12
Dyspnea	5	5	3	10	12
Fatigue	7	10	0	3	10
Muscle aches	9	12	3	14	5
Headache	14	5	5	12	14
Ageusia	7	12	5	10	5
Anosmia	9	12	5	7	5
Sore throat	14	12	7	5	5
Nasal congestion	5	10	3	0	5
Coryza	14	12	12	5	12
Nausea	10	9	5	0	12
Diarrhea	12	10	5	14	5
Median	10	12	5	10	5

Values in the table represent the number of days between increased searching for a particular symptom and a rise in COVID-19 cases.

these terms was followed by a 12-day lag period to a subsequent outbreak in the first wave. However, later in the pandemic, these terms were searched with only 5-day lag (2nd and 4th wave). Fever and cough were other symptoms searched for in the same way. Fever RSVs were correlated moderately with new cases, but higher after application of different time lags (12 days for 0, 1st and 3rd wave and 5 days for 2nd and 4th wave). Cough presented positive correlation in waves 1, 2, 4 but negative during 3rd wave. During the “0” wave, the majority of symptoms presented a negative correlation due to low and stable COVID-19 counts and RSVs diminishing after initially high interest. The most appropriate time lag for each symptom in the subsequent waves is presented in Table 2.

Other symptoms showed various distribution across pandemic waves. Until late 2021, the symptoms that most prominently correlated with new cases were “ageusia” and “anosmia”. However, the 4th wave was connected to

a different set of symptoms, including “fever”, which was the most correlated term, along with “sore throat”, “headache” and “nasal congestion”. Changes in the symptom searching and the highly correlated symptoms across the pandemic’s waves are shown on Figure 1.

Discussion

It is clear from the distribution of search volumes in the current study that searching for COVID-related news and symptoms was a common activity in recent months and more-less resembled the dynamic of ongoing pandemic. Indeed, the most disease-specific symptoms such as anosmia and ageusia were primarily searched in line with patterns of virus transmission. Henry et al [10], demonstrated that search volumes for “anosmia” and “ageusia” could almost perfectly predict a proceeding COVID-19 outbreak in

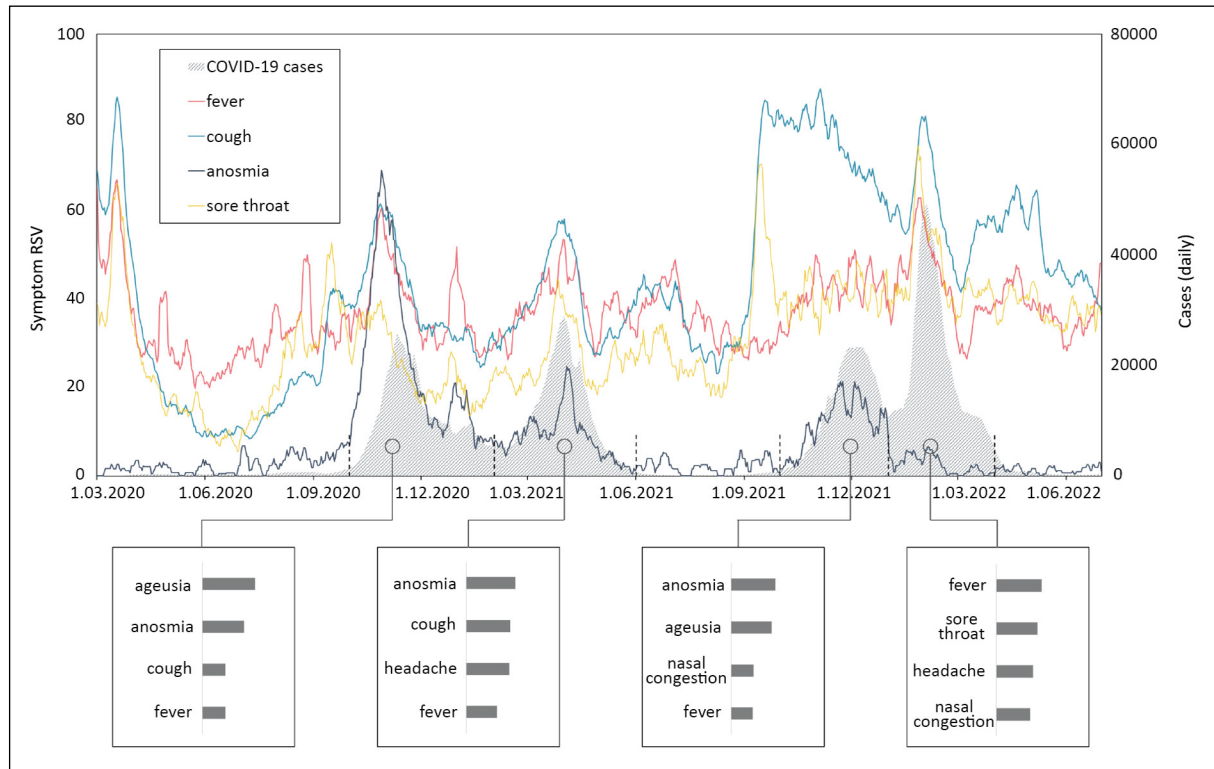


Figure 1. Relative Search Volumes of characteristic symptoms across the study period. Daily new COVID-19 cases are marked by grey area, while relative search volumes (RSVs) of selected symptoms are in color lines. Investigated wave periods are separated by dashed lines on the horizontal axis. Symptoms presenting the highest correlation coefficients in each wave are listed in the brackets below with the bar length representing correlation coefficient proportionally.

Poland within the next 1-week or 2-weeks. Based on daily data, our results revealed that a 12-day delay was more accurate, however this time lag was only observable in 2020. Several months later, these symptoms were searched just 5 days before an outbreak and searching for them almost completely stopped in the spring of 2022. Case prediction based on other symptoms was less accurate, as they occur in many different diseases, including non-infectious and chronic. The role of these symptoms was seldom analyzed in COVID-19 infodemiology research [11] and our study confirms their low suitability for this purpose. For instance, searches for “cough” peaked during COVID-19 waves in 2020 as well as independently of them in September 2021 and April 2022. During the heaviest restrictions in 2020 and 2021 (corresponding to waves 0, 1 and 2 in our study), the circulation of other viruses diminished [12] and searches for common symptoms were more likely to be related to COVID-19 infections, however this was no longer the case in the following months. The issue of low viability of GT in tracking COVID-19 was already raised by Asseo et al. [13] and our long-term observations support their findings.

On the other hand, a shift in symptom searches was manifested in following phases with a diminishing interest in “anosmia” and “ageusia” and an increasing frequency

of “fever”, “sore throat”, and “nasal congestion” searches. These results reflect the substantial change in the prevalence of symptoms noted with the emergence of the Omicron variant. The most frequent symptoms prior to its outbreak were fatigue, headache, cough, and impaired smell or taste, but those infected later were more likely to present with rhinorrhea, sore throat, and fever [14]. Another change was the incubation period of the virus: 5-6 days on average for the ancestral strain, while for the Delta variant it was ~4 days and 3 days for the Omicron [15]. Our results are in line with these reports, as the median time lag for positively-correlated symptoms was 12 days in the Fall of 2020 and decreased to 5 days during the Omicron wave. However, this might also be attributed to greater public awareness, faster recognition of symptoms, and increased availability of testing.

Despite its potential, GT does raise some credibility issues that researchers should be aware of. Foremost, an association between searches and the actual incidence of illnesses remains to be defined and may vary by disease, region and observation period. Furthermore, search data are generally prone to overestimation when there is intense media coverage of the topic [16]. This was the case of the 0 wave in our study, when people were intensively

searching for COVID-19 information, despite the relatively low incidence at that time. It appears that internet search data analysis is an important and promising method, however more complex approaches to building epidemiological models are required to accurately anticipate the spread of infectious agents. Our data shows that the current approach can help predict the general occurrence of an increased spread or changes in symptomatology, however, a precise estimation of cases is not possible by using Google Trends alone. A combination of data from different search engines and social media data, potentially combined and calculated by artificial intelligence, may help to recognize danger quickly [17]. Surely, the future of epidemiology will be based on digital tools to a great extent. Infectious diseases surveillance based on internet sources, molecular sewage monitoring or mobile data tracking has been proven useful before [18-19]. We believe that the possibilities of big data processing and artificial intelligence implementation, instead of individual clinical data may be faster, more accurate and valuable for public health.

Conclusions

The suitability of Google Trends™ analysis for case prediction in infectious diseases is not universal and heavily depends on the proper timing and selection of keywords. This approach may provide overestimation and inaccurate forecasts. Nevertheless, monitoring early changes such as the incubation period and new symptoms of previously known diseases may be a promising application for infodemiology in the future.

Conflicts of interest

None to report.

Funding

Not applicable.

References

1. Mavragani A, Ochoa G. Google Trends in Infodemiology and Infoveillance: Methodology Framework. JMIR Public Heal Surveill [Internet]. 2019;5(2):e13439. Available from: <http://publichealth.jmir.org/2019/2/e13439/>
2. Nuti S V., Wayda B, Ranasinghe I, Wang S, Dreyer RP, Chen SI, et al. The Use of Google Trends in Health Care Research: A Systematic Review. Voracek M, editor. PLoS One [Internet]. 2014;9(10):e109583. Available from: <https://dx.plos.org/10.1371/journal.pone.0109583>
3. Eysenbach G. Infodemiology and Infoveillance: Framework for an Emerging Set of Public Health Informatics Methods to Analyze Search, Communication and Publication Behavior on the Internet. J Med Internet Res [Internet]. 2009;11(1):e11. Available from: <http://www.jmir.org/2009/1/e11>
4. Walker A, Hopkins C, Surda P. Use of Google Trends to investigate loss-of-smell-related searches during the COVID-19 outbreak. Int Forum Allergy Rhinol [Internet]. 2020;10(7):839–47. Available from: <https://onlinelibrary.wiley.com/doi/10.1002/alr.22580>
5. Effenberger M, Kronbichler A, Shin J II, Mayer G, Tilg H, Perco P. Association of the COVID-19 pandemic with Internet Search Volumes: A Google Trends™ Analysis. Int J Infect Dis [Internet]. 2020;95:192–7. Available from: <https://linkinghub.elsevier.com/retrieve/pii/S1201971220302496>
6. Mavragani A. Tracking COVID-19 in Europe: Infodemiology Approach. JMIR Public Heal Surveill [Internet]. 2020;6(2):e18941. Available from: <http://publichealth.jmir.org/2020/2/e18941/>
7. Basics of Google Trends. Google News Initiative [Internet]. 2023 [cited 2023 Sep 26]. Available from: <https://newsinitiative.withgoogle.com/pl-pl/resources/trainings/basics-of-google-trends/>
8. Springer S, Zieger M, Strzelecki A. The rise of infodemiology and infoveillance during COVID-19 crisis. One Heal [Internet]. 2021;13:100288. Available from: <https://www.sciencedirect.com/science/article/pii/S2352771421000781>
9. Mathieu E, Ritchie H, Rod s-Guirao L, Appel C, Gavrilov D, Giattino C, et al. Coronavirus Pandemic (COVID-19) [Internet]. Our World in Data. 2020 [cited 2022 Oct 9]. Available from: <https://ourworldindata.org/coronavirus>
10. Henry BM, Szergyuk I, Santos de Oliveira MH, Lippi G, Juszczyk G, Mikos M. Utility of Google Trends in anticipating Coronavirus Disease 2019 (COVID-19) outbreaks in Poland. Polish Arch Intern Med [Internet]. 2021 Mar 26; Available from: <https://www.mp.pl/paim/issue/article/15894>
11. Yousefinaghani S, Dara R, Mubareka S, Sharif S. Prediction of COVID-19 Waves Using Social Media and Google Search: A Case Study of the US and Canada. Front Public Heal [Internet]. 2021;9. Available from: <https://www.frontiersin.org/articles/10.3389/fpubh.2021.656635/full>

12. Chow EJ, Uyeki TM, Chu HY. The effects of the COVID-19 pandemic on community respiratory virus activity. *Nat Rev Microbiol* [Internet]. 2023;21(3):195–210. Available from: <https://doi.org/10.1038/s41579-022-00807-9>
13. Asseo K, Fierro F, Slavutsky Y, Frasnelli J, Niv MY. Tracking COVID-19 using taste and smell loss Google searches is not a reliable strategy. *Sci Rep* [Internet]. 2020;10(1):20527. Available from: <https://www.nature.com/articles/s41598-020-77316-3>
14. Schulze H, Bayer W. Changes in Symptoms Experienced by SARS-CoV-2-Infected Individuals – From the First Wave to the Omicron Variant. *Front Virol* [Internet]. 2022;2. Available from: <https://www.frontiersin.org/articles/10.3389/fviro.2022.880707/full>
15. Infection [Internet]. European Centre for Disease Prevention and Control. An agency of the European Union. [cited 2022 Oct 31]. Available from: <https://www.ecdc.europa.eu/en/covid-19/latest-evidence/infection>
16. Butler D. When Google got flu wrong: US outbreak foxes a leading web-based method for tracking seasonal flu. *Nature* [Internet]. 2013 Oct 24;494:155–6. Available from: <https://link.gale.com/apps/doc/A319614599/HRCA?u=anon~179f8fd3&sid=googleScholar&xid=6d3dccfb>
17. White BK, Gombert A, Nguyen T, Yau B, Ishizumi A, Kirchner L, et al. Using Machine Learning Technology (Early Artificial Intelligence–Supported Response With Social Listening Platform) to Enhance Digital Social Understanding for the COVID-19 Infodemic: Development and Implementation Study. *JMIR Infodemiology* [Internet]. 2023 Aug 21;3:e47317. Available from: <https://infodemiology.jmir.org/2023/1/e47317>
18. van Boven M, Hetebrij WA, Swart A, Nagelkerke E, van der Beek RF, Stouten S, et al. Patterns of SARS-CoV-2 circulation revealed by a nationwide sewage surveillance programme, the Netherlands, August 2020 to February 2022. *Eurosurveillance* [Internet]. 2023 Jun 22;28(25). Available from: <https://www.eurosurveillance.org/content/10.2807/1560-7917.ES.2023.28.25.2200700>
19. Murray J, Cohen AL. Infectious Disease Surveillance. In: *International Encyclopedia of Public Health* [Internet]. Elsevier; 2017. p. 222–9. Available from: <https://linkinghub.elsevier.com/retrieve/pii/B9780128036785005178>

Interdisciplinary interventional and physiotherapy management of facet joint syndrome

Maciej Broda¹, Julia Miler², Konrad Jankowski², Bartosz Rogowski²,
Mateusz Krakowiak¹ , Paweł Sokal¹ 

¹Department of Neurosurgery and Neurology, Collegium Medicum in Bydgoszcz, Nicolaus Copernicus University, Poland

²Students' Scientific Circle "Neurorehabilitation" at the Department of Neurosurgery and Neurology, Jan Bizioł University Hospital Nr 2, Bydgoszcz, Poland

Abstract

Low back-pain is the most common pain syndrome. Radiofrequency facet denervation (RFD) is a minimally invasive method of treatment of chronic low back pain caused by facet joint syndrome. In this procedure electric current with frequency of radio waves are used to cause thermal injury to a small branch nerve that innervates painful facets. There are numerous studies confirming the effectiveness of this therapy. A good outcome of RFD can be sustained by appropriate and regular exercise. The aim of this article is to recommend such a program of exercises focused on strengthening the muscles and improving stabilization of the lumbar spine.

Keywords: low-back pain • facet joint syndrome • radiofrequency facets denervation • physiotherapy

Citation

Broda M, Miler J, Jankowski K, Rogowski B, Krakowiak M, Sokal P. Interdisciplinary interventional and physiotherapy management of facet joint syndrome. Eur J Transl Clin Med. 2023;6(2):78-84.

DOI: [10.31373/ejtcmm/163576](https://doi.org/10.31373/ejtcmm/163576)

Abbreviations

- LBP – low-back pain
- IJ – intervertebral joints
- FJS – facet joint syndrome
- RFD – lumbar radiofrequency denervation

Introduction

Low-back pain (LBP) is the most common pain syndrome. Diagnosing the cause of LBP is challenging due to its numerous etiologies. Maas et al. reported that lower back pain was classified as “non-specific” in 85-90% of cases [1].

Corresponding author:

Mateusz Krakowiak, Department of Neurosurgery and Neurology, Collegium Medicum in Bydgoszcz, Nicolaus Copernicus University, Poland

e-mail: mateusz.krakowiak@gmail.com

Available online: www.ejtcmm.gumed.edu.pl

Copyright © Medical University of Gdańsk

This is Open Access article distributed under the terms of the Creative Commons Attribution-ShareAlike 4.0 International.



NO APC

OA



LBP is the second most common reason for years lived with disability [2]. Rubin described that 50-80% of adults experience back pain at least once in their lifetime and 15-20% of adults struggle with back pain at least once a year [3]. Frosch et al. indicated that the prevalence of non-specific back pain was increasing among children and adolescents [4]. Yang et al. reported that that 80% of adolescents with LBP could not be clearly diagnosed within a year and the most common final diagnoses were muscle cramps, scoliosis, lumbar degenerative disc disease or disc herniation [5]. Andersson reported that > 50% cases of LBP resolved spontaneously within 2-4 weeks and 90% by 12 weeks. In another study, he reported that 60-70% recovered within 6 weeks and 80-90% in 12 weeks [6]. In another study, spontaneous resolution of LBP of disc origin occurred after 2.33 ± 1.23 months [7]. In their review Chiu et al. reported that the rate of spontaneous resolution of lower back pain was to be 96% for disc sequestration, 70% for disc extrusion, 41% for disc protrusion, and 13% for disc bulging and the rate of complete resolution of disc herniation was 43% for sequestered discs and 15% for extruded discs [8].

A significant number of employees complain of back pain and it is one of the main reasons for absence or resignation from work. Based on data from ZUS (Zakład Ubezpieczeń Społecznych, the institution responsible for social insurance in Poland), cervical pain was the main reason for work absence (51% of employees in Poland), 34% cited LBP and 18% cited thoracic spine pain [9]. The statistical age of patients who seek medical consult due to back pain is systematically decreasing in Poland. The average Polish patient with medically confirmed back pain is currently on average 46 years of age (age ranged from 7 to 95 years of age [9]). Statistics from other European countries show that 10-15% of sick leave from work is due to back pain [6]. Stewart et al. indicate that in the United States LBP is the second most common cause of absenteeism/lost productive time (right after headache) due to pain [10]. Savari et al. showed that the most common reasons for work absence (after respiratory system diseases) were skeletal system diseases (neck and back pains accounted for 12.3% of absences at work) and the most predisposed group was age 20-39 years [11]. The above data clearly shows the scale of the problem that affects our society.

Facet joint syndrome versus radicular pain

When diagnosing a patient, the source of the LBP must be correctly located, which increases the chances of success treatment results. The intervertebral joints (IJ) of the lumbar spine are a common source of pain, accounting for 15-45% of cases apart from other structures like intervertebral discs, sacroiliac joints, and nerve roots [12]. Osteoarthritis of the lumbar spine is the most common cause of intervertebral joint pain (Figure 1). Facet joint syndrome (FJS), also known as facet joint disease, is associated with local pain in the lower back, rarely radiating to the leg. The causes of FJS are: heavy physical work, scoliosis, spondylolisthesis and obesity [13]. It is noteworthy that not every case of chronic LBP originates in the IJ. FJS is related to age and occurs most commonly between the ages of 51 and 60 [12].

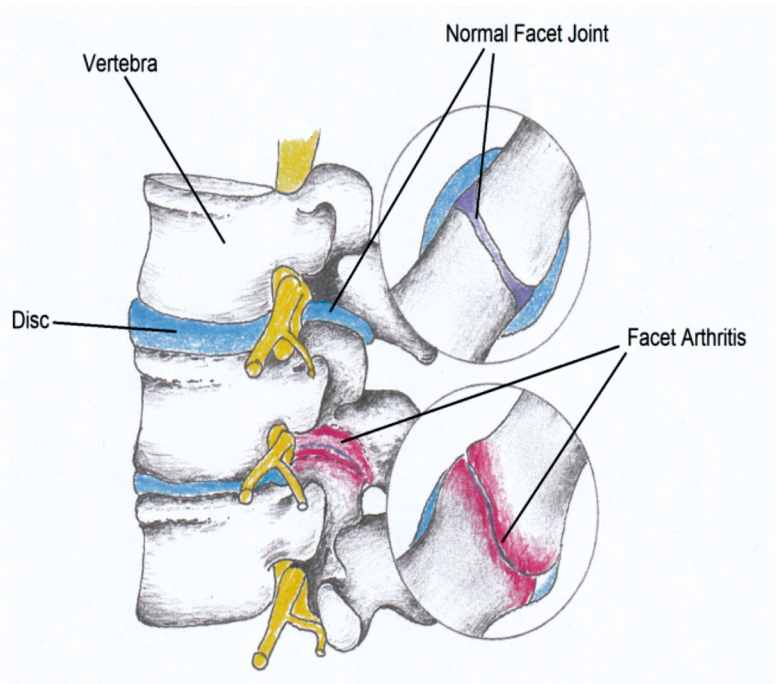


Figure 1. Facet joint syndrome is caused by osteoarthritis of an intervertebral joint which is the source of pain.

Radicular pain is characterized by severe, shooting pain radiating to the extremities. This is accompanied by neurological symptoms such as sensory disturbances, paraesthesia and muscle weakness. Clinical symptoms of lumbosacral radicular syndrome usually result from irritation of L4, L5, S1 roots. Radicular syndromes are most often caused by compression of the spinal roots near the entrance to the intervertebral foramen, the narrowest part of this opening, which is most easily narrowed in the course of degenerative changes of the spine (Figure 2). The second most common cause of spinal root compression is disc displacement [14].

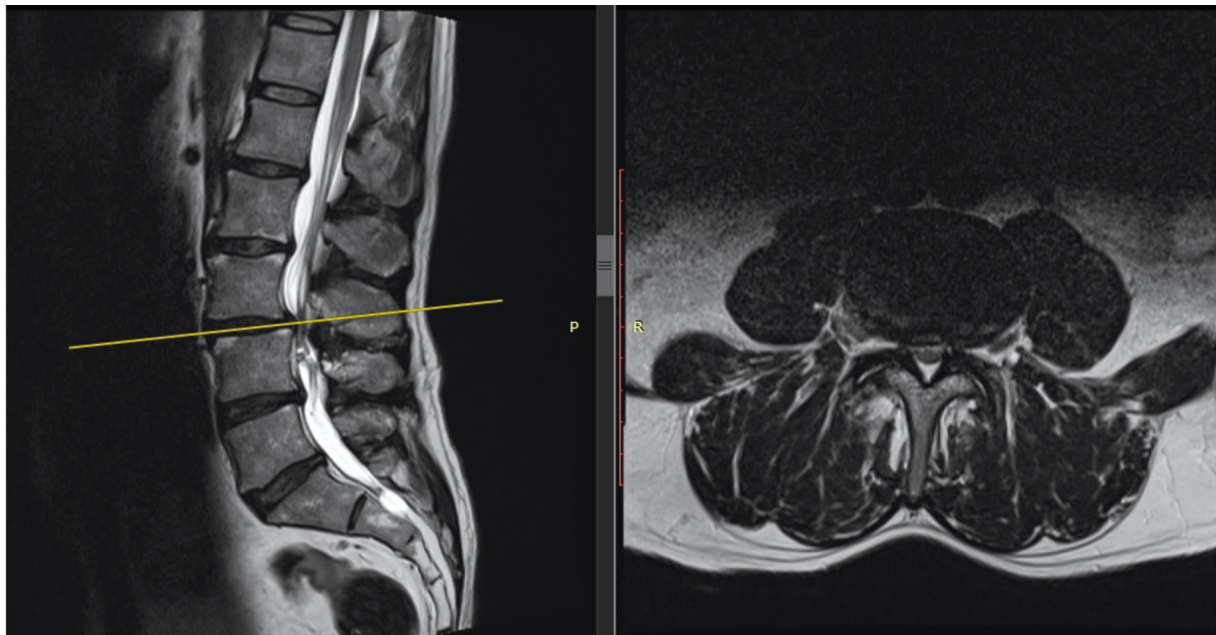


Figure 2. Narrowed spinal canal recess or intervertebral foramen are the causes of compression of the nerve root which is the source of radicular pain.

Lumbar denervation procedure

Lumbar radiofrequency denervation (RFD) is a minimally invasive treatment for chronic LBP that involves targeted percutaneous nerve injury using 300-500 kHz heat-generation for precise and long-lasting pain relief. The indication for this procedure is chronic LBP lasting at least 6 months that cannot be relieved by conventional treatment e.g. analgesics

and physiotherapy. The advantage of RFD is its precision, reproducibility regardless of the patient's age and relatively few contraindications (e.g. heart failure, pregnancy, inflammatory skin changes and certain mental diseases, particularly depression secondary to chronic pain) [15]. The RFD procedure can be performed safely approximately 3 months after stroke and myocardial infarction [16]. See Figure 3-5 for an RFD procedure for facet joint syndrome.

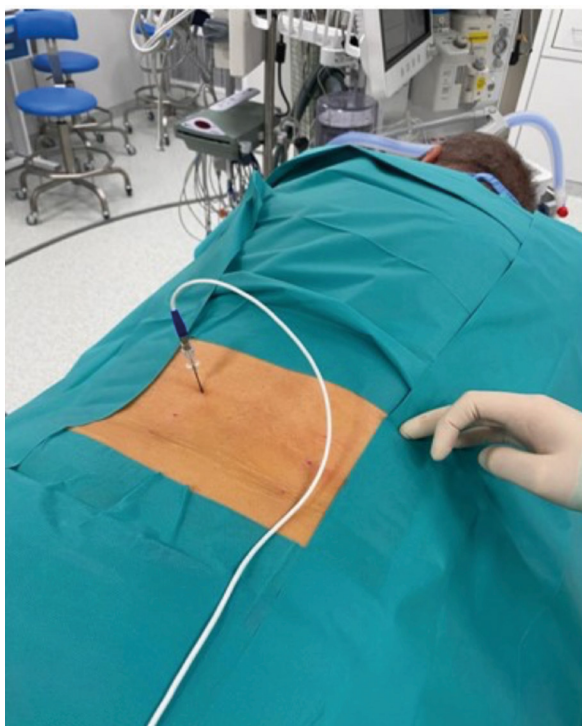


Figure 3. RFD the in operating room under fluoros

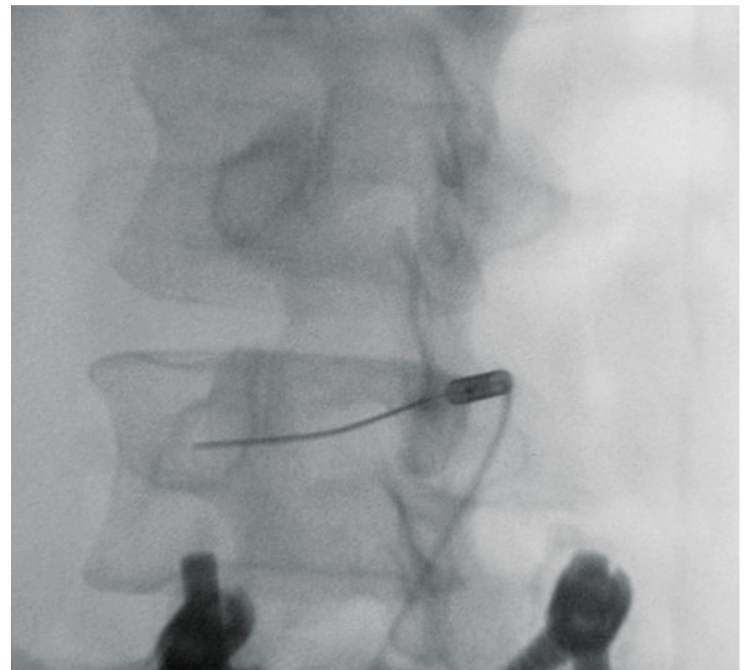


Figure 4. Oblique X-ray of lumbar spine with the needle and electrode lead inserted in the so-called "eye of the scottie dog"

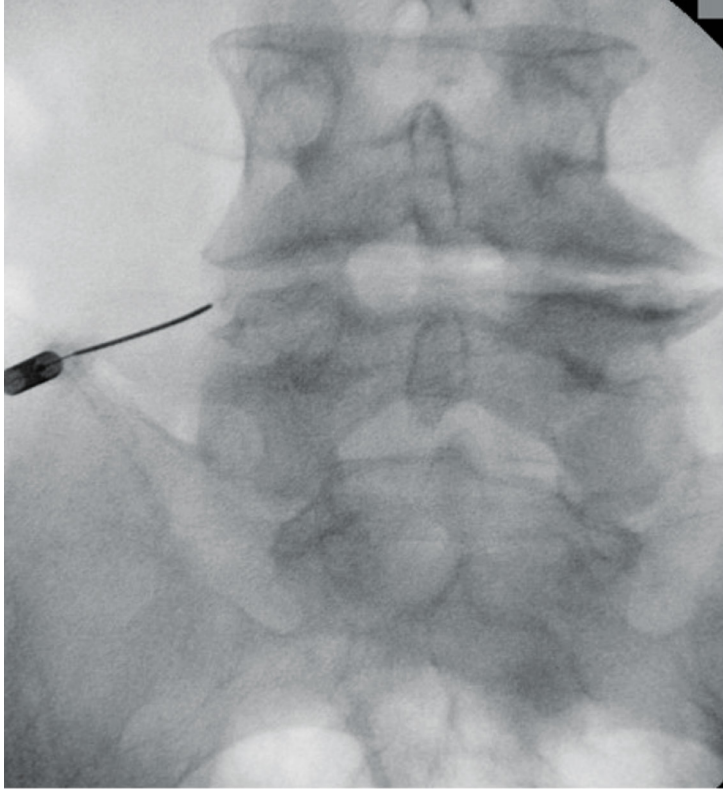


Figure 5. A-P X-ray of the electrode placed on left transverse process of L5

Efficacy of lumbar facet RFD

In a study on 1309 patients with chronic LBP, RFD was shown to provide only short-term pain relief for patients with pain of disc origin, while it was more effective for FJS [1]. Adakli et al demonstrated, comparing RFD with Target Disc Decompression, that RFD was an attractive alternative to conventional surgery for the treatment of radicular symptoms [17]. Pain relief was reported by 41.7% of patients undergoing RFD. In a study on the efficacy of RFD for discogenic lumbar spine pain, Zhang et al noted pain relief in 65% of patients in the first week after treatment, 17 (74%) at 1 month, 18 (78%) at 3 months, 19 (82%) at 6 months, and up to 87% of patients at 12 weeks after treatment [18]. Arici et al. included in their study 164 patients with LBP due to lumbar arthropathy, who underwent RFD and at least 50% of noted pain relief and 68% had good to excellent results. The median time of relief after the procedure was 7.3 months, with 10.2 months for patients with good/excellent results [19]. In a Korean study on 30 patients with discopathy or spinal stenosis underwent RFD, of whom 17 patients scored 'excellent' according to the MacNab criteria, 11 scored 'good' and the remaining 2 patients scored 'fair.' The patients were also assessed with VAS and Oswestry scales in which they showed significant improvement [20]. In their double-blind study, Ertival et al. subjected 96 patients

in 3 randomized groups to RFD with different parameters in terms of temperature and time. The results, regardless of the parameters used, were good (pain relief > 50% in 57% of patients), but were worse in patients who had previously undergone spinal procedures [21]. Masala et al. found significant lumbar pain relief in 70%-81% of patients with FJS [22]. Similar results were also found by Hee Son et al. (85% of patients experienced pain relief) [23] and MacVicar et al. (58% and 53% of patients had a positive treatment outcome) [24].

Physiotherapy approach after RFD treatment on FJS

RFD has been demonstrated to relieve LBP, allowing patients to resume independent daily activities and work. This minimally invasive technique allows patients to start physiotherapy after a week in the form of physical exercises. Patients with LBP tend to have abnormally reduced paraspinal muscle tone caused by long-term chronic overload pain resulting from poor spinal alignment. Therefore, correct body posture and proper shaping of the lumbar lordosis are important [25]. It is important to educate the patient, to implement the correct body posture in everyday activities and the correct sitting position while working in a sitting position, e.g. at the desk. Regular exercises strengthen the lumbar muscles and improve the stabilization of the lumbar spine by correcting its position (from deepened to normal), all of which reduce LBP [26]. The lumbar spine is exposed to heavy loads, and thanks to proper physical activity, we can avoid overload. The greatest pressure is exerted on them during forward tilting of the lumbar spine (lordosis) and rotation of the trunk and pelvis. Active exercises performed regularly, activating the deep muscles of the trunk and aimed at restoring the proper tension and coordination of paraspinal muscles in the lumbar spine [27].

Proper exercise by the patient is based on the principle of performing exercises without increasing pain, gradually increasing the range of motion in the joints of the spine, only to the limit of pain. Regular, daily exercise should be done in isolated, safe positions. Change of exercise position should take place with a stiffened spine. During exercises, the patient should maintain deep breaths by inhaling through the nose and exhaling through the mouth. The effectiveness of individual exercises in terms of reducing pain and improving the patient's functionality has also been demonstrated in other studies [28-29]. Performing RFD treatment in a patient with LBP and performing regular physical exercises under the supervision of a physiotherapist extend the therapeutic effect of RFD treatment in the form of life without LBP symptoms. See Figure 6-10 for a sample set of exercises for patients after RFD.



Figure 6. Exercise 1. While in the supine position, with arms along the torso, knees flexed, raise the pelvis, hold position for 7 seconds, lower the pelvis.



Figure 9. Exercise 4. Arch supports while in the prone position. Hold this position for a few seconds, preferably while inhaling.



Figure 7. Exercise 2. While lying down, use the right heel to touch the left knee and repeat with opposite heel and knee.



Figure 10. Exercise 5. While in the prone position, put your hands on your hips and try to “stick your head” as far as possible in front of you lifting it slightly from the floor.



Figure 8. Exercise 3. Cat (back) stretch. Inhale while pushing the spine towards the ceiling, exhale while lowering the spine to the starting position.

Conclusions

A good outcome of facet joint denervation can be maintained with an appropriate, regular program of exercises to strengthen the muscles and improve the stabilization of the lumbar spine. The exercises described in this article are exemplary. Patients must stay in contact with their doctor or physiotherapist, who work closely together. Combining the RFD treatment with physiotherapy will probably prolong the therapeutic effect and get rid of chronic low back pain. Therefore, it should be remembered that the form of exercise

should always be individual and adapted to the current physical condition of the patient.

Conflict of interest

None.

Funding

None.

References

1. Maas ET, Ostelo RWJG, Niemisto L, Jousimaa J, Hurri H, Malmivaara A, et al. Radiofrequency denervation for chronic low back pain. *Cochrane database Syst Rev* [Internet]. 2015;2015(10):CD008572. Available from: <http://doi.wiley.com/10.1002/14651858.CD008572.pub2>
2. The Lancet. GBD 2017: a fragile world. *Lancet* [Internet]. 2018;392(10159):1683. Available from: <https://linkinghub.elsevier.com/retrieve/pii/S0140673618328587>
3. Rubin DI. Epidemiology and risk factors for spine pain. *Neurol Clin* [Internet]. 2007;25(2):353–71. Available from: <https://linkinghub.elsevier.com/retrieve/pii/S0733861907000059>
4. Frosch M, Mauritz MD, Bielack S, Blödt S, Dirksen U, Dobe M, et al. Etiology, risk factors, and diagnosis of back pain in children and adolescents: evidence- and consensus-based interdisciplinary recommendations. *Children* [Internet]. 2022;9(2):192. Available from: <https://www.mdpi.com/2227-9067/9/2/192>
5. Yang S, Werner BC, Singla A, Abel MF. Low back pain in adolescents: a 1-year analysis of eventual diagnoses. *J Pediatr Orthop* [Internet]. 2017;37(5):344–7. Available from: <https://journals.lww.com/01241398-201707000-00016>
6. Andersson GB. Epidemiological features of chronic low-back pain. *Lancet* [Internet]. 1999;354(9178):581–5. Available from: <https://linkinghub.elsevier.com/retrieve/pii/S0140673699013124>
7. Akpinar A, Akintürk N, Kiliç BM, Kasap M. Spontaneous regression of lumbar disc herniations. *J Turkish Spinal Surg* [Internet]. 2020;31(3):141–7. Available from: http://cms.galenos.com.tr/Uploads/Article_39992/jtss-31-141-En.pdf
8. Chiu C-C, Chuang T-Y, Chang K-H, Wu C-H, Lin P-W, Hsu W-Y. The probability of spontaneous regression of lumbar herniated disc: a systematic review. *Clin Rehabil* [Internet]. 2015;29(2):184–95. Available from: <http://journals.sagepub.com/doi/10.1177/0269215514540919>
9. Zheltoukhova K, Bevan S, Reich A. Fit for work? Musculoskeletal disorders and the Polish labour market [Internet]. London; 2012. Available from: https://www.ceestahc.org/pliki/projekty/f4w/poland_English_060911.pdf
10. Stewart WF. Lost productive time and cost due to common pain conditions in the US workforce. *JAMA* [Internet]. 2003;290(18):2443. Available from: <http://jama.jamanetwork.com/article.aspx?doi=10.1001/jama.290.18.2443>
11. Saravi B, Kabirzadeh A, Rezazadeh E, Khariki M, Zolaykha Z, Asgari A, et al. Prevalence and causes of medical absenteeism among staff (case study at Mazandaran University of Medical Sciences: 2009-2010). *Mater Socio Medica* [Internet]. 2013;25(4):233. Available from: <http://www.scopemed.org/fulltextpdf.php?mno=47883>
12. Manchikanti L, Manchikanti KN, Cash KA, Singh V, Giordano J. Age-related prevalence of facet-joint involvement in chronic neck and low back pain. *Pain Physician* [Internet]. 2008;11(1):67. Available from: <https://www.painphysicianjournal.com/current/pdf?article=OTQ1&journal=39>
13. Perolat R, Kastler A, Nicot B, Pellat J-M, Tahon F, Attaye A, et al. Facet joint syndrome: from diagnosis to interventional management. *Insights Imaging* [Internet]. 2018;9(5):773–89. Available from: <https://insightsimaging.springeropen.com/articles/10.1007/s13244-018-0638-x>
14. Koszewicz M, Budrewicz S. Elektrofizjologiczna diagnostyka zespołów korzeniowych [in Polish]. *Pol Przegląd Neurol* [Internet]. 2010;6(2):86–91. Available from: https://journals.viamedica.pl/polski_przegląd_neurologiczny/article/view/19938
15. Drobniak L, Kowalski G. Analgezja regionalna. Skrypt [in Polish]. Poznań: Szkoła Analgezji Regionalnej; 2012.
16. Raszka A, Waliszewska R, Sokal P, Zieliński P, Harat M. Quality of life in patients after lumbar thermolysis. *J Neurol Neurosurg Nurs* [Internet]. 2016;5(2):76–80. Available from: <https://apcz.umk.pl/PNIN/article/view/38583>

17. Adakli B, Cakar Turhan KS, Asik I. The comparison of the efficacy of radiofrequency nucleoplasty and targeted disc decompression in lumbar radiculopathy. *Biomol Biomed* [Internet]. 2015;15(2):57–61. Available from: <https://www.bjbm.org/ojs/index.php/bjbm/article/view/427>
18. Zhang L, Ding X-L, Zhao X-L, Wang J-N, Li Y-P, Tian M. Fluoroscopy-guided bipolar radiofrequency thermocoagulation treatment for discogenic low back pain. *Chin Med J (Engl)* [Internet]. 2016;129(19):2313–8. Available from: <https://journals.lww.com/00029330-201610050-00008>
19. Arici T. Distal approach for percutaneous radiofrequency thermocoagulation of lumbar medial branches in patients with lumbar facet arthropathy: a retrospective analysis. *Ağrı – J Turkish Soc Algol* [Internet]. 2019;32(1):31–7. Available from: <http://www.agridergisi.com/jvi.aspx?pdire=agri&plng=eng&un=AGRI-15921>
20. Kim HS, Wu PH, Jang I-T. Lumbar degenerative disease part 1: anatomy and pathophysiology of intervertebral discogenic pain and radiofrequency ablation of basivertebral and sinuvertebral nerve treatment for chronic discogenic back pain: a prospective case series and review of literature. *Int J Mol Sci* [Internet]. 2020;21(4):1483. Available from: <https://www.mdpi.com/1422-0067/21/4/1483>
21. Ertilav E, Aydin ON, Erel KV. Facet median branch radiofrequency thermocoagulation treatment at different temperatures and durations in patients with lumbar facet syndrome: a randomized controlled, double-blind study. *Turk Neurosurg* [Internet]. 2021;32(1):149–54. Available from: http://www.turkishneurosurgery.org.tr/summary_en_doi.php?doi=10.5137/1019-5149.JTN.34637-21.2
22. Masala S, Nano G, Mammucari M, Marcia S, Simonetti G. Medial branch neurotomy in low back pain. *Neuroradiology* [Internet]. 2012;54(7):737–44. Available from: <http://link.springer.com/10.1007/s00234-011-0968-6>
23. Son JH, Kim SD, Kim SH, Lim DJ, Park JY. The efficacy of repeated radiofrequency medial branch neurotomy for Lumbar Facet Syndrome. *J Korean Neurosurg Soc* [Internet]. 2010;48(3):240. Available from: <http://jkns.or.kr/journal/view.php?doi=10.3340/jkns.2010.48.3.240>
24. MacVicar J, Borowczyk JM, MacVicar AM, Loughnan BM, Bogduk N. Lumbar medial branch radiofrequency neurotomy in New Zealand. *Pain Med* [Internet]. 2013;14(5):639–45. Available from: <https://academic.oup.com/painmedicine/article-lookup/doi/10.1111/pme.12000>
25. Maeo S, Takahashi T, Takai Y, Kanehisa H. Trunk muscle activities during abdominal bracing: comparison among muscles and exercises. *J Sports Sci Med* [Internet]. 2013;12(3):467–74. Available from: <http://www.ncbi.nlm.nih.gov/pubmed/24149153>
26. Aleksiev AR. Ten-year follow-up of strengthening versus flexibility exercises with or without abdominal bracing in recurrent low back pain. *Spine (Phila Pa 1976)* [Internet]. 2014;39(13):997–1003. Available from: <http://journals.lww.com/00007632-201406010-00002>
27. Saragiotto BT, Maher CG, Yamato TP, Costa LO, Menezes Costa LC, Ostelo RW, et al. Motor control exercise for chronic non-specific low-back pain. *Cochrane Database Syst Rev* [Internet]. 2016;2016(11). Available from: <http://doi.wiley.com/10.1002/14651858.CD012004>
28. Chambon X, Paysant J, Maureira J., André J. Étude comparative et préliminaire d'un réentraînement à l'effort au sein de deux populations de sujets déconditionnés douloureux ou non [in French]. *Ann Réadaptation Médecine Phys* [Internet]. 2003;46(4):198–204. Available from: <https://linkinghub.elsevier.com/retrieve/pii/S0168605403000552>
29. Chatzitheodorou D, Kabitsis C, Malliou P, Mougios V. A pilot study of the effects of high-intensity aerobic exercise versus passive interventions on pain, disability, psychological strain, and serum cortisol concentrations in people with chronic low back pain. *Phys Ther* [Internet]. 2007;87(3):304–12. Available from: <https://academic.oup.com/ptj/article/87/3/304/2742120>

Histopathological characteristics of myocarditis following COVID-19 vaccination: a scoping review

Datis Kalali¹ , Doxakis Anastakis^{1,2} 

¹ Medical School, University of Cyprus, Nicosia, Cyprus

² Laboratory of Autopsy Pathology, Forensic Service of Thessaloniki, Ministry of Justice, Thessaloniki, Greece

Abstract

Introduction: Cases of myocarditis in people were vaccinated against COVID-19 have been reported in the recent years. Nevertheless, the histopathological features and the pathomechanisms in these cases are still unclear. Hence, a scoping review of existing literature was performed to discover the histopathological features of myocarditis induced by the above-mentioned vaccine. **Methods:** A search was performed in the PubMed, Scopus and EMBASE databases to retrieve the relevant records, involving analyses of biopsy and autopsy specimens. Baseline characteristics of the patients and the histopathological characteristics of the respective specimens were extracted and recorded. **Results:** Overall, 24 case reports and case series (involving a total of 54 patients) were included in this scoping review. The following signs of inflammation were present in the specimens: lymphocyte infiltration (64.8%), eosinophilic infiltration (29.6%), neutrophil infiltration (3.7%) and giant-cell formation (1.9%). Other features included myocardial tissue necrosis (20.4%), the presence of the SARS-CoV-2 spike protein (16.7%) and microthrombosis (3.7%). **Conclusions:** The histopathological characteristics of SARS-CoV-2 vaccine-induced myocarditis were heterogenous, the only common characteristic was the presence of lymphocyte infiltration in more than half of the cases. Studies of unreported past cases may provide further insights into the topic.

Keywords: histopathology · COVID-19 vaccine · mRNA vaccines · myocarditis · myocardial inflammation

Citation

Kalali D, Anastakis D. Histopathological characteristics of myocarditis following COVID-19 vaccination: a scoping review. Eur J Transl Clin Med. 2023;6(2):85-90.

DOI: [10.31373/ejtcmm/171985](https://doi.org/10.31373/ejtcmm/171985)

Corresponding author:

Datis Kalali, Medical School, University of Cyprus, Nicosia, Cyprus

e-mail: kalali.datis@ucy.ac.cy

Available online: www.ejtcmm.gumed.edu.pl

Copyright © Medical University of Gdańsk

This is Open Access article distributed under the terms of the Creative Commons Attribution-ShareAlike 4.0 International.



Introduction

Myocarditis is a rare but serious condition where the heart muscle (myocardium) becomes inflamed [1]. According to the histopathological standard for diagnosing myocarditis (the Dallas criteria), myocarditis is defined as an inflammatory infiltration of the myocardium with or without fibrosis of the tissue [2]. Although the latter disease is not generally life-threatening and doesn't cause permanent damage to the myocardium, it can lead to hospitalization and increased risk of developing arrhythmias [3].

Since early 2021, several cases of myocarditis have been reported in people following vaccination against the severe acute respiratory syndrome coronavirus-2 (SARS-CoV-2) virus, particularly in those vaccinated with mRNA vaccines [4-5]. Interestingly, most patients who developed myocarditis presented some common patterns, including the onset of the disease in an average of 2-3 days after receiving the second dose of the SARS-CoV-2 vaccine [6]. Nonetheless, most cases of post-vaccination myocarditis were diagnosed based on medical imaging techniques or laboratory examinations, therefore not enough data and systemic descriptions were available to comprehend the pathophysiology of this condition [7-8]. Hence, there is a significant need for the analysis of biopsy or necropsy specimens of the myocardia of patients with inflammatory cardiomyopathy after receiving the SARS-CoV-2 vaccine. Moreover, according to the proposals of the World Health Organization, it is necessary to systematically evaluate the adverse effects of vaccines [9]. The aim of this study was to conduct a scoping review of the available literature in order to investigate the histopathological features of the myocarditis following SARS-CoV-2 vaccination.

Material and methods

A scoping review was conducted according to the PRISMA Extension for Scoping Reviews (PRISMA-ScR) guidelines with the aim of answering the following research question: "what are the histopathological characteristics of myocarditis following vaccination against SARS-CoV-2, as described in the available literature?" [10]. We systematically searched the PubMed, Scopus and EMBASE electronic databases for English-language articles published from inception until April 2023. The following keywords in combination with Boolean operators (AND, OR) were used in the electronic search: "myocarditis", "inflammatory cardiomyopathy", "histolog*", "histopatholog*", "anatomopatholog*", "surgical pathology", "severe acute respiratory syndrome coronavirus 2", "SARS-CoV-2", "coronavirus disease 19", "COVID-19", "vaccine" and "vaccination".

The inclusion criteria were: case report, case series or observational study reporting the biopsy or necropsy results of patients with myocarditis occurring after the SARS-CoV-2 vaccination. We used the citation manager EndNote (Clarivate, Philadelphia USA and London UK) to remove duplicate records. All remaining records were screened for eligibility based on their titles and abstracts. Finally, we obtained the full-text versions of the remaining records and assessed them in detail.

Data extraction and statistical analyses

Data was extracted from all included studies regarding the number of patients, their gender, the number of vaccine doses they received prior to the onset of myocarditis, the type of vaccine they received, their medical history, the type of specimen taken (biopsy sample or necrotomy specimen) and the histopathological features found within the myocardial specimens. The extracted data was processed and presented using descriptive statistics. All statistical processes were performed using the STATA software package version 17.0 (StataCorp LLC, College Station USA).

Results

The database search retrieved a total of 179 records, of which 94 remained after the duplicates were removed. During the title and abstract screening, a total of 55 citations were deemed ineligible due to irrelevance to the research question. Once the full-text versions of the remaining articles were assessed, 15 were excluded (see Figure 1 for details). Hence, a total of 24 studies were finally included in the review, all of which were case reports and case series [11-34].

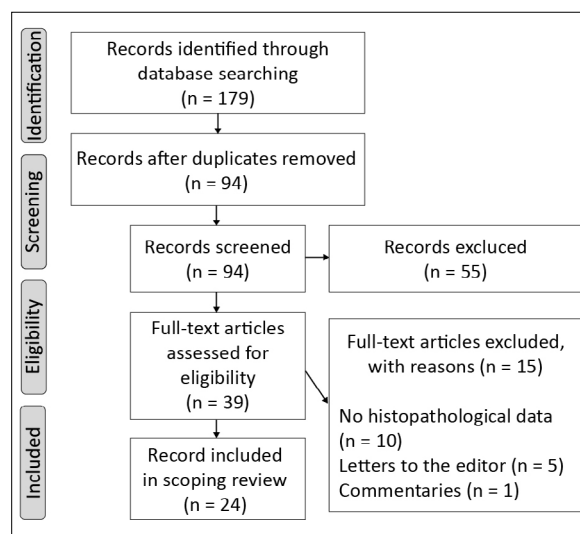


Figure 1. PRISMA diagram of our systematic review

Overall, the included studies described a total of 54 patients who presented with myocarditis after obtaining a dose of the SARS-CoV-2 vaccine. The baseline characteristics and vaccination information of the patients have been recorded in Table 1. Most of the included patients were healthy with no prior history of serious disease and 7 had prior history of myopericarditis, thyroiditis, diabetes mellitus, Parkinson's disease and glioblastoma [22, 24, 26-28, 31-32]. Moreover, all patients except 2, developed myocarditis after receiving either the first or the second dose of the vaccine [23-24]. It is also worth mentioning that majority of the patients who developed myocarditis received an mRNA vaccine.

Table 1. Baseline characteristics of patients in the included studies

VARIABLES	
Total number of patients (n)	54
Mean age (years) ± standard deviation	40.9 ± 17.3
Gender	
Male (n)	35
Female (n)	19
Vaccine doses received prior to myocarditis	
One dose (n)	21
Two doses (n)	31
Three doses (n)	2
Type of vaccine received	
Messenger RNA (n)	49
Viral vector (n)	4
Viral subunit (n)	1
Special health conditions	
Prior history of myopericarditis (n)	1
Thyroiditis (n)	3
Diabetes mellitus (n)	1
Parkinson's disease (n)	1
Glioblastoma (n)	1

All of the specimens (43 from endomyocardial biopsy and 11 from necropsy) in the included studies had undergone anatomopathological analysis. In all the specimens, myocarditis was characterized by inflammatory infiltration, namely lymphocyte infiltration (64.8%), eosinophilic infiltration (29.6%), neutrophil infiltration (3.7%) and giant-cell formation (1.9%). In some specimens, myocardial tissue necrosis was also observed, which was previously reported, particularly in patients with viral myocarditis [35]. Histochemical analyses also revealed that in 16.7% of the specimens, the SARS-CoV-2 spike protein was present. It is also necessary to mention that in 2 specimens, microthrombi were also present and it is known that micro-

thrombosis is associated with SARS-CoV-2 [12, 25, 36]. Table 2 summarizes the histopathological features of the myocardial specimens in the included studies.

Table 2. Histopathological features of myocardial specimens in the included studies

	FREQUENCY (n)	PERCENTAGE (%)
Specimen type		
Endomyocardial biopsy	43	79.6
Necropsy	11	20.4
Lymphocyte infiltration	35	64.8
Eosinophilic infiltration	16	29.6
Neutrophil infiltration	2	3.7
Giant-cell formation	1	1.9
Myocardial tissue necrosis	11	20.4
SARS-CoV-2 spike protein in myocardium	9	16.7
Microthrombosis	2	3.7

Discussion

As seen in this scoping review, the histopathological features of the inflamed myocardia after COVID-19 vaccination vary from case to case. The only prevalent feature amongst the cases was the lymphocytic nature of the myocardial inflammation. Interestingly, the most common type of viral myocarditis is lymphocytic myocarditis as well [37]. Therefore, this histopathological finding may possibly indicate the involvement of the virus in the formation of post-vaccine myocarditis. Indeed, one of the proposed mechanisms is the leakage of vaccine nanoparticles into the bloodstream, which subsequently reach the myocardial cells and cause viral protein expression [38]. The presence of the SARS-CoV-2 spike protein in some of the specimens included in this review may also further support this theory.

Although the present scoping review was performed according to the PRISMA-ScR guidelines it has several significant limitations. First, most included records were case reports, yielding only a small number of included patients and thus decreasing the reliability of the results. Moreover, many of the articles did not provide details of the histopathological characteristics and therefore, possible additional characteristics may not have been recorded in

this review. Lastly, since the search was limited to articles written in the English language, valuable reports written in other languages might have been excluded.

past cases may shed some more light on the histopathological features of myocarditis induced by vaccination against SARS-CoV-2.

Conclusions

Our review demonstrated that myocarditis accompanied with inflammatory infiltration and sometimes myocardial necrosis rarely occurs in patients who were vaccinated against COVID-19, particularly with the novel mRNA vaccines. Further studies are required to validate our results. In particular, retrospective cohort studies of unreported

Conflicts of interest

None to report.

Funding

Not applicable.




References

- Cooper LT. Myocarditis. *N Engl J Med* [Internet]. 2009 Apr 9;360(15):1526–38. Available from: <http://www.nejm.org/doi/abs/10.1056/NEJMra0800028>
- Trachtenberg BH, Hare JM. Inflammatory Cardiomyopathic Syndromes. *Circ Res* [Internet]. 2017 Sep 15;121(7):803–18. Available from: <https://www.ahajournals.org/doi/10.1161/CIRCRESAHA.117.310221>
- Lampejo T, Durkin SM, Bhatt N, Guttman O. Acute myocarditis: aetiology, diagnosis and management. *Clin Med (Northfield Il)* [Internet]. 2021 Sep;21(5):e505–10. Available from: <https://www.rcpjournals.org/lookup/doi/10.7861/clinmed.2021-0121>
- Diaz GA, Parsons GT, Gering SK, Meier AR, Hutchinson I V., Robicsek A. Myocarditis and Pericarditis After Vaccination for COVID-19. *JAMA* [Internet]. 2021 Sep 28;326(12):1210. Available from: <https://jamanetwork.com/journals/jama/fullarticle/2782900>
- Salah HM, Mehta JL. COVID-19 Vaccine and Myocarditis. *Am J Cardiol* [Internet]. 2021 Oct;157:146–8. Available from: <https://linkinghub.elsevier.com/retrieve/pii/S0002914921006391>
- Ali M, Shiwani HA, Elfaki MY, Hamid M, Pharithi R, Kamgang R, et al. COVID-19 and myocarditis: a review of literature. *Egypt Hear J* [Internet]. 2022 Dec 5;74(1):23. Available from: <https://tehr.springeropen.com/articles/10.1186/s43044-022-00260-2>
- Ling RR, Ramanathan K, Tan FL, Tai BC, Somani J, Fisher D, et al. Myopericarditis following COVID-19 vaccination and non-COVID-19 vaccination: a systematic review and meta-analysis. *Lancet Respir Med* [Internet]. 2022 Jul;10(7):679–88. Available from: <https://linkinghub.elsevier.com/retrieve/pii/S2213260022000595>
- Viskin D, Topilsky Y, Aviram G, Mann T, Sadon S, Hadad Y, et al. Myocarditis Associated With COVID-19 Vaccination. *Circ Cardiovasc Imaging* [Internet]. 2021 Sep;14(9):e013236. Available from: <https://www.ahajournals.org/doi/10.1161/CIRCIMA-GING.121.013236>
- Organization WH. Causality assessment of an adverse event following immunization (AEFI): user manual for the revised who classification. 2019; Available from: <https://iris.who.int/bitstream/handle/10665/340802/9789241516990-eng.pdf>
- Tricco AC, Lillie E, Zarin W, O'Brien KK, Colquhoun H, Levac D, et al. PRISMA Extension for Scoping Reviews (PRISMA-ScR): Checklist and Explanation. *Ann Intern Med* [Internet]. 2018 Oct 2;169(7):467–73. Available from: <https://www.acpjournals.org/doi/10.7326/M18-0850>
- Abete R, Valastro P, Iacovoni A, Vittori C, Arbustini E, Pelliccioli F, et al. Acute necrotizing eosinophilic myocarditis presenting with cardiogenic shock after mRNA booster dose for COVID-19: Case report and review of literature. *J Cardiol Cases* [Internet]. 2023 Feb;27(2):52–5. Available from: <https://linkinghub.elsevier.com/retrieve/pii/S1878540922001712>
- Aikawa T, Ogino J, Kita Y, Funayama N. Myocardial microthrombi after COVID-19 mRNA vaccination. *Eur Heart J* [Internet]. 2021 Nov 14;42(43):4501–4501. Available from: <https://academic.oup.com/eurheartj/article/42/43/4501/6384671>
- Ameratunga R, Woon S-T, Sheppard MN, Garland J, Ondruschka B, Wong CX, et al. First Identified Case of Fatal Fulminant Necrotizing Eosinophilic Myocarditis Following the Initial Dose of the Pfizer-BioNTech mRNA COVID-19 Vaccine (BNT162b2, Comirnaty): an Extremely Rare Idiosyncratic Hypersensitivity Reaction. *J Clin Immunol* [Internet]. 2022 Apr 3;42(3):441–7. Available from: <https://link.springer.com/10.1007/s10875-021-01187-0>
- Baumeier C, Aleshcheva G, Harms D, Gross U, Hamm C, Assmus B, et al. Intramyocardial Inflammation after COVID-19 Vaccination: An Endomyocardial Biopsy-Proven Case Series. *Int J Mol Sci* [Internet]. 2022 Jun 22;23(13):6940. Available from: <https://www.mdpi.com/1422-0067/23/13/6940>

15. Bricoli S, Cacciola G, Barocelli F, Guerra C, Zardini M. 553 Myocarditis after COVID-19 vaccination – a case series. *Eur Hear J Suppl* [Internet]. 2021 Dec 8;23(Supplement_G). Available from: <https://academic.oup.com/eurheartjsupp/article/doi/10.1093/eurheartj/suab135.008/6456956>
16. Choi S, Lee S, Seo J-W, Kim M, Jeon YH, Park JH, et al. Myocarditis-induced Sudden Death after BNT162b2 mRNA COVID-19 Vaccination in Korea: Case Report Focusing on Histopathological Findings. *J Korean Med Sci* [Internet]. 2021;36(40). Available from: <https://jkms.org/DOLx.php?id=10.3346/jkms.2021.36.e286>
17. Chow BT, Lai CK. Lymphohistiocytic Myocarditis Possibly Due to Moderna mRNA-1273 Vaccine. *Am J Clin Pathol* [Internet]. 2022 Aug 4;158(2):167–72. Available from: <https://academic.oup.com/ajcp/article/158/2/167/6548250>
18. Dong Y, Liu X, Yang C, Qi Q, Shi W, Li Y, et al. Case report: Myocarditis following COVID-19 protein subunit vaccination. *Front Cardiovasc Med* [Internet]. 2022 Sep 7;9. Available from: <https://www.frontiersin.org/articles/10.3389/fcvm.2022.970045/full>
19. Ehrlich P, Klingel K, Ohlmann-Knafo S, Hüttinger S, Sood N, Pickuth D, et al. Biopsy-proven lymphocytic myocarditis following first mRNA COVID-19 vaccination in a 40-year-old male: case report. *Clin Res Cardiol* [Internet]. 2021 Nov 6;110(11):1855–9. Available from: <https://link.springer.com/10.1007/s00392-021-01936-6>
20. Frustaci A, Verardo R, Galea N, Lavalle C, Bagnato G, Scialla R, et al. Hypersensitivity Myocarditis after COVID-19 mRNA Vaccination. *J Clin Med* [Internet]. 2022 Mar 16;11(6):1660. Available from: <https://www.mdpi.com/2077-0383/11/6/1660>
21. Gill JR, Tashjian R, Duncanson E. Autopsy Histopathologic Cardiac Findings in 2 Adolescents Following the Second COVID-19 Vaccine Dose. *Arch Pathol Lab Med* [Internet]. 2022 Aug 1;146(8):925–9. Available from: <https://meridian.allenpress.com/aplm/article/146/8/925/477788/Autopsy-Histopathologic-Cardiac-Findings-in-2>
22. Kadwalwala M, Chadha B, Ortoleva J, Joyce M. Multimodality imaging and histopathology in a young man presenting with fulminant lymphocytic myocarditis and cardiogenic shock after mRNA-1273 vaccination. *BMJ Case Rep* [Internet]. 2021 Nov 30;14(11):e246059. Available from: <https://casereports.bmj.com/lookup/doi/10.1136/bcr-2021-246059>
23. Mengesha B, Asenov AG, Hirsh-Racah B, Amir O, Pappo O, Asleh R. Severe Acute Myocarditis after the Third (Booster) Dose of mRNA COVID-19 Vaccination. *Vaccines* [Internet]. 2022 Apr 8;10(4):575. Available from: <https://www.mdpi.com/2076-393X/10/4/575>
24. Mörz M. A case report: Multifocal necrotizing encephalitis and myocarditis after BNT162b2 mRNA vaccination against COVID-19. *Vaccines* [Internet]. 2022 Oct 1;10(10):1651. Available from: <https://www.mdpi.com/2076-393X/10/10/1651>
25. Nakatani S, Ohta-Ogo K, Nishio M, Amemiya K, Sato S, Sawano H, et al. Microthrombosis as a cause of fulminant myocarditis-like presentation with COVID-19 proven by endomyocardial biopsy. *Cardiovasc Pathol* [Internet]. 2022 Sep;60:107435. Available from: <https://linkinghub.elsevier.com/retrieve/pii/S1054880722000291>
26. Nunn S, Kersten J, Tadic M, Wolf A, Gonska B, Hüll E, et al. Case Report: Myocarditis After COVID-19 Vaccination – Case Series and Literature Review. *Front Med* [Internet]. 2022 Feb 14;9. Available from: <https://www.frontiersin.org/articles/10.3389/fmed.2022.836620/full>
27. Olmos CV, Trahan S, Rochon A, Ducharme A. Severe myocarditis after SARS-CoV-2 vaccination in a 49-year-old woman. *Can Med Assoc J* [Internet]. 2022 Apr 25;194(16):E581–4. Available from: <http://www.cmaj.ca/lookup/doi/10.1503/cmaj.211687>
28. Onishi N, Konishi Y, Kaneko T, Maekawa N, Suenaga A, Nomura S, et al. Fulminant myocarditis with complete atrioventricular block after mRNA COVID-19 vaccination: A case report. *J Cardiol Cases* [Internet]. 2023 May;27(5):229–32. Available from: <https://linkinghub.elsevier.com/retrieve/pii/S1878540923000051>
29. Otsuka K, Matsuo T, Ishimatsu T, Fukae A, Hamamoto T, Oku K, et al. A case of BNT162b2 COVID-19 vaccine-associated fulminant myocarditis in a very elderly woman. *Clin Case Reports* [Internet]. 2022 Sep 5;10(9):e6161. Available from: <https://onlinelibrary.wiley.com/doi/10.1002/ccr3.6161>
30. Satomi H, Katano H, Kanno H, Kobayashi M, Ohkuma Y, Hashidume N, et al. An autopsy case of fulminant myocarditis after severe acute respiratory syndrome coronavirus 2 vaccine inoculation. *Pathol Int* [Internet]. 2022 Oct 30;72(10):519–24. Available from: <https://onlinelibrary.wiley.com/doi/10.1111/pin.13267>
31. Schwab C, Domke LM, Hartmann L, Stenzinger A, Longerich T, Schirmacher P. Autopsy-based histopathological characterization of myocarditis after anti-SARS-CoV-2-vaccination. *Clin Res Cardiol* [Internet]. 2023 Mar 27;112(3):431–40. Available from: <https://link.springer.com/10.1007/s00392-022-02129-5>
32. Arushi S, Shanil S, Alampoondi VSV, Qiying D, L. HM. Lymphohistiocytic myocarditis following SARS-COV-2 vaccine. *J Am Coll Cardiol* [Internet]. 2022 Mar 8;79(9_Supplement):3384. Available from: [https://doi.org/10.1016/S0735-1097\(22\)04375-3](https://doi.org/10.1016/S0735-1097(22)04375-3)
33. Stervbo U, Van Bracht M, Philippou S, Babel N, Westhoff TH. Case report: SARS-CoV-2 specific T-cells are associated with myocarditis after COVID-19 vaccination with mRNA-1273. *Front Med* [Internet]. 2023 Mar 3;10. Available from: <https://www.frontiersin.org/articles/10.3389/fmed.2023.1088764/full>

34. Yamamoto M, Tajiri K, Ayuzawa S, Ieda M. Pathological findings of clinically suspected myocarditis temporally associated with COVID-19 vaccination. *Eur J Heart Fail* [Internet]. 2022 Jun 15;24(6):1132–8. Available from: <https://onlinelibrary.wiley.com/doi/10.1002/ehf.2523>
35. K hl U, Schultheiss H. Viral myocarditis. *Swiss Med Wkly* [Internet]. 2014 Oct 2; Available from: <https://smw.ch/index.php/smw/article/view/1906>
36. Chen W, Pan JY. Anatomical and Pathological Observation and Analysis of SARS and COVID-19: Microthrombosis Is the Main Cause of Death. *Biol Proced Online* [Internet]. 2021;23(1):4. Available from: <https://doi.org/10.1186/s12575-021-00142-y>
37. A Huber S. Viral myocarditis and dilated cardiomyopathy: etiology and pathogenesis. *Curr Pharm Des* [Internet]. 2016;22(4):408–26. Available from: <https://www.ingentaconnect.com/content/ben/cpd/2016/00000022/00000004/art00002>
38. Kadkhoda K. Post RNA-based COVID vaccines myocarditis: Proposed mechanisms. *Vaccine* [Internet]. 2022 Jan;40(3):406–7. Available from: <https://linkinghub.elsevier.com/retrieve/pii/S0264410X21015942>

Usage of pregabalin in the treatment of pain associated with chronic pancreatitis – a clinically oriented narrative review

Jakub Krzysztof Gałązka¹ , Barbara Skrzydło-Radomańska² ,
Beata Kasztelan-Szczerbińska² , Halina Cichoż-Lach² 

¹Students Scientific Association at Chair and Department of Gastroenterology with Endoscopy Unit,
Medical University of Lublin, Poland

²Chair and Department of Gastroenterology with Endoscopy Unit, Medical University of Lublin, Poland

Abstract

Abdominal pain is one of the main symptoms of pancreatic diseases, including chronic pancreatitis (CP). Once the disease is in remission, pain management is a key element of treatment. Co-analgesics may also be used at any stage of analgesia, among which antiepileptic drugs such as pregabalin. The first data on the beneficial effect of pregabalin on pain in the course of CP was published in a clinical trial in 2011, and it has been known since 2015 that the analgesic effect of pregabalin on CP has a different mechanism of action than conventional analgesics. Currently, research is focused on combining pregabalin with antioxidants and on methods to predict the patient's response to pregabalin administration. Based on current research, pregabalin appears to be a very useful agent for the pharmacologic treatment of pain in the setting of CP.

Keywords: pain • pregabalin • chronic pancreatitis

Citation

Gałązka JK, Skrzydło-Radomańska B, Kasztelan-Szczerbińska B, Cichoż-Lach H. Usage of pregabalin in the treatment of pain associated with chronic pancreatitis – a clinically oriented narrative review. Eur J Transl Clin Med. 2023;6(2):91-94.

DOI: [10.31373/ejtcml/166489](https://doi.org/10.31373/ejtcml/166489)

Corresponding author:

Jakub Krzysztof Gałązka; Students Scientific Association at Chair and Department of Gastroenterology with Endoscopy Unit,
Medical University of Lublin, Poland
e-mail: jakubgałazka2@wp.pl

Available online: www.ejtcml.gumed.edu.pl

Copyright © Medical University of Gdańsk

This is Open Access article distributed under the terms of the Creative Commons Attribution-ShareAlike 4.0 International.



Introduction

Chronic pancreatitis (CP) is one of the most common gastroenterological diseases. In 2017, more than 1.5 million patients were diagnosed with de novo CP, compared to 1 million in 1990. In addition, Poland, along with Belgium and Slovakia, is one of the countries with the highest incidence of CP in the world [1]. According to the most recent definition, chronic pancreatitis is defined as a fibro-inflammatory syndrome of the pancreas, in which there is a persistent immune response associated with a damaging or stress factor, which manifests itself in individuals with a pre-existing genetic or environmental risk [2].

Abdominal pain (less often back pain) is one of the key symptoms of pancreatic diseases, including CP, the presence of which may precede both the loss of exocrine and endocrine function of this organ. Once disease remission is achieved and maintained, analgesia is a key element of patient management. The best-known algorithm is the so-called analgesic ladder, recommending starting with non-steroidal anti-inflammatory drugs (NSAIDs) and if not ineffective, escalate to weak and strong opioids [2]. Currently, the use of surgical methods to reduce pain in patients with CP is being considered [3]. In some patients, the pain can be so severe that it leads to sleep disorders, depression and other mental disorders [4-6].

Co-analgesics may be added at any stage of analgesia. Anti-epileptic drugs have been used as co-analgesics for some time, among them pregabalin. According to the Summary of Product Characteristics (SmPC), treatment of pain with pregabalin can be initiated with a dose of 150 mg daily, administered in two or three divided doses, and then (according to the effects and tolerability of the drug, particularly renal function) the dose can be gradually increased up to up to 600 mg daily [7].

The aim of the article is to summarize the studies conducted so far on the use of pregabalin in patients suffering from pain in the course of chronic pancreatitis.

Material and methods

In order to collect articles on the topic, PubMed and Google Scholar databases were searched using the keywords “pregabalin,” “chronic pancreatitis” and their synonyms.

Results and discussion

The first data on the beneficial effect of pregabalin on pain in the course of CP was published in a 2011 clinical trial in which pregabalin was co-administrated with other analgesics, 36% of patients experienced relief compared to 24% in the placebo group [8]. Since then, more of similar clinical trials have been conducted, the results of which are summarized in Table 1.

In 2015, the results of a study were published showing that the mechanism of analgesic action of pregabalin in patients with CP differs from other agents used in pain management [9]. This implies that pregabalin may be particularly useful in treating patients who do not respond satisfactorily to conventional ladder-based treatment.

Observational studies have shown that one of the mechanisms of neuropathic pain in the course of CP is the adaptation of the structures of the central nervous system (CNS) caused by inflammation [10-11]. This led researchers to try to administer pregabalin together with antioxidant substances (e.g. methionine, selenium, β -carotene, ascorbic acid and α -tocopherol). Clinical trials on the simultaneous administration of pregabalin and antioxidants in patients with pain in the course of CP resulted in greater degree of pain reduction compared to those on pregabalin alone (Table 1) [12-13]. In another clinical trial, conducted on pediatric patients (average age 13 years), it was suggested that the administration of antioxidants (vitamin C, selenium) by itself reduces pain in 68% of patients [14].

Table 1. Summary of the results of clinical trials on the use of pregabalin in the treatment of pain in the course of CP; the VAS scale was used to assess pain in all of the above trials.

Reference	Group size (study+ control group)	Follow-up period	Relative difference in pain intensity between the study and control groups (%)	Comments
Olesen, Bouwense et al. 2011 [8]	64 (32+32)	3 weeks	12	
Olesen, Graversen et al. 2011 [15]	26 (13+13)	3 weeks	14.29	
Talukdar et al. 2016 [13]	87 (42+45)	2 months	20.5	Pregabalin was administered with antioxidants
Sureshkumar et al. 2021 [12]	90 (45+45)	8 weeks	35	

On the other hand, there are claims about the insufficient level of testing of pregabalin in the treatment of pain in the course of CP. The authors of a review from 2016 suggested that in previous studies, insufficient attention was paid to the long-term effects of pregabalin use in patients with CP and its overall impact of such therapy on their quality of life [16].

For some time, it was suspected that frequent diarrhea and changes in the intestinal mucosa typical of CP adversely affected the pharmacokinetics of pregabalin administered orally. These concerns were dispelled in an observational study from 2012, which reported that the pharmacokinetic profile of pregabalin in patients with CP was preserved and dose modification in such patients should be considered only in the case of renal failure [17]. However, it should be noted that according to pregabalin's SmPC, its use in diabetes (a frequent secondary complication of pancreatic diseases) may disturb the bicarbonate balance and require an increase in the dose of hypoglycemic drugs in the patient, including insulin [7].

Due to the proven role of neuroplasticity in the development of pain in some patients with CP, and the frequent digestive system-related adverse effects of pregabalin, attempts have been made to construct methods predicting the response of patients to its use in pain management. In addition to EEG monitoring of analgesia (see below), Quantitative Sensory Testing (QST) may be used. The response was observed only after electrical stimulation of the Th10 dermatome (corresponding with the pancreas) and the effectiveness of such prediction was estimated at 83.9% [18-19].

When treating pain therapy in patients with impaired verbal contact (or unconscious), the level of analgesia can be tested using electroencephalography (EEG). After administration of pregabalin, the normalization of the (previously increased) amplitude of theta waves over the parietal lobes may be an indicator interpretable as analgesia [20].

Conclusion

According to the latest studies, including randomized clinical trials, pregabalin seems to be an effective analgesic in patients with CP. Its use should be considered primarily in patients in whom conventional measures of the analgesic ladder proved unsatisfactory. Pregabalin seems to have a synergistic effect with antioxidants and the degree of its absorption is not significantly affected by the course of CP itself. The patient's response to pregabalin therapy can be predicted using QST, whereas in patients with impaired verbal contact it can be monitored using EEG.

Conflicts of interest

None.

Sources of funding

None.

References

1. Ouyang G, Pan G, Liu Q, Wu Y, Liu Z, Lu W, et al. The global, regional, and national burden of pancreatitis in 195 countries and territories, 1990–2017: a systematic analysis for the Global Burden of Disease Study 2017. *BMC Med* [Internet]. 2020;18:388. Available from: <https://bmcmmedicine.biomedcentral.com/articles/10.1186/s12916-020-01859-5>
2. Shimizu K, Ito T, Irisawa A, Ohtsuka T, Ohara H, Kanno A, et al. Evidence-based clinical practice guidelines for chronic pancreatitis 2021. *J Gastroenterol* [Internet]. 2022;57:709–24. Available from: <https://doi.org/10.1007/s00535-022-01911-6>
3. Goulden MR. The pain of chronic pancreatitis: a persistent clinical challenge. *Br J Pain* [Internet]. 2013;7:8–22. Available from: <http://journals.sagepub.com/doi/10.1177/2049463713479230>
4. Sarkar S, Sarkar P, M R, Hazarika D, Prasanna A, Pandol SJ, et al. Pain, depression, and poor quality of life in chronic pancreatitis: Relationship with altered brain metabolites. *Pancreatol* [Internet]. 2022;22:688–97. Available from: <https://linkinghub.elsevier.com/retrieve/pii/S1424390322002022>
5. Tuck NL, Teo K, Kuhlmann L, Olesen SS, Johnson M, Bean DJ, et al. Pain patterns in chronic pancreatitis and chronic primary pain. *Pancreatol* [Internet]. 2022;22:572–82. Available from: <https://linkinghub.elsevier.com/retrieve/pii/S1424390322001673>
6. Yadav D, Askew RL, Palermo T, Li L, Andersen DK, Chen M, et al. Association of chronic pancreatitis pain features with physical, mental, and social health. *Clin Gastroenterol Hepatol* [Internet]. 2022; Available from: <https://linkinghub.elsevier.com/retrieve/pii/S1542356522009247>
7. Pregabalin Pfizer. Annex I. Summary of product characteristics [Internet]. Eur. Med. Agency. 2019 [cited 2022 Jun 10]. Available from: https://www.ema.europa.eu/en/documents/product-information/pregabalin-pfizer-epar-product-information_en.pdf

8. Olesen SS, Bouwense SAW, Wilder-Smith OHG, van Goor H, Drewes AM. Pregabalin reduces pain in patients with chronic pancreatitis in a randomized, controlled trial. *Gastroenterology* [Internet]. 2011;141:536–43. Available from: <https://linkinghub.elsevier.com/retrieve/pii/S0016508511004744>
9. Bouwense S, Olesen S, Drewes A, van Goor H, Wilder-Smith O. Pregabalin and placebo responders show different effects on central pain processing in chronic pancreatitis patients. *J Pain Res* [Internet]. 2015;375. Available from: <http://www.dovepress.com/pregabalin-and-placebo-responders-show-different-effects-on-central-pa-peer-reviewed-article-JPR>
10. Ceyhan GO, Demir IE, Rauch U, Bergmann F, Müller MW, Büchler MW, et al. Pancreatic neuropathy results in “Neural Remodeling” and altered pancreatic innervation in chronic pancreatitis and pancreatic cancer. *Am J Gastroenterol* [Internet]. 2009;104:2555–65. Available from: <https://journals.lww.com/00000434-200910000-00024>
11. Dimcevski G, Sami SAK, Funch-Jensen P, Le Pera D, Valeriani M, Arendt-Nielsen L, et al. Pain in Chronic Pancreatitis: The Role of reorganization in the central nervous system. *Gastroenterology* [Internet]. 2007;132:1546–56. Available from: <https://linkinghub.elsevier.com/retrieve/pii/S001650850700176X>
12. Sureshkumar S, Omang A, Anandhi A, Rajesh BS, Abdulbasith KM, Vijayakumar C, et al. Efficacy of pregabalin and antioxidants combination in reducing pain in chronic pancreatitis: a double blind randomized trial. *Dig Dis Sci* [Internet]. 2021;66:4017–25. Available from: <https://link.springer.com/10.1007/s10620-020-06711-7>
13. Talukdar R, Lakhtakia S, Reddy DN, Rao GV, Pradeep R, Banerjee R, et al. Ameliorating effect of antioxidants and pregabalin combination in pain recurrence after ductal clearance in chronic pancreatitis: Results of a randomized, double blind, placebo-controlled trial. *J Gastroenterol Hepatol* [Internet]. 2016;31:1654–62. Available from: <https://onlinelibrary.wiley.com/doi/10.1111/jgh.13332>
14. Gopan A, Srivastava A, Mathias A, Yachha SK, Jain SK, Mishra P, et al. Efficacy and predictors of pain response to combined antioxidants in children with chronic pancreatitis. *Dig Dis Sci* [Internet]. 2023;68:1500–10. Available from: <https://link.springer.com/10.1007/s10620-022-07676-5>
15. Olesen SS, Graversen C, Olesen AE, Frøkjær JB, Wilder-Smith O, van Goor H, et al. Randomised clinical trial: pregabalin attenuates experimental visceral pain through sub-cortical mechanisms in patients with painful chronic pancreatitis. *Aliment Pharmacol Ther* [Internet]. 2011;34:878–87. Available from: <https://onlinelibrary.wiley.com/doi/10.1111/j.1365-2036.2011.04802.x>
16. Gurusamy KS, Lusuoku C, Davidson BR. Pregabalin for decreasing pancreatic pain in chronic pancreatitis. *Cochrane Database Syst Rev* [Internet]. 2016;2016. Available from: <http://doi.wiley.com/10.1002/14651858.CD011522.pub2>
17. Olesen AE, Olofsen E, Olesen SS, Staahl C, Andresen T, Dahan A, et al. The Absorption profile of pregabalin in chronic pancreatitis. *Basic Clin Pharmacol Toxicol* [Internet]. 2012;111:385–90. Available from: <https://onlinelibrary.wiley.com/doi/10.1111/j.1742-7843.2012.00914.x>
18. Bouwense SAW, Olesen SS, Drewes AM, Poley J-W, van Goor H, Wilder-Smith OHG. Effects of pregabalin on central sensitization in patients with chronic pancreatitis in a randomized, controlled trial. Eldabe S, editor. *PLoS One* [Internet]. 2012;7:e42096. Available from: <https://dx.plos.org/10.1371/journal.pone.0042096>
19. Olesen SS, Graversen C, Bouwense SAW, van Goor H, Wilder-Smith OHG, Drewes AM. Quantitative sensory testing predicts pregabalin efficacy in painful chronic pancreatitis. Miaskowski C, editor. *PLoS One* [Internet]. 2013;8:e57963. Available from: <https://dx.plos.org/10.1371/journal.pone.0057963>
20. Graversen C, Olesen SS, Olesen AE, Steimle K, Farina D, Wilder-Smith OHG, et al. The analgesic effect of pregabalin in patients with chronic pain is reflected by changes in pharmaco-EEG spectral indices. *Br J Clin Pharmacol* [Internet]. 2012;73:363–72. Available from: <https://onlinelibrary.wiley.com/doi/10.1111/j.1365-2125.2011.04104.x>

Remember by heart – the importance of post-mortem cardiac implantable electronic device analysis

Szymon Rzepczyk , Marcin Migiel , Bartosz Bijata ,
Paweł Świdorski 

Department of Forensic Medicine, Poznań University of Medical Sciences, Poznań, Poland

Abstract

In recent years, the number of patients with a cardiac implantable electronic device (CIED) has been steadily increasing. Implantable cardioverter-defibrillators (ICDs) are currently one of the primary methods of preventing sudden cardiac death (SCD) in patients at risk. A post-mortem CIED examination, which these days is performed very rarely, as well as the analysis of the recordings may provide key information regarding the circumstances of the patient's death. This applies to both the potential impact of a defect or damage to the device in an event of the owner's death and the forensic analysis of the circumstances of death, especially when traditional post-mortem diagnostics do not provide a clear diagnosis. In addition, using the data stored on the device, it is possible to identify the corpse and precisely determine the time of death, which is crucial for the conducted expertise. Since it is a quick, cheap and widely available procedure, CIED analysis should be incorporated as a routine element of post-mortem diagnostics.

Keywords: cardiac implantable electronic device • ICD • sudden cardiac death • post-mortem examination • diagnostic difficulties

Citation

Rzepczyk S, Migiel M, Bijata B, Świdorski P. Remember by heart – the importance of post-mortem cardiac implantable electronic device analysis. Eur J Transl Clin Med. 2023;6(2):95-101.

DOI: [10.31373/ejtcmed/174596](https://doi.org/10.31373/ejtcmed/174596)

Corresponding author:

Szymon Rzepczyk, Department of Forensic Medicine, Poznań University of Medical Sciences, Poznań, Poland

e-mail: szymon.rzepczyk@interia.eu

Available online: www.ejtcmed.gumed.edu.pl

Copyright © Medical University of Gdańsk

This is Open Access article distributed under the terms of the Creative Commons Attribution-ShareAlike 4.0 International.



Introduction

Implantable cardioverter-defibrillator (ICD) is an advanced medical instrument of the cardiac implantable electronic device (CIED) type, which plays a key role in the prevention of sudden cardiac death (SCD) in patients with certain cardiac arrhythmias [1-3]. Its main purpose is to detect and terminate ventricular arrhythmias or bradycardia and to provide resynchronization pacing [4]. This therapy is considered in the context of primary and secondary prevention of SCD [5-7]. Secondary prevention includes cases of patients who were successfully resuscitated after cardiac arrest due to ventricular fibrillation (VF) or ventricular tachycardia (VT), after 48 hours of acute coronary syndrome and have been assessed to benefit from the therapy for at least one year in good condition. Primary prevention is for patients with chronic symptomatic heart failure (NYHA II-III) and low left ventricular ejection fraction (LVEF \leq 35%) for whom three months of optimal pharmacotherapy did not bring improvement in these parameters and are expected to benefit from the therapy for at least one year in good condition [8]. Besides ICDs, permanent pacemakers (PM), also classified as CIEDs, are among the devices used to improve the quality of life and survival time of patients with cardiac problems [9]. PMs are devices used to electrically stimulate the heart's rhythm, especially when dysfunction of the impulse-conducting system occurs, e.g. advanced atrioventricular blocks, causing hemodynamic heart failure [10].

Cardiac Resynchronization Therapy (CRT) is another electronic device permanently implanted in patients with heart failure [11]. Resynchronization therapy improves heart function and the well-being of patients, reduces the severity of symptoms, and decreases morbidity and mortality. There are two main types of CRT devices: a resynchronization stimulator with a defibrillator function (CRT-D, cardiac resynchronization therapy-defibrillator) and resynchronization stimulator without a defibrillator function (CRT-P, cardiac resynchronization therapy-pacemaker) [12]. In recent years, an increase in the number of ICD and other CIEDs implantations has been observed worldwide [13-16]. According to epidemiological data, over 200000 ICD implantations are performed per year [17]. Due to the clear trend in the number of CIED implantations, it is important to explore its role in the post-mortem examination. Such studies are a key element in evaluating the effectiveness of therapy (not only in the context of preventing SCD), but also in identifying potential problems with these devices. The knowledge gathered as a result of post-mortem examinations improves the procedures of implantation, programming and supervision of ICDs, contributing to the improvement of the quality of life of patients with cardiac arrhythmias [18]. Currently, the obligation to extract CIED from the body only applies to cases where cremation is planned

(for safety reasons, including the risk of explosion due to high temperature). Furthermore, explantation of the device during autopsy and postmortem analysis of its recordings is rare and applies mainly to forensic examinations, while the device itself is usually treated as medical waste [19-21].

CIED flaws and malfunctions

Despite the high efficacy demonstrated by implantable cardioverter-defibrillators, it is imperative to acknowledge the potential existence of operational imperfections within these devices. This acknowledgment underscores the significance of considering the presence of defects that might impact the seamless functioning of CIEDs despite their overall effectiveness. These may include electrode failures or displacements, abnormalities regarding arrhythmia detection and treatment, mechanical failures of the control unit and pulse generator, or improper programming of the device and software errors, including spontaneous reset or shutdown [22-23]. These defects can lead to inappropriate therapy or the lack of it in critical situations, which in turn may result in a threat to the patient's life [24-25]. The analysis of the literature shows that many technical defects of the ICD are not recognized during the life of the patient, which may contribute to their death [26]. A post-mortem examination conducted on 262 CIEDs showed device malfunction resulting from its defect or damage in as many as 15% of cases [27]. Additionally, in more than 3% of cases the flaw of the device was a potential threat to the patient's life [28]. The most common failure was battery depletion, although there were also cases of damaged electrodes, as well as errors in the software or infection at the implantation site [27]. Thanks to post-mortem CIED analysis, it is possible to identify defects in the device, which enables modification of subsequent therapies and potentially saving the lives of future patients with similar devices. There is also a risk of misdiagnoses of arrhythmias or false alarms, which can lead to unnecessary pacing. Inadequate ICD interventions, (to rhythms other than VT or VF) occur most often in the case of atrial fibrillation (AF) with rapid ventricular action, sinus tachycardia or supraventricular tachycardia (SVT). This flaw is a result of the difficulty in differentiating the various types of arrhythmias and accurately identifying which of them are in fact life-threatening. This can lead to unnecessary electric shocks, even repeated several times, which is not only unpleasant for the patient, but also increases the risk of complications [29-32].

There have also been cases of death of patients with ICDs, which were directly caused by a pacemaker dysfunction [28] and traffic accidents resulting from loss of consciousness after receiving a stimulation [33]. In cases of death of patients with CIED, the possibility of infection and infection of the device should also be considered in the post-mortem diagnosis.

Despite their infrequent occurrence, such events carry a high mortality rate [34-35]. Then, it becomes particularly important to examine the device pocket in situ during the post-mortem examination and the histopathological examination together with the analysis of the patient's medical records [36]. These results underline the importance of the forensic aspect of such cases and the need to discuss and question the natural cause of death in such cases. What is more, inclusion of ICD analysis during a routine autopsy becomes an important issue, as it may reveal a cause of death different from what was originally assumed. Moreover, the integration of comprehensive scrutiny of implantable cardioverter-defibrillators (ICDs) within the framework of routine post-mortem examinations assumes paramount significance, as it holds the capacity to elucidate an underlying cause of death that diverges from the initial hypotheses.

Forensic medicine

The reading and analysis of data recorded by CIED's provides key information for the conducted forensic medical examination [37-40]. This is particularly important in the case of unknown circumstances of the event or lack of witnesses [41]. One of its basic advantages is the possibility of identification of corpses, which is particularly important in the case of mass events, significant body damage, advanced decomposition or inability to be identify using commonly used methods, such as dental analysis or fingerprints [42]. Body identification is possible by reading the patient's data uploaded during device preparation before implantation. In the event of damage preventing the download of data, it is possible to determine the patient's identity indirectly, by reading the serial number placed on the device's case [43]. The analysis of the information recorded by the CIED also enables determination of the precise time of death, which is crucial information for the investigation, allowing, among other things, to identify the perpetrator [44-46]. Confirmation or exclusion of a suspect's alibi is one of the key pieces of information for an investigation. Moreover, determination of the exact time of death is possible even in the case of a long time since death [47]. In this case, one should also remember about possible time shifts resulting, for example, from changing the time zone, and to correlate the time shown by the device with the real time.

An autopsy remains the gold standard for determining the cause of death but in sometimes it does not provide a clear conclusion as to its circumstances [48]. In such cases, it is required to perform additional tests, which may be post-mortem analysis of the CIED record. Post-mortem reading of the data recorded by the CIED helps to determine the cause and mechanism of death by analyzing the electrophysiology and rhythm of the heart [39, 49]. This is particularly important in unclear cases when traditional post-mortem diagnostics do

not show significant changes that could have led to death [18, 50]. Such situations include, among others, sudden cardiac death as a result of cardiac arrhythmias in the functional mechanism, which may not cause any specific changes that can be visualized during an autopsy [51-53]. It is also important in the case of poisoning or overdose of drugs that may not leave macroscopically visible changes during post-mortem examination but may affect the cardiac function. In addition, reading a time-correlated heart rate record from the CIED allows a reliable determination of the sequence of events and the cause of death in cases, where potentially fatal events occur suddenly, e.g. a car accident or a fall due to loss of consciousness resulting from cardiac arrhythmias [54-56]. Moreover, the analysis of the record allows to determine the patient's condition in the period immediately prior to death and determine whether the death was sudden or preceded by agony and to determine the manner of death [57]. It is essential to correctly separate the lifetime record from the artifacts created after death, e.g. as a result of body transport or medical rescue operations. The impact of the low temperature in which the corpse is stored in the mortuary on the operation and recording of the device should also be taken into account. Another important aspect is the possibility of damage to the CIED as a result of violence, which can be life-threatening.

Conclusions

Post-mortem analysis of data recorded by CIEDs is an important addition to the traditional post-mortem examination, often providing crucial information for expert opinion on the time and circumstances of death, as well as identification of the body. Since it is a quick, cheap and widely available procedure, CIED analysis should be incorporated as a routine element of post-mortem diagnostics. Cooperation between forensic medicine specialists and cardiologists seems to be of key importance in order to assess the record and its interpretation in the context of the patient's available medical documentation as accurately as possible. This procedure would allow for a reliable assessment of the circumstances of death and identification of any defects or faults of the device, which is of key importance for the legal and medical proceedings and for improving the safety of future patients using CIEDs. It is necessary to conduct further research on post-mortem CIEDs analysis, determining the frequency of occurrence of potentially life-threatening events caused by malfunctioning of the device, which will also enable safety-improving design modifications. In addition, routine post-mortem examination of CIEDs will help to determine the cause of death in cases when the traditional post-mortem examination is inconclusive. Consideration should also be given to the CIED feature that allows transferring the recorded data from the device to an external server in order to prevent record loss.

Funding

None to report.

Conflicts of interest

All authors declare that they have no conflicts of interest.

References

1. Borne RT, Katz D, Betz J, Peterson PN, Masoudi FA. Implantable Cardioverter – Defibrillators for Secondary Prevention of Sudden Cardiac Death: A Review. *J Am Heart Assoc* [Internet]. 2017;6(3):e005515. Available from: <https://doi.org/10.1161/JAHA.117.005515>
2. DiMarco JP. Implantable Cardioverter – Defibrillators. *N Engl J Med* [Internet]. 2003;349(19):1836-47. Available from: <https://doi.org/10.1056/NEJMra035432>
3. Wasiak M, Tajstra M, Kosior D, Gąsior M. An implantable cardioverter-defibrillator for primary prevention in non-ischemic cardiomyopathy: A systematic review and meta-analysis. *Cardiol J* [Internet]. 2023;30(1):117-24. Available from: <https://doi.org/10.5603/CJ.a2021.0041>
4. Al-Khatib SM, Stevenson WG, Ackerman MJ, Bryant WJ, Callans DJ, Curtis AB, et al. 2017 AHA/ACC/HRS Guideline for Management of Patients With Ventricular Arrhythmias and the Prevention of Sudden Cardiac Death. *J Am Coll Cardiol* [Internet]. 2018;72(14):e91-220. Available from: <https://doi.org/10.1016/j.jacc.2017.10.054>
5. Ezekowitz JA, Armstrong PW, McAlister FA. Implantable Cardioverter Defibrillators in Primary and Secondary Prevention. *Ann Intern Med* [Internet]. 2003;138(6):445-52. Available from: <https://www.acpjournals.org/doi/abs/10.7326/0003-4819-138-6-200303180-00007>
6. Maron BJ, Spirito P, Shen W-K, Haas TS, Formisano F, Link MS, et al. Implantable Cardioverter-Defibrillators and Prevention of Sudden Cardiac Death in Hypertrophic Cardiomyopathy. *JAMA* [Internet]. 2007;298(4):405-12. Available from: <https://doi.org/10.1001/jama.298.4.405>
7. Noordman ABP, Rienstra M, Blaauw Y, Mulder BA, Maass AH. Appropriate Implantable Cardioverter-Defibrillator Therapy in Patients with Ventricular Arrhythmia of Unclear Cause in Secondary Prevention of Sudden Cardiac Death. *J Clin Med* [Internet]. 2023;12(13):4479. Available from: <https://www.mdpi.com/2077-0383/12/13/4479>
8. Zeppenfeld K, Tfelt-Hansen J, de Riva M, Winkel BG, Behr ER, Blom NA, et al. 2022 ESC Guidelines for the management of patients with ventricular arrhythmias and the prevention of sudden cardiac death: Developed by the task force for the management of patients with ventricular arrhythmias and the prevention of sudden cardiac death. *Eur Heart J* [Internet]. 2022;43(40):3997-4126. Available from: <https://doi.org/10.1093/eurheartj/ehac262>
9. Greenspon AJ, Patel JD, Lau E, Ochoa JA, Frisch DR, Ho RT, et al. Trends in Permanent Pacemaker Implantation in the United States From 1993 to 2009. *J Am Coll Cardiol* [Internet]. 2012;60(16):1540-5. Available from: <https://doi.org/10.1016/j.jacc.2012.07.017>
10. Gregoratos G. Indications and recommendations for pacemaker therapy. *Am Fam Physician* [Internet]. 2005;71(8):1563-70. Available from: <https://www.aafp.org/pubs/afp/issues/2005/0415/p1563.html>
11. Steffen MM, Osborn JS, Cutler MJ. Cardiac Implantable Electronic Device Therapy. *Med Clin North Am* [Internet]. 2019;103(5):931-43. Available from: <https://linkinghub.elsevier.com/retrieve/pii/S002571251930046X>
12. Glikson M, Nielsen JC, Kronborg MB, Michowitz Y, Auricchio A, Barbash IM, et al. 2021 ESC Guidelines on cardiac pacing and cardiac resynchronization therapy: Developed by the Task Force on cardiac pacing and cardiac resynchronization therapy of the European Society of Cardiology (ESC) With the special contribution of the European Hear. *Eur Heart J* [Internet]. 2021;42(35):3427-520. Available from: <https://doi.org/10.1093/eurheartj/ehab364>
13. Fernández Lozano I, Osca Asensi J, Alzueta Rodríguez J. Spanish implantable cardioverter-defibrillator registry. 18th official report of the Heart Rhythm Association of the Spanish Society of Cardiology (2021). *Rev Española Cardiol (English Ed)* [Internet]. 2022;75(11):933-45. Available from: <https://www.sciencedirect.com/science/article/pii/S1885585722002432>
14. Gadler F, Valzania C, Linde C. Current use of implantable electrical devices in Sweden: data from the Swedish pacemaker and implantable cardioverter-defibrillator registry. *EP Eur* [Internet]. 2015;17(1):69-77. Available from: <https://doi.org/10.1093/europace/euu233>
15. Raatikainen MJP, Arnar DO, Merkely B, Nielsen JC, Hindricks G, Heidbuchel H, et al. A Decade of Information on the Use of Cardiac Implantable Electronic Devices and Interventional Electrophysiological Procedures in the European Society of Cardiology Countries: 2017 Report from the European Heart Rhythm Association. *EP Eur* [Internet]. 2017;19(suppl_2):ii1-90. Available from: <https://doi.org/10.1093/europace/eux258>
16. Zecchin M, Torre M, Carrani E, Sampaolo L, Ciminello E, Ortis B, et al. Seventeen-year trend (2001–2017) in pacemaker and implantable cardioverter-defibrillator utilization based on hospital discharge database data: An analysis by age groups. *Eur J Intern Med* [Internet]. 2021;84:38-45. Available from: <https://www.sciencedirect.com/science/article/pii/S0953620520303484>

17. Ammannaya GKK. Implantable cardioverter defibrillators – the past, present and future. *Arch Med Sci – Atheroscler Dis* [Internet]. 2020;5(1):163-70. Available from: <https://doi.org/10.5114/amsad.2020.97103>
18. Mauf S, Jentzsch T, Laberke PJ, Thali MJ, Bartsch C. Why We Need Postmortem Analysis of Cardiac Implantable Electronic Devices. *J Forensic Sci* [Internet]. 2016;61(4):988-92. Available from: <https://doi.org/10.1111/1556-4029.13075>
19. Kirkpatrick JN, Ghani SN, Burke MC, Knight BP. Postmortem Interrogation and Retrieval of Implantable Pacemakers and Defibrillators: A Survey of Morticians and Patients. *J Cardiovasc Electrophysiol* [Internet]. 2007;18(5):478-82. Available from: <https://doi.org/10.1111/j.1540-8167.2007.00773.x>
20. Oliveira JC de, Fagundes AA, Alkmim-Teixeira R, Baggio JM, Armaganijan L, D'Avila A, et al. Recomendações para o Manejo de Dispositivos Cardíacos Eletrônicos Implantáveis Post Mortem. *Arq Bras Cardiol* [Internet]. 2020;115(6):1178-9. Available from: <http://abccardiol.org/article/recomendacoes-para-o-manejo-de-dispositivos-cardiacos-eletronicos-implantaveis-post-mortem/>
21. Van Heuverswyn FE, Timmers L, Stroobandt RX, Barold SS. Implantable Cardioverter-Defibrillators: Is There Life after Death? *Pacing Clin Electrophysiol* [Internet]. 2013;36(1):2-6. Available from: <https://doi.org/10.1111/pace.12023>
22. Tajstra M, Dyrbuś M, Nożyński J, Niedziela J, Gadula-Gacek E, Zembala-Nożyńska E, et al. The clinical value of routine analysis of cardiac implantable electronic devices after death in the tertiary cardiovascular centre. *Polish Arch Intern Med* [Internet]. 2020; Available from: <https://www.mp.pl/paim/issue/article/15343>
23. Tseng ZH, Hayward RM, Clark NM, Mulvanny CG, Colburn BJ, Ursell PC, et al. Sudden Death in Patients With Cardiac Implantable Electronic Devices. *JAMA Intern Med* [Internet]. 2015;175(8):1342-50. Available from: <https://doi.org/10.1001/jamainternmed.2015.2641>
24. Tukker M, Schinkel AFL, Dereci A, Caliskan K. Clinical outcomes of implantable cardioverter-defibrillator therapy in noncompaction cardiomyopathy: a systematic review and meta-analysis. *Heart Fail Rev* [Internet]. 2022;28(1):241-8. Available from: <https://doi.org/10.1007/s10741-022-10250-w>
25. Schinkel AFL. Implantable Cardioverter Defibrillators in Arrhythmogenic Right Ventricular Dysplasia/Cardiomyopathy. *Circ Arrhythmia Electrophysiol* [Internet]. 2013;6(3):562-8. Available from: <https://doi.org/10.1161/CIRCEP.113.000392>
26. Irnich W. Pacemaker-Related Patient Mortality. *Pacing Clin Electrophysiol* [Internet]. 1999;22(9):1279-83. Available from: <https://doi.org/10.1111/j.1540-8159.1999.tb00620.x>
27. Bartsch C, Irnich W, Riße M, Junge M, Weiler G. Postmortem in situ diagnosis of pacemakers and electrodes to detect dysfunction. *Leg Med* [Internet]. 2003;5:S397-400. Available from: <https://www.sciencedirect.com/science/article/pii/S1344622302001712>
28. Bartsch C, Irnich W, Junge M, Stertmann WA, Risse M, Weiler G. Post-mortem evaluation of 415 pacemakers: in situ measurements and bench tests. *EP Eur* [Internet]. 2005;7(2):175-80. Available from: <https://doi.org/10.1016/j.eupc.2004.12.010>
29. Mazurek M, Lenarczyk R, Kowalski O, Kalarus Z. Co lekarz praktyk powinien wiedzieć o automatycznym kardiowerterze-defibrylatorze? [in Polish]. *Chor Serca i Naczyn*. 2014;11(3):128-37. Available from: https://journals.viamedica.pl/choroby_serca_i_naczyn/article/view/38789
30. Maria E De, Giacomelli D, Borghi A, Modonesi L, Cappelli S. Antitachycardia pacing programming in implantable cardioverter defibrillator: A systematic review. *World J Cardiol* [Internet]. 2017;9(5):429. Available from: <http://www.wjgnet.com/1949-8462/full/v9/i5/429.htm>
31. Wilkoff BL, Ousdigian KT, Sterns LD, Wang ZJ, Wilson RD, Morgan JM. A Comparison of Empiric to Physician-Tailored Programming of Implantable Cardioverter-Defibrillators. *J Am Coll Cardiol* [Internet]. 2006;48(2):330-9. Available from: <https://www.sciencedirect.com/science/article/pii/S073510970601045X>
32. Wang N, Xie A, Tjahjono R, Tian DH, Phan S, Yan TD, et al. Implantable cardioverter defibrillator therapy in hypertrophic cardiomyopathy: an updated systematic review and meta-analysis of outcomes and complications. *Ann Cardiothorac Surg* [Internet]. 2017;6(4):298-306. Available from: <http://www.annalscts.com/article/view/15739/15847>
33. Curtis AB, Conti JB, Tucker KJ, Kubilis PS, Reilly RE, Woodard DA. Motor vehicle accidents in patients with an implantable cardioverter-defibrillator. *J Am Coll Cardiol* [Internet]. 1995;26(1):180-4. Available from: <https://www.sciencedirect.com/science/article/pii/073510979500133K>
34. Sgreccia D, Vitolo M, Valenti AC, Manicardi M, Boriani G. Burden of disease and costs of infections associated with cardiac implantable electronic devices. *Expert Rev Pharmacoecon Outcomes Res* [Internet]. 2022;22(1):7-16. Available from: <https://www.tandfonline.com/doi/full/10.1080/14737167.2021.1980386>
35. Ngiam JN, Liong TS, Sim MY, Chew NWS, Sia C-H, Chan SP, et al. Risk Factors for Mortality in Cardiac Implantable Electronic Device (CIED) Infections: A Systematic Review and Meta-Analysis. *J Clin Med*. 2022;11(11):3063. Available from: <https://www.mdpi.com/2077-0383/11/11/3063>

36. Boriani G, Proietti M, Bertini M, Diemberger I, Palmisano P, Baccarini S, et al. Incidence and Predictors of Infections and All-Cause Death in Patients with Cardiac Implantable Electronic Devices: The Italian Nationwide RI-AIAC Registry. *J Pers Med* [Internet]. 2022;12(1):91. Available from: <https://www.mdpi.com/2075-4426/12/1/91>
37. Ellouze N, Rekhis S, Boudriga N, Allouche M. Cardiac Implantable Medical Devices forensics: Postmortem analysis of lethal attacks scenarios. *Digit Investig* [Internet]. 2017;21:11-30. Available from: <https://www.sciencedirect.com/science/article/pii/S1742287616301426>
38. Fischer F, Lafleur L, Lackermair K. Aktive kardiale Implantate in der Rechtsmedizin. *Herzschrittmachertherapie + Elektrophysiologie* [Internet]. 2023;34(3):212-7. Available from: <https://doi.org/10.1007/s00399-023-00952-5>
39. Lacour P, Buschmann C, Storm C, Nee J, Parwani AS, Huemer M, et al. Cardiac Implantable Electronic Device Interrogation at Forensic Autopsy. *Circulation* [Internet]. 2018;137(25):2730-40. Available from: <https://doi.org/10.1161/CIRCULATIONAHA.117.032367>
40. Raasch FO. Pacemaker postmortem. *West J Med* [Internet]. 1978;128(1):48-9. Available from: <http://www.ncbi.nlm.nih.gov/pubmed/625967>
41. Stevenson IH, Mond HG. A Coroner's Request for Closure: The Value of the Stored Electrogram. *Pacing Clin Electrophysiol* [Internet]. 2006;29(6):670-3. Available from: <https://doi.org/10.1111/j.1540-8159.2006.00415.x>
42. Makinae H, Numata N, Kitaoka H, Daimon M, Yamamoto T, Amano A. Use of pacemaker programmers for disaster victim identification. *Forensic Sci Med Pathol* [Internet]. 2013;9(4):551-3. Available from: <https://doi.org/10.1007/s12024-013-9432-8>
43. Saint-Martin P, Rogers C, Muto J, Boyle NG, Rieders D, Sathyavagiswaran L. Pacemaker/Defibrillator Evaluation at Los Angeles County Department of Coroner. *J Forensic Sci* [Internet]. 2008;53(5):1160-5. Available from: <https://doi.org/10.1111/j.1556-4029.2008.00805.x>
44. Bhatt A, Ajugiya V, Bhandari D, Khobragade N. Forensic Significance of Cardiac Implantable Device (Pacemaker). *Int J Sci Res Sci Eng Technol* [Internet]. 2019;340-5. Available from: <http://ijsrset.com/paper/5932.pdf>
45. Lackermair K, Fischer F, Manhart J, Scheurer E, Graw M, Boy D, et al. Determination of time of death by blinded post-mortem interrogation of cardiac implantable electrical devices. *Sci Rep* [Internet]. 2022;12(1):8199. Available from: <https://doi.org/10.1038/s41598-022-12390-3>
46. Paratz ED, Block TJ, Stub DA, La Gerche A, Kistler PM, Kalman JM, et al. Postmortem Interrogation of Cardiac Implantable Electronic Devices. *JACC Clin Electrophysiol* [Internet]. 2022;8(3):356-66. Available from: <https://doi.org/10.1016/j.jacep.2021.10.011>
47. Block T, Paratz E, La Gerche A, Stub D, Strathmore N, Mond H, et al. Unearthing the evidence: post-mortem interrogation of cardiac implantable electronic devices. *Eur Heart J* [Internet]. 2021;42(Supplement_1):ehab724.0407. Available from: <https://doi.org/10.1093/eurheartj/ehab724.0407>
48. Ely SF, Gill JR. Chapter 5 – The forensic autopsy. In: Ely SF, Gill JRBT-P of FP, editors. Academic Press; 2023. p. 103-26. Available from: <https://www.sciencedirect.com/science/article/pii/B9780323917964000143>
49. Sinha SK, Crain B, Flickinger K, Calkins H, Rickard J, Cheng A, et al. Clinical Inferences of Cardiovascular Implantable Electronic Device Analysis at Autopsy. *J Am Coll Cardiol* [Internet]. 2016;68(12):1255-64. Available from: <https://doi.org/10.1016/j.jacc.2016.06.052>
50. Bernardes-Souza B, Tiecher RD, Do DH, Saint-Martin P, Sathyavagiswaran L, Ukpo OC, et al. Forensic cardiac device analysis at the Los Angeles County Department of the Coroner: A 20-year experience. *J Forensic Sci* [Internet]. 2022;67(5):1924-31. Available from: <https://doi.org/10.1111/1556-4029.15107>
51. Basso C, Burke M, Fornes P, Gallagher PJ, de Gouveia RH, Sheppard M, et al. Guidelines for autopsy investigation of sudden cardiac death. *Virchows Arch* [Internet]. 2008;452(1):11-8. Available from: <https://doi.org/10.1007/s00428-007-0505-5>
52. Nikolaidou T, Johnson MJ, Ghosh JM, Marincowitz C, Shah S, Lammiman MJ, et al. Postmortem ICD interrogation in mode of death classification. *J Cardiovasc Electrophysiol* [Internet]. 2018;29(4):573-83. Available from: <https://doi.org/10.1111/jce.13414>
53. Rzepczyk S, Świdarski P, Bijata B, Rusek D, Bożek B, Żaba C. The lethal assault, fall trauma or cardiac arrhythmia? – diagnostic difficulties associated with determining the cause of death in a patient with an ICD. *Pomeranian J Life Sci* [Internet]. 2023;69(3):50-3. Available from: <https://intapi.sciendo.com/pdf/10.21164/pomilifesci.921>
54. Dolinak D, Guileyardo J. Automatic Implantable Cardioverter Defibrillator Rhythm Strip Data as Used in Interpretation of a Motor Vehicle Accident. *Am J Forensic Med Pathol* [Internet]. 2001;22(3):256-60. Available from: https://journals.lww.com/amjforensicmedicine/fulltext/2001/09000/automatic_implantable_cardioverter_defibrillator.11.aspx

55. Janowski M, Chan C-E, Poleszak K, Kozak M, Wysocka A, Główniak A. Death caused by cervical spine trauma from a car accident, secondary to ventricular arrhythmia recorded by implantable cardioverter-defibrillator. *Polish Arch Intern Med* [Internet]. 2023; Available from: <https://www.mp.pl/paim/issue/article/16414>
56. Kaliszan M, Daniłowicz-Szymanowicz L, Kempa M, Tomczak E, Krzyżanowska M, Jankowski Z, et al. Postmortem Analysis of Electrogram Records from an Implantable Cardioverter-Defibrillator (ICD) in the Reconstruction of a Road Traffic Accident. *J Forensic Sci* [Internet]. 2019;64(5):1551-4. Available from: <https://doi.org/10.1111/1556-4029.14037>
57. Mond HG, Valentine BC, Randall RD, Kelsall R, Gregory M. Anatomy of a Murder: Telemetric Footprints. *Pacing Clin Electro-physiol* [Internet]. 2002;25(9):1406-8. Available from: <https://doi.org/10.1046/j.1460-9592.2002.01406.x>
58. Junge M, Weckmüller J, Nägele H, Püschel K. "Natural death" of a patient with a deactivated implantable-cardioverter-defibrillator (ICD)? *Forensic Sci Int* [Internet]. 2002;125(2):172-7. Available from: <https://www.sciencedirect.com/science/article/pii/S0379073801006338>
59. Kaya A, Çelik C, Güler H, Şenol E, Aktaş EÖ. Medicolegal Evaluation of the Case of Implantable Cardioverter Defibrillator (ICD) Lead Fracture Due to Domestic Violence. *Düzce Tıp Fakültesi Derg* [Internet]. 2020 Aug 30;22(2):134-6. Available from: <http://dergipark.org.tr/en/doi/10.18678/dtfd.729969>

